Université Louis Pasteur
Strasbourg I
2007

THESE

présentée à la

FACULTE DES SCIENCES

Pour obtenir le titre de

DOCTEUR DE L'UNIVERSITE LOUIS PASTEUR

Discipline : SCIENCES DU VIVANT
Spécialité : ASPECTS MOLECULAIRES ET CELLULAIRES DE LA BIOLOGIE
Option : NEUROSCIENCES

par

Michał ŚLĘZAK

New transgenic mouse models for astrocyte-specific, inducible somatic mutagenesis

Soutenance publique le 10 juillet 2007 devant la Comission d'Examen:

Directeur de Thése : Frank W. PFRIEGER
Rapporteur Interne : Manuel MARK
Rapporteur Externe : Philip G. HAYDON
Rapporteur Externe : Leszek KACZMAREK
Examinateur : Elisabeth GEORGES-LABOUESSE

INCI – UMR 7168 / LC2 Dept. Neurotransmission et Sécrétion Neuroendocrine

Pamięci Oli Barańskiej

i Tobie, Zbyszku...

I would like to thank Prof. Haydon, Prof. Kaczmarek, Prof. Mark and Dr. Georges-Labouesse for honoring me with their acceptation to be a member of my jury.

₪

Agnieszko, jesteś światełkiem na mojej drodze. Dziękuję.

₪

Frank: Wenn ich etwas über dich sagen soll, dann, dass du ein guter Mensch bist, ein exzellenter Wissenschaftler und ein herausragender Chef, genau in dieser Reihenfolge. Danke, dass du „ Das Narrenschiff“ auf deine Webseite genommen hast, es hat mir den Weg gezeigt. Danke für alle wissenschaftlichen Diskussionen, für das Formen meines kritischen Denkens, dafür, dass du mir die Welt der Wissenschaft in seiner meist faszinierenden Weise gezeigt hast, für alle Meetings zu denen du mich ermutigt hast (und die du mir ermöglicht hast!). Am meisten aber, danke für das Vertrauen und für den Zwang, wann immer möglich, zu denken und dafür, keine Antworten gegeben zu haben. Ich hoffe, das ist nicht das Ende unseres wissenschaftlichen Abenteuers. Danke für München, für die Mojitos, für deine leckere Art zu kochen und für deine wichtigen Worte, wenn ich sie am meisten brauchte.

Dear Pfrieger team! I am happy that I know you all. Thank you for all scientific help that I received from each of you. Thank you for all great moments we had outside of the lab. I have beautiful memories from these last five years… I would like also to thank
Aurore – pour les traductions, ton sourire, ton indépendance et pour partager ton bonheur avec moi.
Céline – pour m’avoir accueilli quand je suis arrivé et pour avoir adopté avec beaucoup d’enthousiame les coutumes polonaises.
Isa – pour ta spontanéïté, ton sourire, ton ironie, ma première conversation francaise et pour ce dernier mail.
Katja - danke für die ersten Monate, als ich noch etwas verloren war und du für mich da warst…und für die Chats, die wir später hatten…sie haben mir einige gute Einfälle gebracht.
Dominique – pour l’aide apportée avec cette administration francaise de m***e, pour le canapé et pour le photo d’Aga.
Renaud – pour ton optimisme et pour m’avoir soutenu dans le pire moment de ma vie.
Thomas – pour la table, le taxi et pour toutes nos pauses clopes.
I wish you all, and also Anina, Daniela, Christian all the best in your scientific and private future. I hope we meet soon somewhere where they have a beer….

₪

I would like to thank Bernard Poulain, Marie-France Bader and all members of NSN for their scientific help, constant support and some nice moments inside and outside of the work.

₪

Daniel, merci de m'avoir permis de préparer une thèse dans un domaine aussi inattendu, de m'avoir donné l'opportunité de travailler dans ton laboratoire, de m'avoir aidé et pour ton enthousiasme pour la vrai science.
Michael, danke für den Unterricht in molekularer Biologie, für deine Geduld, deine Solidität und deinen deutschen Humor.
Meister, merci d'avoir partagé avec moi ces choses que seulement le Dieu sait et pour ton sens de l'humour.
Pierre, merci pour ton aide, ta douce folie, cet enthousiame envers la Pologne et les polonais et pour m'avoir invité à ton mariage.
Celine, Delphine, merci pour votre sourire, votre thé et pour apporter de la soleil au labo.
Mei, thank you for your critical comments during this project and help.
I would like to thank all members of Metzger's team: Krishna, Letitia, Magali, Susan, Ying, Eduardo, Arup, Roman, Ali, Takeshi, Ming, Zhang, Koumar, Milan, also Andre and Stephane for these years, for your support and for scientific discussions. I learned a lot of positive things…

I would like to gratefully acknowledge technical staff from IGBMC, ICS and INCI for their outstanding assistance and help during my project.
Leila – merci!

₪

Krzysztofie, dziękuję za Twój optymizm, wiarę, uczciwość, upór, wszelką pomoc. Następny doktorat obronię w kraju.
Zuzanno, dziękuję za wszelką pomoc. Uściski dla wszystkich kolaborantów.

₪

During these years I met a lot of outstanding people that made them unforgettable.
Dziękuję Wam.
Olu, dziękuję za Twoje wsparcie i przyjaźń, za poświęcenie kawałka siebie, żebym dziś mógł to pisać. Za wszystko.
Radosławie, za Twoje męstwo, honor, uczciwość, ironię, wszelką pomoc, niepowtarzalny humor. Dziękuję za Dijon, szanty, wspólne mieszkanie. Za przyjaźń.
Madziu, za pomoc w ciężkich chwilach, za wspólne obiady, imprezy, humor, za łzy. Za przyjaźń.
Isabelle, pour les soirées avecle foot, pour les sorties au cinéma, pour Julie et Julien. Merci pour ta sagesse, que tu partages avec moi. Merci pour ta amitié.
Marto, za naukowe i zdecydowanie pozanaukowe dyskusje, wspólne obiady, wszystkie imprezy. Za wsparcie, za krytykę, która uczyniła mnie lepszym.
Sergiuszu, Rajnerze, za Waszą mądrość i za wspólne granie.
Wojtku, za wszelką pomoc naukową, umożliwienie mi przeprowadzenia eksperymentów, za imprezy, tańce, hulanki, swawole i za trzy cudowne córki, które za każdym razem wzbudzały tyle radości.
Kasiu, dziękuję za Twoją oryginalność, ciepło i poczucie humoru.
Petre, dovol mi pdekovat za pomoc kterou jsi mi poskytl kdykoliv jsem potreboval. Dekuji take za radostne a krasne chvile ktere jsme spolecne prozili. Jsem vdecny za tve pratelstvi a tesim se na budouci zazitky.
Malika, merci pour la sérénité, que j'ai retrouvé chez toi et tes soeurs.

Joanno, Moniko, Georgij, Iwono, Kasiu, Rafale, Aleksandrze, Sophie, Wojtku, Wiolu, Madziu, Moniko, Asiu, Wojtku, Tariku, Kasiu, Karolino, Pawle, Kingo, Joanno, Aniu, Kasiu, Olo – to z Wami dzieliłem przeżycia tych pięciu lat. Dziękuję za Waszą obecność, humor, wsparcie, mądrość, imprezy... za piękne chwile.
Życzę Wam samego szczęścia. A sobie – spotkania równie wspaniałych przyjaciół.

Wszystkim dzieciakom za ich uśmiech – ogromna buźka.

Przyjaciołom w Polsce i w niebie – dziękuję za wszystko.

Madziu, Maćku, Marto i mała Madziu (wybaczysz tę poufałość, prawda?) – ogromnie się cieszę, ze Was poznałem. Dziękuję za piękne chwile w Dijon, w Strasbougu, w Białce. Liczę na dużo więcej! Ściskajcie ode mnie dijonowców, których poznałem dzięki Wam.
Agnieszko, Kamilo, Paulino, Aniu, Olu, Karino, Kasiu, Edyto, Marysiu, Agnieszko, Miśku – dziękuję za całą radość jaka mnie spotkała dzięki Wam.
Asiu, Olu, Moniko, Sylwio, Urszulo, Joanno – dziękuję za piękne wakacje. Dałyście mi wiarę w siebie. Dziękuję.
I would like to thank friends from European Doctoral College: Piotr, Petr, Ginka, Akmer, Sasza, Ozgur, Mme Naud, Michael Vorbeck for broadening my horizons, great parties, for their friendship.

₪

Mamo, dziękuję za wsparcie. Dziękuję za wszelką pomoc. Dziękuję, że przyjechałaś.
Tato, dziękuję za to, że wiem jak być dobrym ojcem.
Młody, dzięki że jesteś. Teraz i zawsze, kiedy Cię potrzebuję.
Basiu, Wojtku, Aniu, Mirku – dziękuję za wsparcie i Waszą obecność.
Babciu, Dziadku – dziękuję, że pamiętacie o mnie i zawsze wspieracie.

₪

Iwono, dziękuję za czary.

Elżbieto, dziękuję za nadzieję i inspirację.

Zbyszku, dziękuję że jesteś dla mnie.

₪

I would like to acknowledge European Doctoral College, which enabled me to share a part of this project with the Jagiellonian University and to participate in a special multicultural course of European interests presented by international experts.

₪

I also gratefully acknowledge Centre National de la Recherche Scientifique and Max-Planck Gesellchaft for financial support during my PhD.

TABLE OF CONTENTS

RESUME EN FRANCAIS

Les astrocytes sont le type cellulaire le plus représenté dans le cerveau des Mammifères. Ces cellules gliales forment une population hétérogène, différant dans leur morphologie, leur protéome et leurs propriétés physiologiques. Les avancées de la recherche ces dernières décennies ont générées des hypothèses attribuant aux astrocytes un rôle actif dans la formation et le fonctionnement des synapse, la balance énergétique cérébrale, la capture des ions dans le milieu extracellulaire, les processus homéostasiques ou encore la réponse immunitaire dans le système nerveux central. Jusqu'ici la majorité des hypothèses formulées sur leurs fonctions sont basées sur des études *in vitro* , à cause du manque d'outils permettant de manipuler génétiquement ces cellules *in vivo* . Le but de ma thèse était d'établir de nouveaux modèles transgéniques murins permettant d'éliminer des gènes d'intérêt spécifiquement dans les astrocytes.

Nous avons choisi une approche utilisant le système Cre/loxP qui permet une mutagenèse somatique inductible dans un type cellulaire donné. Le contrôle temporel de la mutagenèse est permis par le recours à une version inductible de la Cre recombinase ($CreER^{T2}$) par le Tamoxifène (TAM), la protéine Cre restant inactive jusqu'à l'administration de ce ligand synthétique.

Nous voulions établir des lignées ciblant différentes sous-populations d'astrocytes, permettant une approche comparative. C'est pourquoi nous avons choisi cinq promoteurs contrôlant l'expression de gènes astrocytaires, à savoir les promoteurs des gènes codant pour le transporteur Glutamate/Aspartate (Glast), la connexine 30 (Cx30), l'aquaporine 4 (Aqp4), l'apolipoprotein E (ApoE) et la glial fibrillary acidic protein (Gfap). Enfin, nous avons opté pour une transgenèse basée sur l'utilisation de chromosomes bactériens artificiels (BAC). Les BACs contiennent de grands fragments d'ADN génomique murin (20-200 kb) insérés dans des bactéries et présentent plusieurs avantages au regard de la transgenèse. Ils peuvent porter la plupart des éléments de régulation de l'expression d'un gène donné, leur intégration dans le génome est moins soumis aux effets de positionnement, et leur utilisation réduit le nombre de lignées qui doivent être dépistées pour identifier celles présentant une forte expression du transgène.

Pour générer le transgène, la région entourant le codon ATG (codon initiateur) a été remplacée par la séquence codante $CreER^{T2}$ dans chaque BAC comportant un gène exprimé dans les astrocytes. Ceci par recombinaison homologue dans des souches bactériennes spécifiquement développées. L'utilisation de différentes enzymes de restriction a permis de vérifier la bonne insertion de la cassette contenant la séquence $CreER^{T2}$. Les BACs correctement modifiés ont par la suite été purifiés et microinjectés dans des œufs fécondés de

souris. Une fois la transgenèse réalisée, deux à cinq lignées fondatrices ont été obtenues pour chaque transgène. Parmi celles-ci, quatre lignées (Glast-CreER^{T2}, Cx30-CreER^{T2}, Aqp4-CreER^{T2} et ApoE-CreER^{T2}) ont transmis le transgène à leur descendance. Aucune transmission germinale n'a été obtenue pour les lignées Gfap-CreER^{T2}.

Par la suite, il nous a fallu déterminer si ces lignées transgéniques permettent de cibler les gènes astrocytaires à l'aide de différentes approches. Tout d'abord, j'ai réalisé des RT-PCR (reverse transcriptase polymerase chain reaction) afin de tester si les niveaux de transcrits pour CreER^{T2} sont comparables au niveau de transcription des gènes endogènes correspondants, dans différentes régions cérébrales et dans les organes périphériques. Dans une des lignées utilisant le promoteur Glast et dans toutes les lignées utilisant le promoteur Cx30, l'expression de CreER^{T2} correspondait fortement aux niveaux de transcription de Glast et Cx30 respectivement. Pour les autres promoteurs (ApoE et Aqp4) les niveaux d'ARNm codant pour CreER^{T2} étaient bien plus bas, et montraient une plus faible corrélation avec le niveau de transcrits du gène endogène correspondant. Dans un deuxième temps, nous avons tester l'activité de la recombinase CreER^{T2} en croisant les différentes lignées avec la lignée « rapporteuse » RXRαaf2/+ qui permet la détection de la recombinaison génique avec une grande sensibilité. Différents protocoles d'injection du Tamoxifen (TAM) ont été appliqués, le plus efficace consistant en une injection journalière de 2 mg de TAM pendant 5 jours consécutifs. Les souris adultes ayant reçues des injections de TAM sont sacrifiées une semaine après la dernière injection. A noter que l'activité de la recombinase détéctée en l'absence de traitement au TAM été tres rare dans les différentes lignées. Dans la lignée Tg(Glast-CreER^{T2}), l'activité recombinase de Cre-ER^{T2} faisant suite à l'injection de TAM a été observée dans le cervelet, le cortex, l'hippocampe, le mésencéphale, le bulbe olfactif, la médulla et dans les yeux, la rate et la peau. Dans la lignée Tg(Cx30-CreER^{T2}), l'activité recombinase était la plus forte dans le cervelet, le cortex, l'hippocampe, le mésencéphale, le tronc cérébral et la peau. Aucune activité n'a été observée dans les yeux et les autres organes testés. Pour ces deux lignées, le motif de distribution de l'activité de l'enzyme correspond à celui de l'activité du promoteur décrite dans la littérature, et à celui indiqué par nos données de RT-PCR.

Dans la lignée Tg(ApoE-CreER^{T2}) l'activité de la recombinase Cre a été observée dans le cervelet, mais est relativement faible ou absente dans les autres régions du cerveau. Une activité recombinase a également été mise en évidence dans le foie. Dans le cas de la lignée Tg (Aqp4-CreER^{T2}), l'activité de Cre s'est révélée être très faible dans le cerveau mais élevée

dans le cœur, les reins et les muscles. Ces données sont en accord avec les données publiées sur l'activité des deux promoteurs.

Dans le but de déterminer de manière plus précise la distribution de la recombinaison induite par la protéine CreER^{T2} dans les différentes régions du système nerveux central, les lignées transgéniques ont été croisées avec la lignée rapporteuse Z/AP qui présente la particularité de ne plus exprimer la β-galactosidase (β-gal) après action de Cre, mais exprime l'alcaline phosphatase placentaire humaine (hPLAP), pouvant être visualisée à l'aide de marquage cytochimique trois semaines après la dernière injection de TAM. Dans la lignée Tg(Glast-CreER^{T2})T45-72 l'activité recombinase a été détectée dans des cellules à morphologie radiaire dans le cervelet, le gyrus denté de l'hippocampe, la paroi du 3ème ventricule et dans la rétine, ainsi que dans certaines cellules à morphologie étoilée dans le cortex, l'hippocampe et l'hypothalamus. Dans la lignée Tg(Cx30-CreER^{T2})T53-33 l'activité recombinase fut observée dans des cellules radiaires de la matière grise du cervelet et dans de nombreuses cellules étoilées, particulièrement dans le thalamus ou le tronc cérébral, mais aussi dans la matière blanche du cervelet, le cortex et l'hippocampe. Pour les lignées Tg(ApoE-CreER^{T2}) et Tg(Aqp4-CreER^{T2}), très peu de cellules exprimaient hPLAP, indiquant qu'elles ne permettaient pas d'induire une recombinaison génique très étendue dans le cerveau.

A ce stade, les résultats obtenus nous ont incités à nous focaliser sur la caractérisation des lignées basées sur les promoteurs Glast et Cx30. Pour confirmer l'identité des cellules dans lesquelles la recombinaison génique a eu lieu, chacune des deux lignées transgéniques a été croisée avec la lignée rapporteuse ROSA26, qui en présence d'activité recombinase Cre va exprimer la β-gal, qui peut être visualisée par marquage immunohistochimique. Ceci présentant l'avantage de pouvoir identifier les cellules exprimant la β-gal à l'aide d'un double marquage en utilisant un second marqueur spécifique. Le marquage sur des coupes de cerveaux d'animaux injectés au TAM a montré que le nombre de cellules présentant une recombinaison est plus important dans cette lignée rapporteuse que dans la lignée Z/AP. Le motif général de distribution de l'activité est en revanche similaire. Pour les deux lignées, la grande majorité des cellules exprimant β-gal était également positive pour l'un des marqueurs astrocytaires GFAP ou S100β, mais pas pour le marqueur neuronal NeuN ou pour le marqueur oligodendrocytaire CNPase. Ceci confirme que les deux lignées Tg(Glast-CreER^{T2})T45-72 et Tg(Cx30-CreER^{T2})T53-33 permettent de cibler spécifiquement les astrocytes dans le cerveau adulte.

L'efficacité de la recombinaison induite par Cre-ER^{T2} a été estimée en comptant le nombre de cellules positives pour β-gal et S100β. Dans la lignée Tg(Glast-CreER^{T2})T45-72 l'expression de β-gal a été observée en moyenne dans 98% des glies de Bergmann positives pour S100β dans le cervelet, 30% des glies de Müller dans la rétine et 20% des astrocytes du cortex et de l'hippocampe. L'activité de Cre-ER^{T2} a également été mise en évidence dans deux zones de neurogenèse chez l'adulte: la zone sous-ventriculaire et la couche sous-granulaire du gyrus denté. En collaboration avec les Drs C. Goeritz et J. Frisen (Karolinska Institute, Stockholm), nous avons pû confirmer que la lignée Tg(Glast-CreER^{T2})T45-72 peut être utilisée pour cibler les précurseurs neuronaux dans le cerveau adulte. Dans la lignée Tg(Cx30-CreER^{T2})T53-33 j'ai déterminé que les cellules exprimant la β-gal représentaient environ 80% des glies de Bergmann, 80% des astrocytes du thalamus, plus de la moitié de ceux du tronc cérébral, et 40% des astrocytes du cortex et de l'hippocampe.

Ainsi, mon travail de thèse a abouti à la génération et la caractérisation d'au moins deux lignées de souris transgéniques qui peuvent être utilisées pour inactiver efficacement et de manière inductible des gènes dans les astrocytes. Ces lignées viennent compléter le petit nombre d'animaux transgéniques permettant de cibler ces cellules, et devraient être utiles pour déterminer la fonction des astrocytes dans le cerveau en développement et le cerveau adulte par des approches perte- ou gain-de-fonction.

ABBREVIATION LIST

AMPA	Amino-3-hydroxy-5 -methyisoxazol-4-propionic acid
AMPAR	Amino-3-hydroxy-5 -methyisoxazol-4-propionic acid receptor
ApoE	Apolipoprotein E
Aqp4	Aquaporin-4
ATP	Adenosine tri-phosphate
BAC	Bacterial artificial chromosome
BDNF	Brain-derived neurotrophic factor
βGIVS	β-globin intervening sequences
BMP	Bone morphogenic protein
Bon	Bone
BrdU	5-bromo-2-deoxyuridine
BSA	Bovine serum albumin
CA1	Cornu Ammonis 1
cAMP	Cyclic adenosine monophosphate
CBP	cAMP response element-binding (CREB) binding protein
Cer	Cerebellum
CNPase	2',3'-cyclic nucleotide 3'-phsosphodiesterase
CNS	Central nervous system Ciliary neurotrophic factor
CNTF	Ciliary nerutor
Cre	Cyclization recombination
Ctx	Cortex
Cx26, 30, 43	Connexin-26, -30, -43
DAG	Diacylglycerol
DNA	Desoxyribonucleic acid
EAAT	Excitatory amino acid transporter
EDTA	Ethylene-diamine tetraacetic acid
EGFP	Enhanced green fluorescent protein
EPSC	Excitatory postsynaptic current
mEPSC	Miniature excitatory postsynaptic current
FGF	Fibroblast growth factor
Flp	Flippase
GABA	Gamma-aminobutyric acid
GDNF	Glia-derived neurotrophic factor

Gfap	Glial fibrillary acidic protein
GFP	Green fluorescent protein
GLAST	Glutamate/aspartate transporter
GLT-1	Glial glutamate transporter
GRP	Glia-restricted progenitors
GS	Glutamine synthetase
20-HETE	20-hydroxyeicosatetraenoic acid
Hip	Hippocampus
Hrt	Heart
IP_3	Inositol tri-phosphate
IPSC	Inhibitory postsynaptic current
mIPSC	Miniature inhibitory postsynaptic current
Kid	Kidney
Kir	Potassium inward rectifier channel
LIF	Leukemia inhibitory factor
Liv	Liver
LTD	Long-term depression
LTP	Long-term potentiation
MCT	Monocarboxylase transporter
Med	Medulla oblongata
Mid	Midbrain
mGluR	Metabotropic glutamate receptor
NG2	Neuron/glial proteoglican
Ngn1	Neurogenin 1
NMDA	N-methyl-D-aspartate
NMDAR	N-methyl-D-aspartate receptor
NT-3	Neurotrophin-3
4-OHT	4-hydroxy-tamoxifen
PCR	Polymerase chain reaction
PDGF	Platelet derived growth factor
PGE_2	Prostaglandin E_2
PLC	Phospholipase C
RGC	Retinal ganglion cells
RT-PCR	Reverse-transcriptase polymerase chain reaction

RXRα	Retinoid X receptor alpha
SAT	System A transporter
SDS	Sodium dodecyl sulphate
SGL	Subgranular layer
SN1	System N transporter
SNARE	Soluble N-ethylmaleimid sensitive factor attachment protein receptor
SOC	Slow outward current
Spl	Spleen
STAT	Signal transducer and activator of transcription
SVZ	Subventricular zone
TAM	Tamoxifen
TCA	Tricarboxylic acid cycle
Tes	Testis
TNFα	Tumor necrosis factor alpha
Tris	Tris (hydroxymethyl) aminomethane
TSP	Thrombospondin
VAMP	Vesicle associated membrane protein

INTRODUCTION

The nervous tissue is composed of many types of cells that classically are divided in neurons and glia, the latter further subdivided in astrocytes, oligodendrocytes and microglia (Kandel et al., 2000; Kettenmann and Ransom, 2004). While neurons are responsible for fast communication, glial cells were originally thought to perform supplementary functions. Over a century of research passed from the first description of glia byVirchow (1846) to hypotheses on their contribution to synaptic transmission by Orkand (1966). The rapid development of techniques during the last two decades revealed unexpected functions of all types of glial cells. In particular, a revolution in our understanding of astrocytes was initiated with the discovery of a communication between astrocytes based on calcium (Dani et al., 1992) and of modification of neuronal function by astrocytes (Parpura et al., 1994; Nedergaard, 1994; Hassinger et al., 1995). With time the influence of astrocytes on neuronal development (Freeman, 2006), synaptogenesis (Slezak and Pfrieger, 2003), synaptic transmission (Haydon, 2001), brain energy balance (Magistretti, 2006) and immunological responses (Bechmann et al., 2007) has been investigated. The summary of selected results on the function of these fascinating cells will be presented in the introduction of this thesis.

One important limitation of the research of astrocytes has been the lack of appropriate tools to investigate their biology *in vivo* . This urgent need prompted my project, which aimed to generate new transgenic models enabling astrocyte-specific and temporally-controled gene manipulation.

1. GENERATION OF ASTROCYTES

Astrocytes, as well as neurons, arise from neuroectoderm, but the molecular mechanisms that define the different stages of their generation are still poorly understood.

1.1. Genetic regulation of glial fate in invertebrates

In invertebrates, glia and neurons arise probably from the same set of progenitors, and their fate is regulated genetically. A gene responsible for the switch of the neuronal versus glial cell fate has been identified, and named *glial cell missing/glial deficient* (*gcm/glide* (Giangrande, 1995; Hosoya et al., 1995; Jones et al., 1995). Flies lacking *gcm* display loss of certain types of glial cells, whereas overexpression of this gene leads to differentiation of neuroblasts towards glia. This suggested the existence of common progenitor of both cell types, with cell fate depending on *gcm* activation, at least for specific glial cells studied. Recently, the vertebrate ortholog of *gcm* has been described to play a role in the development of chick spinal cord (Soustelle et al., 2007).

1.2. The search for astrocyte progenitors in developing mammalian brain

In the developing mammalian brain, differentiation of the diverse cell types proceeds in a precise order. In the rat, astrocytes begin to differentiate at embryonic day 17 (E17) and their number rises until postnatal day 24 (P24) (Nixdorf-Bergweiler et al., 1994).

Diverse classes of astrocytic precursors were identified. Detailed analyses of protein expression and morphological features in mice suggested that cortical astrocytes arise from radial glia and acquire stellate morphology perinatally (Takahashi et al., 1990). Based on clonal analysis from developing rat optic nerve, astrocytes were proposed to originate from progenitors common for both types of macroglia, named O2A (Raff et al., 1983). Further discoveries led to a more precise characterization of cell lineages (Liu and Rao, 2004). A2B5-positive progenitors from E13.5 rat spinal cord, named glia-restricted progenitors (GRPs, for all abbreviations see list at the beginning of the manuscript), were shown to give rise to three types of cells: oligodendrocytes, type 1- (fibrous, A2B5-, Gfap+) and type 2- (protoplasmic, A2B5+, Gfap+) astrocytes (Rao et al., 1998). Restricted astroglial lineage were shown for precursors extracted from E16 mouse cerebellum [nestin+, A2B5-, (Seidman et al., 1997)], neonatal rat spinal cord [nestin-, A2B5+, (Fok-Seang and Miller, 1992)] and developing rat optic nerve [nestin+, A2B5+, (Mi and Barres, 1999)]. It is possible that depending on the brain region astrocytes arise from different type of precursors. Another explanation is that

heterogeneity of precursors reflects later diversity of astrocytic phenotypes. Finally, it is not clear to which degree cells growing *in vitro* recapitulate their natural development. This question is raised by the fact that type 2 astrocytes observed *in vitro* have not been detected in living brains.

The existence of common precursors can also be addressed by cell-fate mapping *in vivo* using transgenic lines that express Cre recombinase in progenitors. Targeting radial glia during development was possible with transgenic lines like hGfap-Cre (Malatesta et al., 2003), BLBP-Cre (Anthony et al., 2004) or mGfap-Cre (Casper and McCarthy, 2006). Analysis of these transgenic animals caused some dissappointment, however, since authors were unable to confirm astrocytic lineage. Recently, using a new transgenic mouse model where Cre expression is controlled by the endogenous promoter for Glast, Mori et al. (2006) have shown that 42% of cortical grey matter, 30% of cortical white matter and 43% of striatal astrocytes are derived from E18-traced radial glia and that from this stage on Glast-positive precursors do not give rive to neurons, except for distinct neurogenic regions. Additionally, Mori et al. (2006) and Casper and McCarthy (2006) found a significant proportion of oligodendrocytes originating from Glast- or Gfap-positive progenitors, respectively. It is unclear, however, whether astrocytes and oligodendrocytes originate from the same, or from different set of precursors. On the other hand, cell-fate mapping studies in spinal cord, using *Olig1*-Cre and *Olig2*-Cre transgenic lines indicated that oligodendrocytes and motoneurons, but not astrocytes, arise from a common progenitor cell (Lu et al., 2002). This is in contrast to recent studies showing the opposite, namely that motoneurons and oligodendrocytes do not share a common precursor (Wu et al., 2006) and that astrocytes may also originate from *Olig2*-positive precursors (Masahira et al., 2006, Cai et al., 2007). One important limitation of these studies is still the scarcity of stage-specific markers that would enable identification of progenitors.

1.3. Molecular determinants of astrocytic fate

In vivo experiments allowed also to uncover some of the molecular mechanisms underlying astrocytic differentiation. Many growth factors were proposed to regulate astrogliogenesis. Eliminating genes encoding for the epidermal growth factor (Sibilia et al., 1998), the fibroblast growth factor receptor (Vaccarino et al., 1999) or gp130 (Nakashima et al., 1999) diminished the pool of astrocytes in transgenic mice. There is evidence for a role of neurogenin (Ngn) 1 and 2 as crucial factors determining neurogenic versus gliogenic fate. The transcription factors *Id*1 and *Id*3 are expressed in zones and at times of gliogenesis and inhibit

the activity of the *Ngn*1 promoter (Nakashima et al., 2001). High levels of *Ngn*1 during the neurogenic period (around E14) promoted neuronal differentiation and inhibited differentiation towards astrocytes by sequestering the CBP/p300 complex from STAT (Sun et al. 2001). Phosphorylation of the latter was shown to be induced by different astrogenic factors including CNTF-, LIF- or BMP and appears to be the main regulator of astrogliogenesis (He et al., 2005). The cellular source of the different external factors regulating astrocyte generation is not clear though.

1.4. Astrocytes turnover in the adult brain

There is increasing evidence that neurons and astrocytes are generated in the adult brain (Kempermann et al., 2004; Emsley and Macklis, 2006). Whereas neurogenesis is restricted to specific brain regions, astrocytes appear to be generated throughout the CNS. Adult born astrocytes were detected throughout the CNS with double immunolabelling against BrdU and astrocytic markers 7 days after after single BrdU injection. The analysis of turnover of S100β- or Gfap-population revealed that ca. 10% of astrocytes are labeled with BrdU (Emsley and Macklis, 2006).

In the adult hippocampus, radial type glial cells were shown to act as precursors of both glia and neurons and differentiation of both was reported to occur at similar rates (Steiner et al., 2004). Conflicting results exist concerning the survival of newly generated astrocytes in adult brain. Steiner et al. (2004) reported the disappearance of BrdU-, S100β-double positive cells within 4 weeks, whereas another study reported relatively stable pool of BrdU/Gfap-double positive cells (Rietze et al., 2000).

Despite some conflicting data, these results indicate a turnover of astrocytic population in the adult brain.

2. MORPHOLOGY OF ASTROCYTES

The name "astrocyte" implies a star-shaped appearance, but in fact, the morphology of what we call now astrocytes varies widely ranging from protoplasmic cells with myriads of finely branching processes radiating from the soma to the sleek radial appearance of Bergmann glia or Muller cells (Reichenbach et al., 1992; Wolff and Chao, 2004).

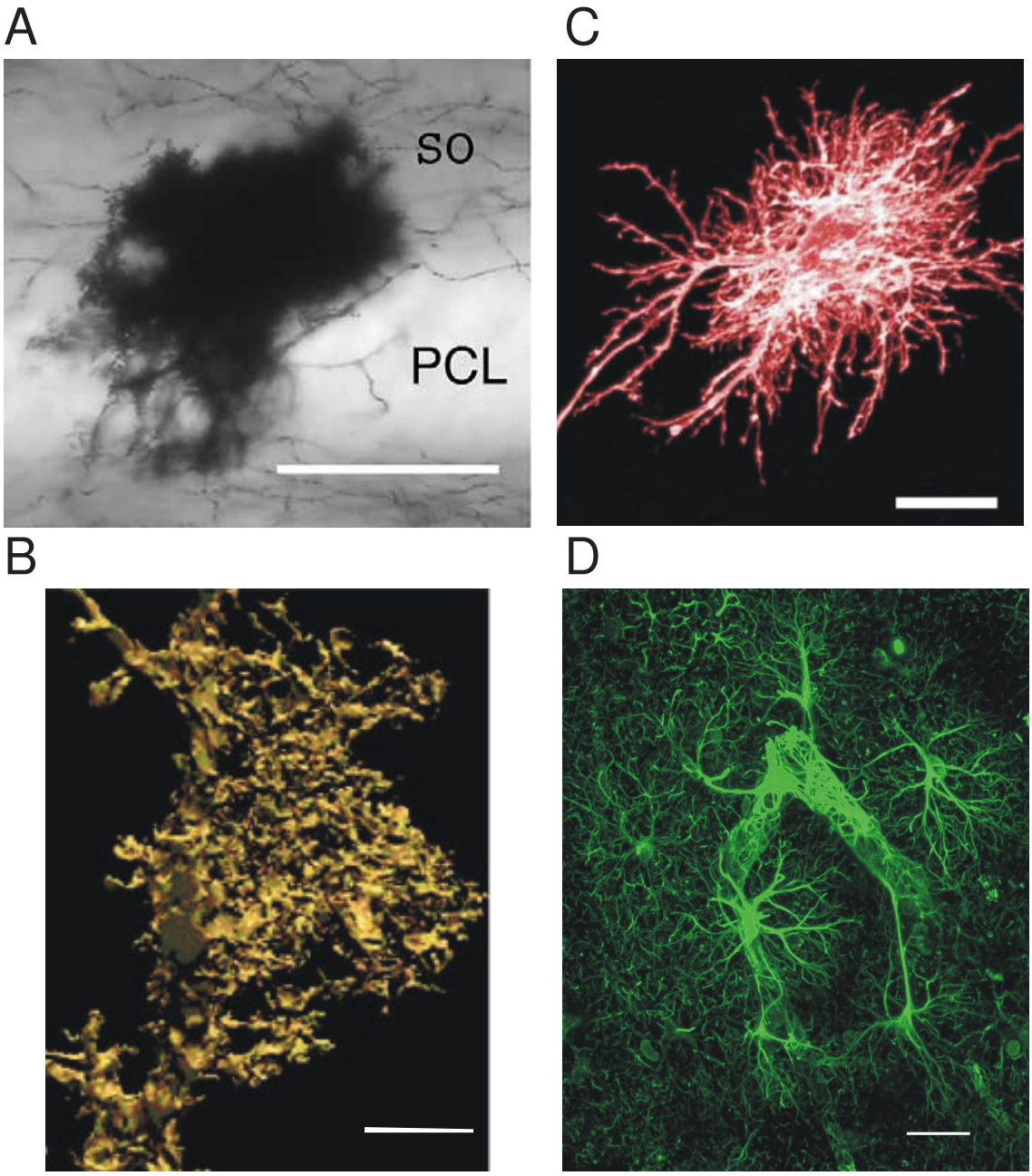

Fig. 1. Morphological diversity of astrocytes.
A. Bright field micrograph of Golgi-labeled astrocyte from mouse hippocampus (Ogata and Kosaka, 2002). B. Three-dimensional z-stack reconstruction from ultrathin sections analyzed with electron microscopy of single Bergman glia process from mouse cerebellum (Grosche et al., 1999). C. The z-stack reconstruction of rat hippocampal astrocyte after gene gun transfer of dye-coding vector (Benediktsson et al., 2005). D. The z-stack reconstruction of 25 µm-thick section of mouse cortex immunolabeled against Gfap (Z. Soltys, with permission). Scale bars: A, 50µm, B, 5µm, C, 20µm, D, 25 µm.

2.1. Approaches to study the morphology of astrocytes

The first identification of astrocytes was achieved in silver chromate (Golgi) impregnated tissue. The characteristic star-shaped cells were recognized as a distinct population of cells, and named "astrocytes" by Mihaly von Lenhossek (Verkhratsky, 2006). The discovery of Gfap in the 1970s, which was supposed to be an astrocytic marker, allowed for extensive studies of their morphology under different conditions (Eng et al., 2000). Electron microscopy and dye-filling revealed their extreme ramification in fixed tissue (Grosche et al., 1999; Ventura and Harris, 1999; Bushong et al., 2002). Examples of morphological appearances of astrocytes obtained with different staining methods are presented in Fig. 1.

Finally, the discovery of astrocyte-specific dyes (Nimmerjahn et al., 2004), viral targeting (Benediktsson et al. 2005) and development of transgenic mouse models (Benediktsson et al., 2005; Hirrlinger et al., 2004) together with *in vivo* imaging allowed visualization of astrocytic morphology in the living brain tissue. Simultaneous time-lapse analysis of neurons and astrocytes marked with different fluorescent proteins revealed that astrocytic protrusions were more mobile than dendritic ones (Haber et al., 2006; Nishida and Okabe, 2007). The motility of their protrusions has been shown to depend on the actin cytoskeleton, since it was inhibited by cytochalazin-D (Haber et al., 2006) and by expression of a dominant-negative form of Rac1 (Nishida and Okabe, 2007).

2.2. Organization of astrocytes in the brain

The average density of astrocytes varies strongly between CNS regions, with the average value 80-100 cells/mm^2 (Emsley and Macklis, 2006). In the hippocampus astrocytes occupy distinct domains and show very little overlap with neighboring astrocytes (Bushong et al., 2002). This parcellation of the hippocampal volume by individual astrocytes may be the result of space economy, but may also have functional consequences, as each astrocytic domain may represent a functional unit, somewhat similar to cortical columns. Thanks to intracellular dye injections, single or closely apposed pairs of astrocytes have been labelled recently in the CA1 region of rat hippocampus. These studies revealed that a single astrocyte covers with its processes up to 66,000 μm^3 (Bushong et al., 2002). Comparing this value with the density of synapses in the neuropil, one can estimate that a single astrocyte contacts up to 140,000 synapses. An electron microscopic study revealed that in the CA1 area of rat hippocampus, about 60% of synapses are ensheated by astrocytes (Ventura and Harris, 1999) with a preferential localization of their processes next to the postsynaptic side (Witcher et al.

2007). Nearly every astrocyte has also at least one contact with blood vessels (Bushong et al., 2002). Gfap-positive processes contact arterioles with a diameter of more than 8 μm, whereas Gfap-negative processes contact capillaries (Simard et al., 2003). The functional consequences of this arrangement will be discussed in following chapters.

Astrocytes are coupled via gap junctions and form a syncytium (Giaume and McCarthy, 1996). Gap junctions are formed by connexin (Cx) hemichannels, with a very restrictive pattern of expression (Rash et al. 2001a). Astrocytic junctions are composed of Cx26, Cx 30 and Cx43 (Rash et al. 2001b). The coupling by gap-junctions may represent a morphological basis for astrocytic functions, such as potassium buffering and homeostatic processes (see below). Glial syncytium may regulate the three-dimensional shapes of neurons (Denis-Donini et al., 1984) and the volume of larger brain structures such as cortical columns (Steindler, 1993).

2.3. Approaches formalizing the morphological description of astrocytes

Astrocytes show a wide range of morphologies and have been described as “bushy”, “stellate”, “velate”, “fibrous” and many other terms (Emsley and Macklis, 2006). Since these diverse forms may also reflect functional diversity and since morphological changes may be connected to complex processes or define disease states, such vocabulary appears inadequate and a more formal description appears desirable. So far, there are only few attempts to transform images of ramified astrocytes to meaningful numbers, which is prerequisite for their quantitative description and modelling – an issue that is underestimated in biological sciences (Lazebnik, 2002). One approach involves measurements of fractal dimensions (Mandelbrot, 1982), which allows to define the space-filing capacity of the cell. Such measurements were done on different cell types, including astrocytes (Reichenbach et al., 1992) and it was concluded that the morphology of astrocytes is coupled to their role as potassium buffering cells (Reichenbach et al., 1992).

3. ELECTROPHYSIOLOGICAL PROPERTIES OF ASTROCYTES

Currently, the defining electrophysiological properties of mature astrocytes are a negative membrane resting potential (-70 to -85mV), coupling via gap junctions, expression of glutamate transporters and the absence of action potentials.

The ability of neurons to propagate action potentials in very short time is at the basis of brain function. Astrocytes and other types of glial cells do not have this property, hence they were originally thought not to play a role in complex brain function. Within the last years, however, electrophysiologically distinct subpopulations of astrocytes have been identified. A crucial requirement to define their electrophysiological properties is their identification during or after the recording. This has been achieved by the injection of bio-compatible dyes like biocytin and analysis of their morphology, occasionally coupled to post-recording immunohistochemistry or electron microscopy.

Initial patch-clamp recordings from cultured astrocytes extracted from white matter suggested the presence of sodium and calcium channels in astrocytes (Barres et al., 1988; 1990). Analysis of hippocampal sections from P10-P12 mice identified four subgroups of glial cells based on the current profile, as well as morphological and ultrastructural criteria, but without the final proof of their cellular identity (Steinhauser et al., 1992). Further studies on hippocampal astrocytes described “outward rectifiying” and “variable rectifying” currents in freshly isolated cells from P7 to P15 rats (Zhou and Kimelberg, 2000), or “complex”, “inward rectifiers” and “linear cells” in acute slices from P23-30 rats (D'Ambrosio et al., 1998). Astrocytes were also subdivided based on the resting potential: a subset at -70 mV and another one at –45mV (D'Ambrosio et al., 1998; McKhann et al., 1997). This classification was further shown to depend on the presence of distinct potassium channels, with Kir channels defining the first, and ether-a-go-go channels the second phenotype (Emmi et al., 2000).

A new classification of hippocampal astrocytes emerged from studies on hGfap-EGFP transgenic mice, where Gfap-positive cells are fluorescently labelled. Here, two main subpopulations were identified: GluR cells, expressing AMPAR-mediated currents, but no glutamate transporter currents (identical to earlier “complex” cells), and GluT cells, expressing exclusively transporter currents, but not AMPA receptors (“passive” cells) (Matthias et al., 2003). This categorization also predicted the level of hGfap promoter activity. Weak promoter activity occured in GluR cells, whereas strong activity was observed in GluT cells. Evidently, these studies focused only on Gfap-positive astrocytes, and so the

properties of astrocytes, which lack this marker, but still represent a considerable fraction depending on the brain region, were not studied.

A detailed study on the electrophysiological phenotypes of "complex" astrocyte-like cells from rat hippocampus at different stages of development revealed that outwardly or variably rectifying, Glast-positive cells are dominant in early postnatal development, whereas in adult brain there was a clear segregation between variably rectifying, NG2-positive cells, and passive, Glast-positive cells (Zhou et al., 2006). Since a subpopulation of GluR cells was reported to express NG2 (Matthias et al.., 2003) and the NG2-positive cells were suggested to be separate population of glial cells (synantocytes, Butt et al., 2002; polidendrocytes, Nishiyama, 2007), it is possible that many observations concerning GluR cells (or "complex" astrocytes) concerned in fact NG2-positive polidendrocytes.

4. ASTROCYTE FUNCTION

4.1. Roles of astrocytes in neuronal development

There is evidence from studies on different culture preparations that astrocytes produce a broad spectrum of neurotrophic factors, essential for neuronal growth and survival, like CNTF, GDNF, BDNF, LIF, PDGF, FGF and NT-3 (Davies, 1998). Apart from peptide factors, also lipids were shown to have neurotrophic action. Thus oleic acid, whose synthesis and release are promoted by blood-derived albumin, promotes neuronal growth (Medina and Tabernero, 2002). On the other hand, the existence of neurotoxic, astroglia-derived factor(s) was suggested. Although the factor(s) itself is not yet identified, it was shown to induce neuronal apoptosis *in vitro* , possibly by the inhibition of $GABA_A$- or glycine receptors (Hans et al., 2002). In addition, another unidentified factor from astrocytes extracted from neonatal rat brain was shown to inhibit *in vitro* the proliferation of neocortical precursor cells (de Lima and Voigt, 1999).

In the developing brain immature glial cells regulate neuronal survival and differentiation. In the adult brain this function may be exerted by astrocytes. Two studies investigated the astrocytic control of adult neurogenesis. Astrocytes (Gfap, S100β-positive cells) from the subventricular zone (SVZ) or from the cortex of early postnatal mice induced neurogenesis of SVZ progenitors *in vitro* (Lim and Alvarez-Buylla, 1999), whereas astrocytes isolated from adult rat hippocampus stimulated neurogenesis of progenitors from the subgranular layer of the dentate gyrus (Song et al., 2002a; Song et al., 2002b). The astrocytic potential to induce this process appeared restricted to particular regions, since

spinal cord astrocytes failed to stimulate neurogenesis from SGL progenitors. Song et al. (2002a) showed also that so far unknown soluble and membrane-bound factors mediated the astrocytic effect. One possible factor could be neurogenesin1, a neurogenic factor that appears secreted by astrocytes and dentate granule cells (Ueki et al., 2003).

It remains controversial, whether astrocytes regulate adult neurogenesis or give rise to neuronal progenitors. De-differentiation of astrocytes towards a radial glia phenotype – a putative progenitor of adult born neurons – was demonstrated in a transplantation model (Leavitt et al., 1999). Aditionally, Gfap-positive progenitors were shown to be the main source of new neurons in adult brain (Garcia et al. 2004). The lack of markers that differentiate between astrocytes and adult neuronal progenitors from neurogenic regions precluded so far a detailed study of the relationships between both populations *in vivo* .

4.2. Astrocytic influence on synaptogenesis

There is increasing evidence that astrocytes influence the formation of synapses, a crucial phase during brain development (Slezak and Pfrieger, 2003). First direct evidence for such an effect was reported in a study on immunoisolated retinal ganglion cells (Pfrieger and Barres, 1997), which showed that glial cells strongly increased the level of synaptic activity in these neurons. Subsequent studies on the same culture preparation showed that astrocytes enhanced the formation of glutamatergic synapses (Nagler et al., 2001; Ullian et al., 2001) by promoting dendritogenesis (Goritz et al., 2005). A study on immunoisolated hippocampal and cerebellar neurons from postnatal mice revealed, however, that neurons in these preparations formed excitatory and inhibitory synapses in the absence of glial cells (Steinmetz et al., 2006).

Apart from effects on synapse number, glial signals also enhanced the pre- and postsynaptic efficacy of synapses formed by RGCs (Nagler et al., 2001; Steinmetz et al., 2006) and by hippocampal and cerebellar neurons (Steinmetz et al., 2006). Studies on cultures derived from embryonic mice provided evidence for glial participation in inhibitory synapse formation. Glia-conditioned medium enhanced synaptic localization of $GABA_A$ receptors, the number of presynaptic terminals and the frequency of mIPSC in hippocampal cultures and the postsynaptic effects required neurotrophin signaling (Elmariah et al., 2005). The discrepancy between results obtained by Steinmetz et al. (2006) and Elmariah et al. (2005) may be explained by differences in culture conditions and in the age of animals, from which neurons were obtained.

Two of the molecules that mediate the glial influence on synapses development in RGCs were identified. Cholesterol, which is released from astrocytes via lipoproteins, was necessary for dendrite differentiation (Goritz et al., 2005) and the formation of synapses (Mauch et al., 2001) and thrombospondin was shown to promote formation of synapses by inducing the apposition of pre- and postsynaptic sites (Christopherson et al., 2005). Expression of thrombospondin-1 was enhanced by ATP via activation of astrocytic P2Y receptors (Tran and Neary, 2006), which suggests a possible link between purinergic signalling and glia-induced synaptogenesis. The exact mechanisms by which both signals promote synapse formation remains unknown. Cholesterol is a precursor for neurosteroids and recent studies indicate that astrocyte-derived estrogen increased the number and activity of synapses in cultured neonatal cortical neurons (Hu et al., 2007).

Apart from soluble factors, direct astrocyte-to-neuron signalling may also instruct synaptogenesis. In a special hippocampal coculture system integrin-mediated contact with astrocytes induced synapse formation and this effect was not mimicked by soluble factors (Hama et al., 2004).

The suggestion from *in vitro* studies that the synaptogenic effect of astrocytes may result at least in part from action on dendrites (Goeritz et al., 2005) is supported by recent studies of hippocampal slices employing advanced genetics and imaging techniques. Newly formed dendritic protrusions that contact with astrocytes had a longer lifetime than those without contact (Haber et al. 2006; Nishida and Okabe 2007). In addition, contact to astrocytes promoted the probability of spine formation from a dendritic protrusion and this effect involved ephrin/Eph receptor signaling, as interference with ligand or receptor abolished these effects (Nishida and Okabe, 2007).

4.3. Astrocytes role in potassium buffering

Potassium buffering is one of the best documented physiological roles of astrocytes with good evidence for its relevance *in vivo* . The activity-induced rise of extracellular potassium depolarizes neurons and undermines their excitability. Therefore, fast removal of excess potassium is crucial for normal brain function. Two main mechanisms were proposed to achieve this goal: net uptake or spatial buffering. Astrocytes were shown to perform both.

Net uptake of potassium can be realized by ion pumps and transporters: Na^+/K^+-ATPase, $Na^+/K^+/2Cl^-$-cotransporter or cooperation between K^+ and Cl^- channels to restore the electrochemical gradient. Pharmacological blockade of neuronal and glial Na^+/K^+/ATPase results in inhibition of potassium clearance, as measured with a potasium-sensitive electrode,

after neuronal stimulation in the hippocampal slices from P30 rats (D'Ambrosio et al., 2002). The role of astrocyte-specific $Na^+/K^+/2Cl^-$-transporter in the uptake of potassium was confirmed in the isolated rat optic nerve, where neuronal stimulation resulted in astrocyte swelling, which could be abolished by specific inhibitors of this transporter (MacVicar et al., 2002).

The mechanism of spatial buffering was proposed already by Orkand in 1966. It was shown that glial elements of amphibian optic nerve take up potassium at the site of neuronal activity and release it elsewhere. To accomplish spatial buffering two conditions must be fulfilled: the resting membrane potential of the cell should match the Nernst potential of potassium to allow for sensitive detection of the extracellular potassium concentration and the cell should be member of a syncytium (Kofuji and Newman, 2004). It is well known that astrocytes meet these conditions, but only recent experiments have brought final proof for the relevance of this mechanism *in vivo* .

Spatial buffering has best been described for Muller cells in the retina, where it is also called potassium siphoning (Newman et al., 1984). Muller cells do not form syncytia, but span throughout from the subretinal space to the inner surface of the retina, where their endfeet form the inner limiting membrane and contact the vitreous humour. Measurements of potassium conductance across Muller cells revelead an uneven distribution with 94% of the total conductance at the endfeet (Kofuji and Newman, 2004; Newman et al., 1984). The main potassium channel subtype responsible for this effect is Kir 4.1, whose subcellular distribution matches the conductance density (Kofuji et al., 2000). Genetic ablation of Kir4.1 in mice decreases Muller cell conductance by 10-fold (Kofuji et al. 2000) and the impaired potassium uptake by Muller cells leads to imbalance of osmotic homeostasis (Kofuji and Newman 2004).

In other parts of the CNS potassium buffering has also been demonstrated. Spatial buffering was shown in rat cortical slices (Holthoff and Witte, 2000), although a glial participation in this process remained unproven. An elegant study on mouse hippocampal slices provided direct evidence for a role of astroglial coupling in potassium buffering. Cell-type specific elimination of two main astrocytic gap junction proteins, Cx43 and Cx30, caused a complete uncoupling of the astrocytic syncytium and enhanced the actvity-induced rise of extracellular potassium and slowed its decay. Moreover, the expected rise of extracellular potassium at a distant region was much smaller in mutant mice. Together, these findings favour the hypothesis that astrocytes play a crucial role in spatial buffering (Wallraff et al., 2004). The contribution of water transport to potassium buffering was indicated by the

observation that animals lacking α-syntrophin, the protein responsible for assemble of Kir4.1 and AQP4, leads to mislocalization of AQP4 and two-time slower potassium clearance than wildtype mice following stimulation of hippocampal slices (Amiry-Moghaddam et al., 2003).

4.4. Astrocytic influence on neuronal activity

4.4.1. Calcium signaling

An important finding in the field of glial biology was the discovery of calcium-based communication in astrocytes. In 1990 Smith and coworkers (Cornell-Bell et al., 1990) made two important observations following application of glutamate to cultured astrocytes. First, this induced repetitive, transient increases in the intracellular calcium concentration (calcium transients) and second, these calcium transients propagated to neighbouring cells over hundreds of micrometers at 19 μm/s (calcium waves) (Cornell-Bell et al., 1990).

4.4.1.1. Calcium transients as a mode of signal processing in astrocytes

Subsequent studies have shown that also physiological stimuli induce intracellular calcium transients in astrocytes. This was shown in rat hippocampal slices after stimulation of Schaffer collaterals (Porter and McCarthy, 1996; Pasti et al., 1997) and cholinergic afferents (Araque et al., 2002), in Bergmann glia after stimulation of parallel fibers (Grosche et al., 1999), in retinal Muller cells as response to light flashes (Newman, 2005) and finally in the barrel cortex of living mice after whisker stimulation (Wang et al., 2006). The basic mechanism of calcium transients in astrocyte relies on activation of mGluR-induced activation of PLC, hydrolysis of phospholipids to DAG and IP_3, with the latter releasing calcium from IP_3-dependent internal calcium stores (Scemes, 2000). Since astrocytes express G-protein coupled receptors similar to mGluRs for most, if not all, neurotransmitters (Porter and McCarthy, 1997), other transmitters as well as hormones can induce calcium transients (Verkhratsky et al., 1998; Fiacco and McCarthy, 2006).

Although it has been shown that calcium transients in astrocytes are evoked by physiological stimulation, it remains unclear, whether they contribute to brain function. So far, there is evidence that calcium transients fulfill some of the criteria that appear necessary for this. First, the size and pattern of calcium transients follows the simulus intensity. In hippocampal slices, for example, stimulation of Schaffer collaterals led to single calcium spikes, to spikes followed by plateaus, or to oscillatory patterns, depending on the frequency of activating stimulus (Pasti et al., 1997). It was also reported that joint AMPAR and mGluR

stimulation in rat hipoccampal slices was much stronger in evoking glial calcium oscillation than stimulation of either receptor alone (Bezzi et al., 1998, Fig. 2).

A recent study indicates that astrocytes are able to differentiate between different synaptic inputs. In slices from rats, hippocampal astrocytes responded to glutamate originating from Schaffer collaterals, but not to glutamate from alveus axons, although they responded to acetylcholine released from the latter (Perea and Araque, 2005). Moreover, simultaneous stimulation of glutamatergic and cholinergic inputs to hippocampal astrocytes lead to non-linear enhancement of calcium transients suggesting intracellular integration of incoming stimuli (Perea and Araque, 2005). Recent studies provided further evidence for integration of inputs from different neurotransmitters including glutamate and ATP (Beierlein and Regehr, 2006; Piet and Jahr, 2007). Interestingly, a form of memory for synaptic activity in astrocytes is suggested by the observation that calcium oscillations induced by repetitive stimulation of Schaffer collaterals lasted up to 3 hours (Pasti et al., 1997). Another key requirement that calcium transients contribute to brain function is that they generate an output signal that feeds back on neuronal activity. Evidence for this will be presented in chapter 5.

4.4.1.2 Calcium waves

Several mechanisms have been proposed to mediate the intercellular propagation of glial calcium waves, including diffusion of IP_3 through gap junctions (Venance et al., 1995), through secreted factors (Hassinger et al. 1996), namely ATP (Guthrie et al., 1999), or a combination of both, namely ATP release from connexin hemichannels (Cotrina et al., 1998, Fig. 4). However, a technical aspect may have influenced the interpretation of results, since agents used in earlier studies to block gap junctions were recently shown to antagonize P2X7 receptors, whereas the latter was also reported as the main pathway of ATP release from astrocytes (Suadicani et al., 2006).

So far, the intercellular propagation of calcium transients was mainly observed in cultured astrocytes. In more intact preparations, the rise of intracellular calcium appears restricted to single cells, with rare examples of transmission to neighboring astrocytes (Fiacco and McCarthy, 2004; Sul et al., 2004; Takano et al., 2006; Wang et al., 2006). It is possible that calcium waves occur only *in vitro* or during development (Parri et al., 2001), in specialized regions, like retina (Newman and Zahs, 1997), or under pathological conditions (Basarsky et al., 1998). The use of genetically coded calcium indicators (Miyawaki et al., 1999; Heim et al., 2007) appears as a promising new tool to resolve the physiological significance of calcium waves.

In the following, I will summarize evidence that astrocytes feed back on neurons and influence their electrical and synaptic activity.

4.4.2. Calcium-dependent “gliotransmitter” release.

There is now good evidence that astrocytes release neuromodulatory substances and that this release is induced by intracellular calcium transients. In initial studies, bradykinin-induced calcium transients led to the release of glutamate from cultured rat astrocytes (Parpura et al., 1994). Calcium-induced glutamate release was later shown in hippocampal slices in response of stimulation of Schaffer collaterals (Pasti et al., 1997) as well as *in vivo* in the somatosensory cortex after whisker (Takano et al., 2006; Wang et al., 2006) or forepaw stimulation (Zonta et al., 2003).

The dependence on calcium, together with the detection of components of the SNARE complex in astrocytes suggested that glutamate may be released by vesicular exocytosis (Parpura et al., 1995; Pfrieger and Barres, 1996). Experimental support for this idea was obtained within the last decade. In brain slices, glutamate release from astrocytes could be blocked by tetanus toxin, which cleaves synaptobrevin/VAMP2 (Schiavo et al., 1992), a component of the exocytotic machinery. Small vesicles containing components of the SNARE-complex have been detected in astrocytes from developing and adult rat hipoccampal slices using electron microscopy coupled to immunogold labeling (Bezzi et al., 2004; Jourdain et al., 2007). Time-lapse imaging revealed punctate release of glutamate from stimulated rat astrocytes in culture (Bezzi et al., 2004; Montana et al., 2004; Kang et al., 2005). Vesicular release was also shown for other substances including ATP (Coco et al., 2003; Pascual et al., 2005) and D-serine (Mothet et al., 2005). Interestingly, a recent study provided first evidence that astrocytes release different transmitters depending on the target neuron. In the rat olfactory bulb, astrocytes released GABA to induce hyperpolarization of mitral cells and they released glutamate or GABA onto granule cells, although it remains unclear, whether this was mediated by distinct processes of a single cell or by distinct astrocytes (Kozlov et al., 2006). Expression of a dominant-negative form of synaptotagmin-IV, a SNARE component that was suggested to be astrocyte-specific (Zhang et al., 2004) altered synaptic function in transgenic animals (Pascual et al., 2005), bringing the first *in vivo* proof that exocytotic release from astrocytes is crucial for neuron-to-neuron communication.

Apart from vesicular exocytosis, other modes of glutamate release from astrocytes have been proposed and experimentally proven. These include reverse action of glutamate transporters (in *in vivo* model of ischemia, Seki et al., 1999), connexin hemichannels (rat

astrocytes *in vitro* in divalent cation-free solution, Ye et al., 2003), P2X7 receptors (murine cortical astrocytes *in vitro* , Duan et al., 2003) and volume-sensitive anion channels (rat astrocytes in culture in hypotonic conditions, Takano et al., 2005). Since these mechanisms were observed in artificial or pathological conditions, their physiological role awaits further confirmation.

4.4.3. Astrocytic influence on neuronal activity and synaptic transmission

Studies in the mid 90s proved for the first time that activation of astrocytes induces changes in neurons. Parpura et al. (1994) showed *in vitro* that calcium transients and glutamate release from astrocytes induces calcium transients in cocultured neurons. Similarly, Nedergaard (1994) observed a rise of calcium in neurons cultured on an astrocytic monolayer after electrical stimulation of a single astrocyte. Finally, Pasti et al. (1997) reported AMPA- and NMDA-dependent rise in intracellular calcium in neurons following stimulation-induced calcium oscillations in astrocytes (Pasti et al., 1997). Some of mechanisms presented below are summarized in Fig. 2.

Direct effects of astrocytes on synaptic transmission have been shown by several groups. In a first study, Araque and colleagues observed that glutamate released from astrocytes reduced the magnitude of action potential-evoked EPSC and IPSC in cocultured neurons by acting on presynaptic mGluR, therefore diminishing the probability of transmitter release (Araque et al., 1998a). Additionally, astrocyte-derived glutamate was shown to increase the frequency of mEPSCs and mIPSCs by acting on extrasynaptic NMDA receptors (Araque et al., 1998b). Astrocyte-derived glutamate was also shown to enhance spontaneous transmitter release by activation of extrasynaptic mGluR1 receptors in mouse hippocampal slices (Fiacco and McCarthy, 2004). A more detailed study corroborated a presynaptic action of astrocyte-derived glutamate (Jourdain et al., 2007). These authors revealed in hippocampal slices that NMDA receptors located on nerve terminals can be activated by glutamate released from vesicle-containing astrocytic processes, which in turn leads to an increase of neurotransmitter release (Jourdain et al., 2007, Fig. 2).

First evidence for a postsynaptic action of astrocyte-derived glutamate came from an *in vitro* study. It showed that mechanically-induced calcium-dependent glutamate release evoked slow inward currents (SICs) in cocultured neurons (Araque et al., 1998b). Neuronal

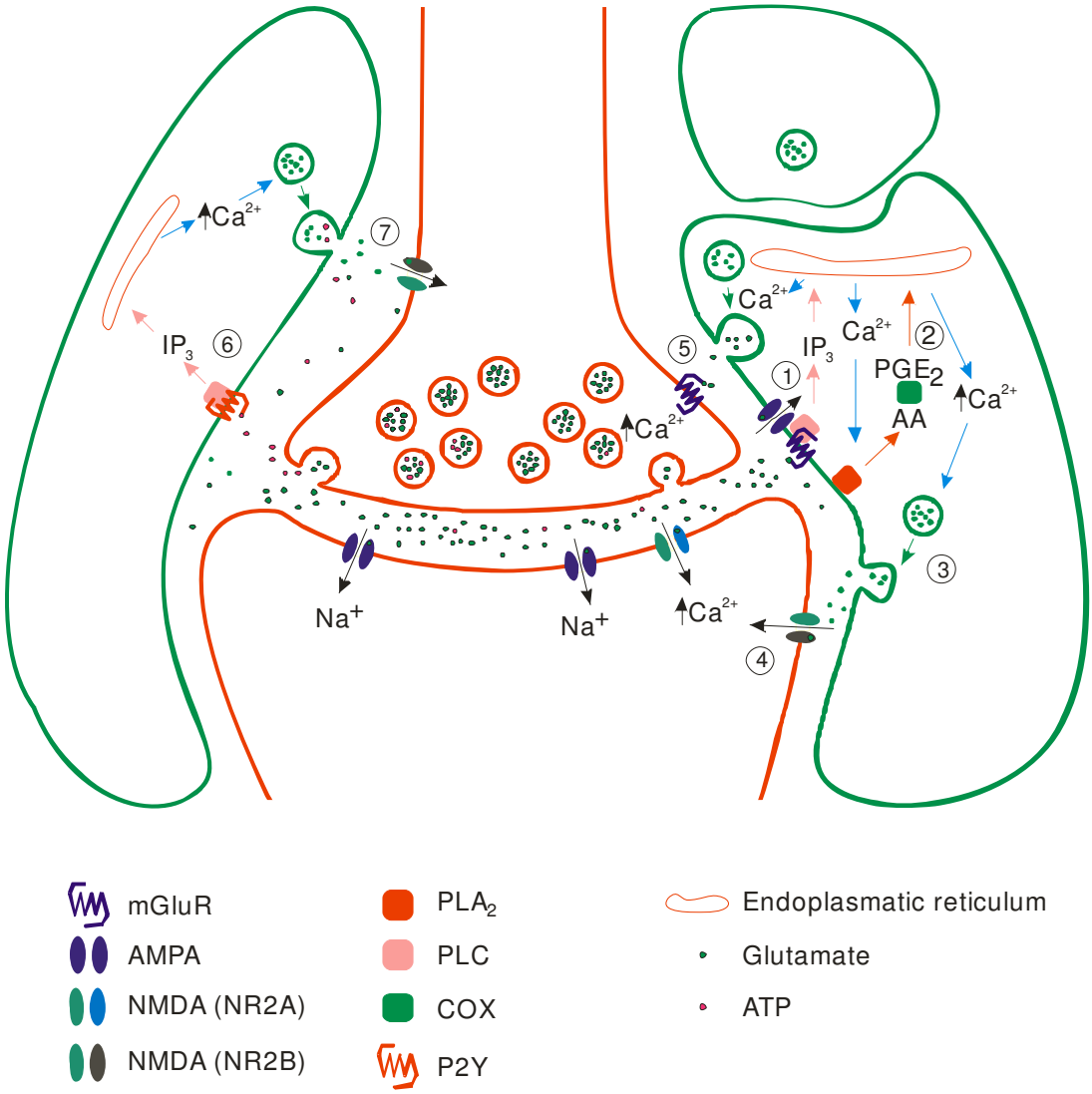

Fig. 2. Schematic representation of interactions between astrocytes and glutamatergic synapses.

(1) Neurons release glutamate that activates astrocytic glutamate receptors AMPA and/or mGluR5 and induces a transient increase in intracellular calcium concentration in astrocytes. (2) This results in activation of cyclooxygenase pathway and production of PGE_2 that amplifies the calcium transient. (3) The latter may lead to vesicular release of gliotransmitters, including glutamate that (4) activates postsynaptic NMDA receptors bearing NR2B subunit or (5) activates presynaptic mGluR receptors changing the calcium concentration in presynaptic terminals and thus the release efficacy. (6) Activity-dependent ATP release may activate astrocytic P2Y receptors that (7) leads to release of glutamate activating presynaptic NR2B-bearing NMDA receptors.

SICs due to calcium-dependent glutamate release from astrocytes were subsequently observed in slices from different brain regions and confirmed to be mediated by extrasynaptic NMDA receptors (Angulo et al., 2004; Fellin et al., 2004; Kang et al., 2005; Perea and Araque, 2005; D'Ascenzo et al., 2007; Fig. 2). Further experiments showed that astrocyte-induced, NMDA-dependent SICs depolarize postsynaptic neurons and thus enhance their excitability (Fellin et al., 2006a; Fellin et al., 2006b). These results were recently questioned by a study on transgenic mice expressing an exogenous ligand-activated metabotropic receptors specifically in astrocytes (Fiacco and McCarthy, 2007). Here, ligand-evoked calcium transients in astrocytes from hippocampal slices did not raise the neuronal calcium level modulate mEPSCs or induce neuronal SICs (Fiacco and McCarthy, 2007), but this approach has limitations including the timing of calcium transients as well as their spatial restriction that do not allow for a definite answer.

On the other hand, there is evidence that astrocytic release of glutamate modulates the activity of inhibitory neurons. In hippocampal slices, electrical stimulation of astrocytes was sufficient to increase the frequency of mIPSCs (Kang et al., 1998) and evoked IPSCs (Liu et al., 2004) in a glutamate-dependent manner, probably via activation of kainate receptors on interneurons (Liu et al., 2004). Astrocytes were also shown to induce slow outward currents in inhibitory mitral cells in the olfactory bulb (Kozlov et al., 2006) by releasing GABA.

Another way how astrocytes can modulate synaptic transmission is by the release of D-serine. This amino acid binds to the glycine binding site of NMDA receptors (Mothet et al., 2000), is produced selectively by astrocytes (Wolosker et al., 1999) and is released in a calcium-dependent, vesicular mode (Mothet et al. 2005). A tonic level of D-serine allows for NMDA-mediated transmission, whereas its enzymatic degradation reduces the NMDA component of EPSCs in the hippocampus (Mothet et al., 2000; Yang et al., 2003), hypothalamic supraoptic nucleus (Panatier et al., 2006) and in the retina (Stevens et al., 2003).

Recently, evidence is growing on the role of the ATP as the gliotransmitter. In the retina, for example, light-stimulated glutamate release from neurons and activation of mGluR on Müller glia causes a calcium-dependent release of ATP. ATP is subsequently hydrolyzed to adenosine and lowers the firing rate of retinal ganglion cells (Newman, 2004). Moreover, studies indicate that ATP released by astrocytes participates in a homeostatic control mechanism that ensures high fidelity synaptic transmission. Application of an A1 adenosine receptor antagonist to hippocampal slices increased basal synaptic transmission and this was overcome by inhibition of exonucleotidase activity, which in turn induced inhibition of transmission via P2Y purinergic receptors (Coco et al. 2003; Zhang et al. 2003; Pascual et al.

2005). Notably, blockade of vesicular release from astrocytes also abolished the tonic inhibition (Pascual et al., 2005). On the other hand, inhibition of glial glutamate transporters revealed that in the absence of neuronal activity NMDA currents may be tonically active (Angulo et al., 2004). Hence, astrocytes may regulate the basal level of activity by releasing ATP and by regulating the ambient glutamate.

Finally, there is evidence that astrocytes modulate activity-dependent changes in synaptic transmission. In hippocampal slices, tetanus stimulation of Schaffer collaterals leads to long term potentiation of synapses in stimulated pathway. NMDA receptors play a crucial role in long-term potentiation and application of the enzyme that degrades D-serine blocked long-term potentiation in hippocampal slices (Yang et al., 2003). An elegant study on slices from the rat supraoptic nucleus revealed that lactation-induced retraction of astrocytic processes reduced the ambient level of D-serine around synapses and thereby converted long-term potentiation to long-term depression (Panatier et al., 2006). LTP is accompanied by decrease in neurotransmitter release from neighboring synapses (Manzoni et al., 1994). This phenomenon, known as heterosynaptic depression, is abolished in transgenic animals with impaired vesicular released from astrocytes (Pascual et al., 2005). The mechanism was analysed in more detail by Serrano et al. (2006), who showed that activity-dependent interneuronal release of GABA activates $GABA_B$ receptors on astrocytes, which in turn induce calcium-dependent release of ATP. The hydrolysis product adenosine inhibited distal presynaptic neurons via A1 receptors (Serrano et al., 2006, Fig. 3).

A recent study showed that astrocytes may play a role in so-called synaptic scaling. This is an activity-dependent homeostatic mechanism where the number of receptors in postsynaptic membrane is dynamically regulated in order to maintain excitability of neurons. It has been shown that glia-derived TNFα, which regulates AMPA receptor density (Beattie et al., 2002), mediates the upregulation of hippocampal synapses in response to chronic block of electrical activity (Stellwagen and Malenka, 2006). The latter example supports the general idea that astrocytes play a role in long-term processes in the brain, which are necessary to maintain neuronal function (Slezak et al., 2006).

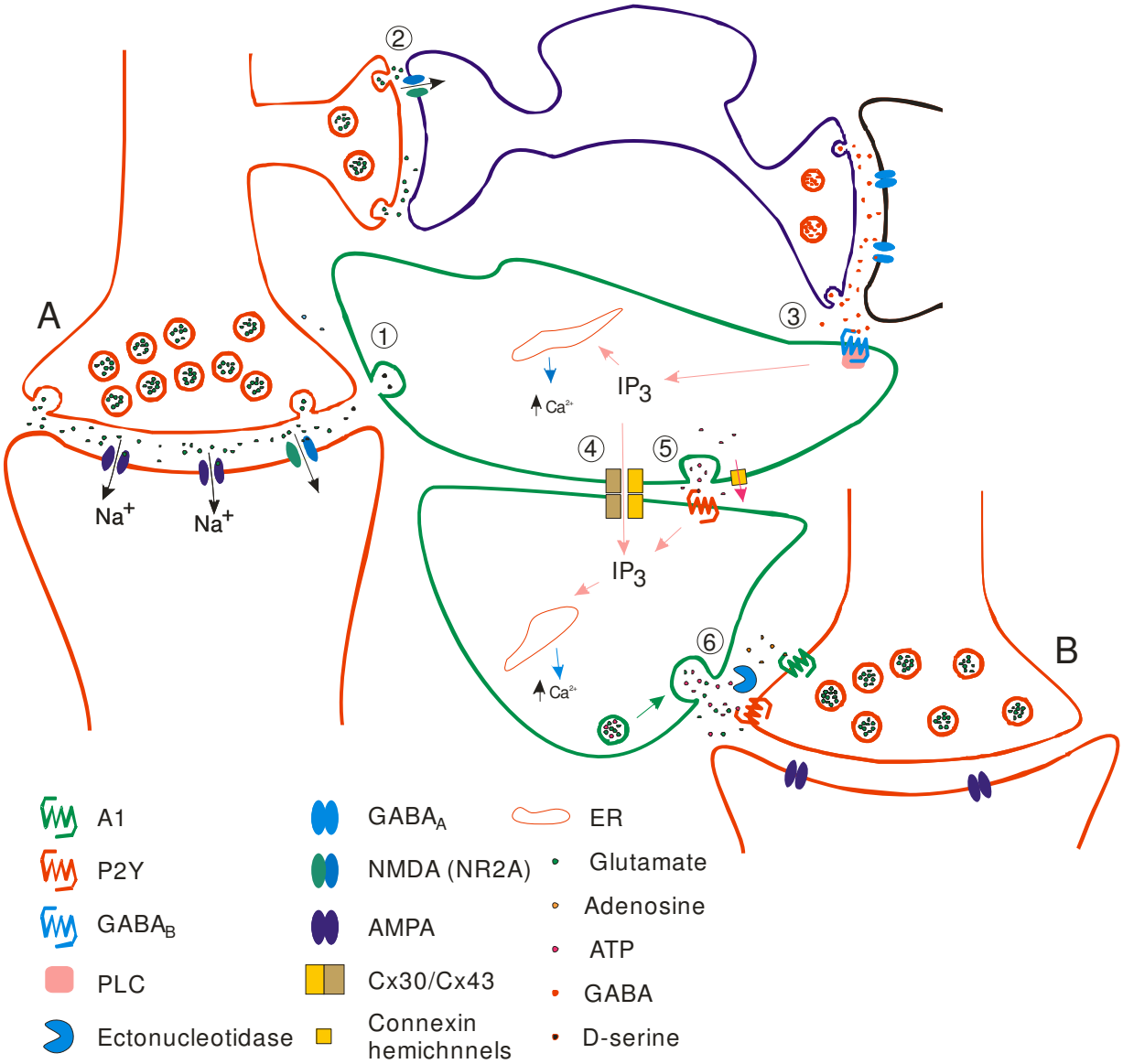

Fig. 4. **Astrocytic modulation of neuronal network: heterosynaptic depression as example.**
Tetanic stimulation of synapse A induces LTP, that depends on (1) glia-derived D-serine. In parallel (2) NMDA-dependent activation of interneurons leads to (3) release of GABA, that acts on astrocytic $GABA_B$ receptors. Activation of calcium transient in astrocyte may propagate to neighboring cells via (4) gap-junctions or (5) ATP release, resulting in (6) release of ATP that is hydrolyzed to adenosine that acts on distal synapse B, inhibiting neurotransmitter release from presynaptic terminals.

4.5. Role of astrocytes in glutamate homeostasis and brain energy balance

Some of mechanisms described in this chapter are summarized in Fig. 4.

4.5.1. Glutamate homeostasis

One of the best-described functions of astrocytes is to remove excess glutamate, the main neurotransmitter in the CNS, from the synaptic cleft and to replenish the transmitter pool of glutamate in presynaptic terminals of glutamatergic neurons.

Astrocytes are well-equipped to maintain the extracellular concentration of glutamate. High-affinity glutamate transporters allow to accumulate intracellular glutamate up to 10,000-fold compared to extracellular concentration (Bergles and Jahr, 1998, Maragakis and Rothstein, 2006). Two proteins are responsible for astrocytic uptake of glutamate: Glast (glutamate/aspartate transporter, EAAT1, Slc1a3; Storck et al., 1992) and GLT-1 (EAAT2, Slc1a3; Pines et al., 1992; Danbolt, 2001). Their astrocytic localization was confirmed in rodents by in situ hybridization, immunohistochemistry and electron microscopy (Rothstein et al. 1994; Furuta et al., 1997; Voutsinos-Porche et al., 2003a). The transporter-mediated inward current in astrocyte was found to faithfully reflect the synaptic activity of neighbouring neurons, and it was therefore used to measure the latter in rat hippocampal slices (Diamond et al., 1998). The crucial role of astrocytic transporters for the clearance of extracellular glutamate was confirmed *in vivo* using administration of antisense oligonucleotide (Rothstein et al., 1996) and in knock-out animals (Tanaka et al., 1997). The lack of glutamate transporters resulted in a significant increase of ambient glutamate levels in the brain causing motor impairment, as well as spontaneous seizures and increased glutamatergic excitotoxicity.

Glutamate taken up by astrocytes is converted at least in part to glutamine (Fig. 3). Expression of the enzyme that catalyses this reaction, glutamine synthetase, was shown to be restricted to astrocytes (Derouiche and Rauen, 1995). Pharmacological blockade of glutamine synthetase results in depletion of neuronal glutamate and a rise in astrocytic glutamate concentration (Hertz and Zielke, 2004). Glutamine is released from astrocytes by glia-specific glutamine transporters, mainly SN1 (system N, Broer et al., 2004) and taken up by neurons by neuron-specific glutamine transporters (Liang et al., 2006, Fig. 3). This cycle of glutamate uptake and glutamine release, also called glutamate-glutamine shuttle, allows for resupply of the neurotransmitter to neurons (Daikhin and Yudkoff, 2000). An alternative source of glutamate for neurons is de novo synthesis from glucose. This process occurs exclusively in

astrocytes, since neurons lack pyruvate carboxylase, which is a crucial enzyme in this pathway (Waagepetersen et al., 2001).

4.5.2. Metabolic coupling

The human brain constitutes around 2% of body weight but utilizes as much as 20% of total energy (Magistretti and Pellerin, 1999). Although these numbers may differ between species, efficient energy supply to brain cells is key for all animals. Theoretical considerations on glutamatergic transmission suggest that most of the energy is spent on action potential generation and postsynaptic receptor signalling (Attwell and Laughlin, 2001). The rest is used to sustain the resting membrane potential (Na^+/K^+/ATPase), protein synthesis and calcium signaling.

If glutamatergic transmission is such an energy expensive process, then glutamate itself or glutamate-dependent signaling molecules should regulate energy supply. Indeed, glutamate uptake was shown to activate glucose uptake, glycolysis and the production of energy metabolites for neurons. The original concept derived from *in vitro* studies postulated the following cascade (Pellerin and Magistretti, 1994): glutamate uptake in astrocytes leads to an increase in sodium ions, which then activate Na^+/K^+/ATPase. The latter is coupled to enzymes of the glycolytic pathway so that activation of Na^+/K^+/ATPase results in increased aerobic glycolysis. This in turn stimulates production of lactate, which may be released from astrocytes and taken up by neurons, which utilize it as energy source (Pellerin and Magistretti, 1994, Fig. 3).

Support for the idea that astrocytes are a source of energy for neurons came from a study of hippocampal slices using multiphoton microscopy, where activity-induced depression of the neuronal NADH signal (i.e. increase of oxidative metabolism) was followed by a slower (>10s) increase in the signal from astrocytic compartments (Kasischke et al., 2004). The role of astrocytic glutamate transporters in these hypotheses was corroborated by the observation that astroglial cultures derived from Glast-deficient mice showed a 60% reduction in lactate release in response to application of glutamate (Voutsinos-Porche et al., 2003b). Moreover, the same study proved that the influx of Na^+ ions, that normally accompanies Glast-mediated glutamate uptake, was necessary and sufficient to initiate glycolysis in astrocytes (Voutsinos-Porche et al., 2003b).

The induction of glucose uptake by glutamate uptake was shown directly in cultured astrocytes (Loaiza et al., 2003). Physiologically, this process requires the communication of astrocytes with blood vessels, and is presented in the next chapter.

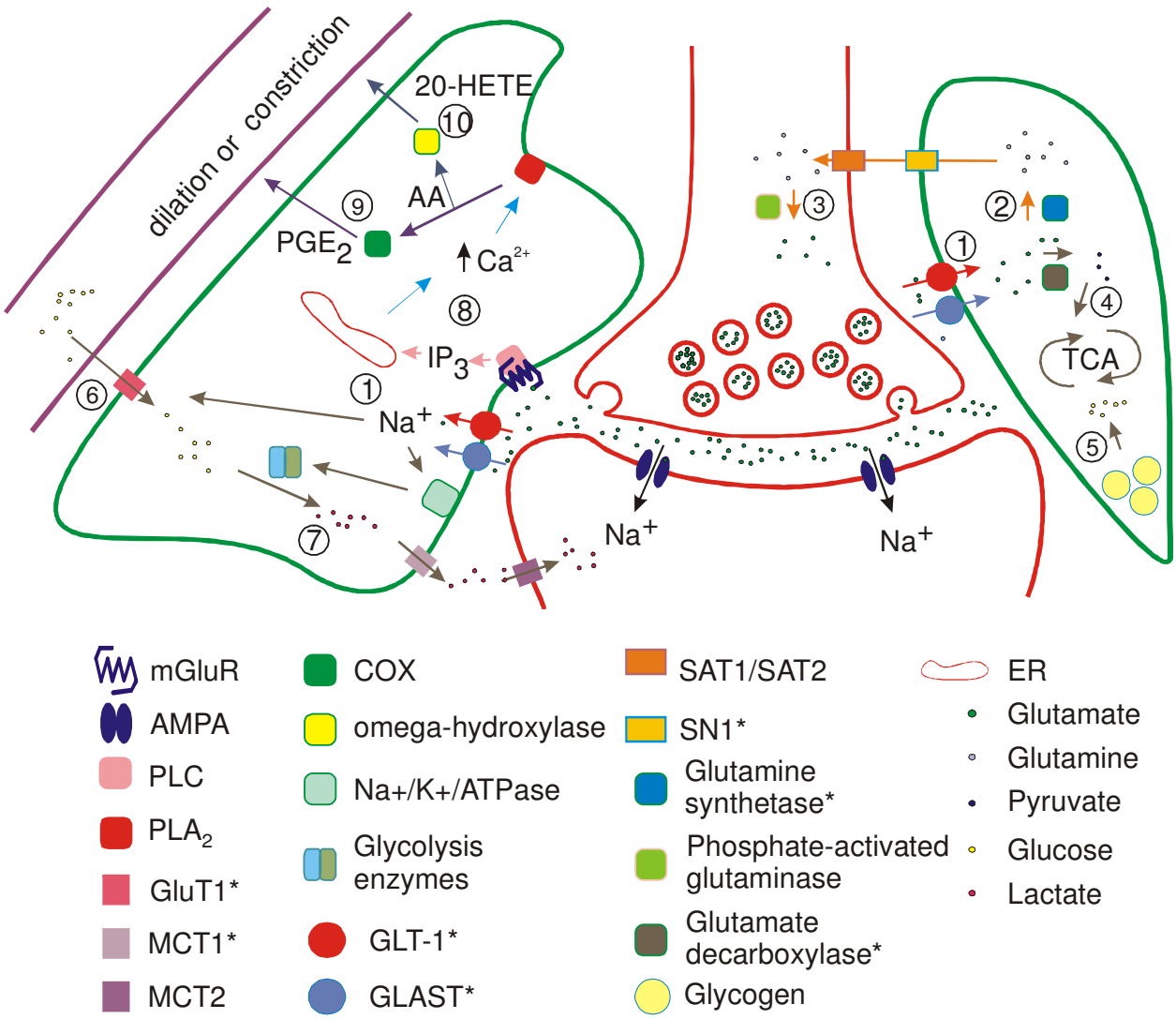

Fig. 4. Schematic representation of astrocytes role in couplic gluatamatergic synapse activity with brain energy metabolism.
(1) Glutamate uptake by astrocytic glutamate transporters leads to activation of metabolic cascades in astrocytes. (2) Glutamate may be aminated by glutamine synthetase, and (3) delivered back to neurons as glutamine. (4) After decarboxylation glutamate may enter the TCA cycle. (5) Glutamate uptake may activate glycogenolysis and (6) activate glucose uptake from blood, followed by glycolysis and (7) production of lactate, which is delivered to neurons as energy source via monocarboxylate transporters. (8) Glutamate uptake and/or activation of glial mGluR receptors may change the blood flow, via activation of calcium-dependent enzymes synthetising vasoactive factors including COX-2 (9) and ω-hydrolase (10). Asterisks indicate astrocyte-specific components.

4.5.3. Neurovascular coupling.

Ultimately, brain cells acquire glucose and oxygen from blood. Consequently, increased local neuronal activity should enhance local cerebral blood flow, a phenomenon known as functional hyperemia.

The arrangement of astrocytes around blood vessels (see 2.2) provoked the hypothesis that they are involved in the local regulation of blood flow (Raichle, 1998; Magistretti et al., 1999). Recent studies provide clear evidence for this hypothesis. In cortical slices, stimulation of neuronal afferents leads to vasodilation that is preceded by an increase in intracellular calcium concentration in astrocytes contacting blood vessels (Zonta et al., 2003a; Zonta et al., 2003b). The use of specific pharmacological agents showed that both events are dependent on activation of mGluRs. The authors concluded that neuronal glutamate induced calcium transients by activation of glial mGluRs, which then stimulated the production of vasodilating agents. The signals responsible for this effect were identified as cyclooxygenase products (Zonta et al., 2003a; Zonta et al., 2003b). Surprisingly, using a similar preparation a second study showed that uncaging of astrocytic calcium causes vasoconstriction (Mulligan and MacVicar, 2004). The pathway involved in calcium-dependent production of arachidonic acid, which in turn stimulated the release of vasoconstricors, such as 20-HETE from endothelial cells or smooth muscle (Mulligan and MacVicar, 2004). The opposing findings may be explained by differences in preparations. Another recent study revealed that uncaging of calcium in mouse cortical astrocytes *in situ* induces vasodilation with a short (0.6 s) delay after increase in astrocytic $[Ca^{2+}]_i$ (Takano et al., 2006). Taken together, there is now evidence that neuronal activity-dependent synthesis of vasoactive factors in astrocytes participates in the control of cerebral blood flow.

5. TRANSGENIC APPROACHES TO STUDY THE ROLE OF ASTROCYTES *IN VIVO*

As stated above, most of the data on the role of astrocytes for brain function and development are derived from *in vitro* or *in situ* studies. Verification *in vivo* requires appropriate models, which were scarce at the beginning of my thesis.

5.1. Conventional "knock-outs" of astrocyte-specific genes

Several genes were reported to be expressed exclusively in astrocytes in the CNS, including Gfap (Brenner and Messing, 1994), Glast (Chaudhry et al., 1995), GLT-1 (Furuta et al., 1997), glutamine synthetase (Sonnewald et al., 1993), connexin 30 (Rash et al., 2001a),

connexin 43 (Rash et al., 2001a), Kir 4.1 (Kofuji et al., 2000), Aqp4 (Rash et al., 1998), S100β (Ogata and Kosaka, 2002). For these genes, conventional gene elimination by homologous recombination in embryonic stem cells and creation of transgenic mice should result in a loss of function in astrocytes. As mentioned in previous chapters, knockouts of these genes caused pathological conditions like epileptic seizures and neurodegeneration and thus illustrated the importance of astrocytes *in vivo* .

Despite these advances, conventional knockouts have two important drawbacks that need to be taken into account. First, the function of these genes is lost at the moment when they are normally expressed. Hence, eventual developmental defects may influence the adult outcome. Second, the gene of interest may have an essential function in other types of cells, possibly even outside the brain. Therefore a loss of function outside the brain may hamper an analysis of brain-specific defects. An example for this is Cx43, a gap junction component, which in the brain is selectively expressed by astrocytes (Rash et al., 2001a). Knockout of Cx43 results in early death of animals due to the malformation of the heart (Eckardt et al., 2004). To overcome these limitations, experimental models for cell-type specific and temporally controlled gene manipulation have been established.

5.2. Cell-type specific gene ablation

Recombinases from bacteriophage P1 (Cre recombinase, Sauer and Henderson, 1988) and from baker yeast (flippase, Flp; Sadowski, 1995) were used to develop gene ablation in transgenic animals (Cre: Lakso et al., 1992; Orban et al., 1992; Gu et al., 1994); Flp: Dymecki, 1996). Both enzymes catalyze the homologous recombination of DNA fragments that are flanked by their respective recognition sites (loxP for Cre, frt for Flp). In the following, I will focus on the Cre/loxP system. The outcome of Cre-mediated recombination depends on the orientation of the loxP sites. Cre activity may result in excision, if they are situated in the same direction, inversion, if inversely oriented, or translocation, if only single loxP sites occur in each DNA strand (Van Duyne, 2001). To use this system for gene targeting, two independent transgenic lines are necessary. First, a line where expression of Cre recombinase is driven by a cell-specific promoter and second, a line where essential exons of the gene of interest are flanked by loxP sites. In double transgenic mice, the gene will be excised from genomic DNA in cells expressing Cre recombinase.

5.3. Inducible gene ablation

To allow for temporal control over gene ablation and thus to avoid uncontrolled developmental defects, mainly embryonic lethality of gene deficiency, inducible versions of recombinases were established. To accomplish this, mutated versions of ligand binding domains (LBDs) of specific steroid receptors, which bind only non-endogenous ligands like tamoxifen or RU486, were fused to Cre recombinase, resulting in $CreER^{T}$ (Metzger et al., 1995). $CreER^{T2}$ (Feil et al., 1996), iCre (Shimshek et al., 2002), MerCreMer (Verrou et al., 1999), CrePR (Kellendonk et al., 1996; Wunderlich et al., 2001). In these models, the fusion protein stays in the cytoplasm due to the binding of heat shock proteins. Application of exogenous ligand leads to the dissociation of the latter, therefore enabling the translocation of recombinase to the nucleus, where it exerts its action.

5.4. Genetic targeting of astrocytes

5.4.1. Cellular specificity of transgene expression

The most extensively used way to target astrocytes engaged the human (Brenner et al., 1994) or mouse (Mucke et al., 1991) version of the Gfap promoter. The use of reporter proteins suggested that in the adult brain these promoters drive astrocyte-specific expression of lacZ (Mucke et al., 1991; Brenner et al., 1994), GFP (Zhuo et al., 1997) or EGFP (Nolte et al., 2001). Subsequent studies revealed, however, a few limitations of the Gfap promoter. First, a detailed analysis of transgenic mice that employed the mouse and human version revealed that both of them drive the expression of transgenes in neurons (Su et al., 2004). This observation undermined the value of studies using Gfap promoters to drive astrocyte-specific expression of transgene, where this fact was unsufficiently verified. Second, both promoter versions are active at an early embronic stage, before astrocytes are born. At this stage, however, neuronal progenitors are Gfap-positive (Malatesta et al., 2003). This observation is of particular interest for studies using Cre recombinase, since once active, it leads to the excision of the flanked gene in the progenitor, hence its progeny also lacks the gene. Indeed, studies on hGfap-Cre or mGfap-Cre transgenic mice confirmed that the majority of neurons underwent Cre mediated recombination during their development (Zhuo et al., 2001; Malatesta et al., 2003; Casper and McCarthy, 2006). This again questions studies where astrocyte-specific elimination of genes was undertaken with this system (Marino et al., 2000; Bajenaru et al., 2002; Uhlmann et al., 2002; Garcia et al., 2004) and stressed the necessity to verify cell-specific elimination of the gene of interest post factum.

In summary, at the beginning of my thesis, there were no transgenic models for inducible gene ablation in astrocytes in the adult brain.

5.4.2. Strategies of transgene delivery

Expression of transgene may be achieved in a few ways. The most popular method is the use of a construct carrying a short, cell-type specific promoter, followed by gene to be expressed and regulatory sequences. Few limitations are inherently connected with this approach: the position effect variegation, since short constructs may stay under the control of surrouding DNA sequences; a lack of eventual regulatory sequences responsible for cell-specific expression in minimal promoters; the necessity of screening large number of transgenic lines due to variability of transgene expression between lines and due to inefficient germline transmission of these constructs (Giraldo and Montoliu, 2001).

Another mode is targeted insertion of the transgene to the defined endogenous locus (knock-in). This allows the external gene to be regulated by natural promoter elements, which should assure faithful and efficient gene expression. This approach may however suffer from the accompanying heterozygousity of the endogenous gene, since one of its allele is replaced with transgene.

A recently developed approach using bacterial artificial chromosome (Shizuya et al., 1992) as the transgene carrier was reported to avoid limitations related to previous approaches (Heintz et al., 2001). It is based on the use of large (up to 250 kb) fragments of mouse genomic DNA, that are cloned to bacteria. The existence of an efficient method to target defined locus in the BAC (Lee et al., 2001), as well as subsequent succesfull generation of transgenic mice with modified BAC (Yang et al., 1997) prompted us to use this method for the generation of transgenic lines.

AIMS AND GENERAL APPROACH

The goal of this project was to establish new transgenic mouse lines that allow for inducible gene ablation in astrocytes. We planned to generate a series of transgenic lines that target defined subpopulations of astrocytes and allow for a comparative approach to study astrocyte function in the brain.

To achieve these goals we decided to use advanced tools from molecular genetics. The spatiotemporal control of genetic manipulation should be accomplished by the CreER^{T2}/loxP system. This enables the Cre recombinase-mediated excision of any gene that is flanked by loxP sites. Temporal control is achieved by the dependency of CreER^{T2} activity on the exogenous ligand tamoxifen. To direct recombinase activity to astrocytes, Cre transcription was controlled by regulatory sequences of different genes with well-established expression in astrocytes including apolipoprotein e (Apoe), aquaporin-4 (Aqp4), connexin-30 (Cx30), glial fibrillary acidic protein (Gfap) and glia-specific glutamate transporter (Glast).

To improve the chances for faithful regulation of CreER^{T2} by these promoters, transgenesis constructs were made of bacterial artificial chromosomes (BACs) containing genomic mouse DNA. This method was shown to enable specific and efficient transgene expression.

MATERIALS AND METHODS

1. GENERATION OF TRANSGENESIS CONSTRUCT

BACs (CHORI, Oakland, USA) were purified using the NucleoBond® BAC 100 kit (Macherey-Nagel) following the manufacturer's instructions. The concentration of BAC DNA was verified based on absorbance at 260/280 nm using a spectrophotometer (Beckman, DU640).

Promoter	BAC code	Region upstream (Kbp)	Region downstream (Kbp)	Total length (Kbp)	Transgenic lines
ApoE	RP24-294K20	65	73	140	T54-29
Aqp4	RP24-374B16 (RP23-189N2)	30 38	123 141	155 181	T55-8 T55-27 T55-30
Cx30	RP24-368M7	123	40	165	T53-15 T53-33
Cx30	RP23-213N5	45	52	99	T56-7
Gfap	RP24-155G1	100	50	159	T46
Glast	RP23-63O21	30	90	201	T45-5 T45-30 T45-52 T45-57 T45-72

Table 1. Summary of BAC clones used in the study. Numbers indicate the approximate size surrounding the ATG starting codon of the given gene and the total length of the BACs

1.1 Modification of the Cre expression cassette

To attach homology arms to the Cre expression cassette, PCR primers were designed to amplify regions in the BACs that surround the ATG codon of each gene using Primer3 (Rozen and Skaletsky, 2000). Although efficient recombination can be achieved by homology arms as short as 50 bp (Muyrers et al., 1999), previous experience advised on the use of longer (200-300 bp) sequences (D. Metzger, personal communication). Each primer contained restriction sites that are also contained in the pC17 plasmid (see below) located 6 bp from the 5'-end (XXX-LF, -LR, -RL, -RR primers, see Table 2 for sequences of all primers used in this study, Table 3 for the localization of respective primers with regard to ATG).

1	GLRHAf	5’-TCTACTTAAGCATTGTGGGTGAGTCGTTTG-3’
2	GLRHAr	5’-TCAAGGCCGGCCCACCGGAGAGCGTTTATCTC-3’
3	GLLHAf	5’- ATGCGTCGACAAATGTGGGTGCTTGGTCTC-3’
4	GLLHAr	5’-TCTACCTAGGAGGAATTTATCACGTCCTTGC-3’
5	CxLHAf	5’-ATGCGTCGACGTGAAAGGCGCGGTTATTAT-3’
6	CxLHAr	5’-ACTACCTAGGCGTGCAGGCTTATTCTTAAAC-3’
7	CxRHAf	5’-TAAGCTTAAGACCAGCATAGGGAAGGTGTG-3’
8	CxRHAr	5’-TGTAGGCCGGCCACCTTCTGCCGTTTGATGTC-3’
9	ApoLHAf	5’-ATGCGTCGACGAGGGAGCTGGAATTTTTGG-3’
10	ApoELHAr	5’-ACAACCTAGGTCTTCGCAATTGTGATTGG-3’
11	ApoERHAf	5’-AACACTTAAGTGGTCACATTGCTGACAGG-3’
12	ApoERHAr	5’-ACAAGGCCGGCCGGAATTGGCTCTCTCCTTC-3’
13	Aqp4LHAf	5’-AAGCGTCGACGCAGAGGAGAAGCAGAGGAA-3’
14	Aqp4LHAr	5’-ACAACCTAGGATCTCCCAAGCAGCCTCAG-3’
15	Aqp4RHAf	5’-ATCACTTAAGCAGGGACTGTTTCCTACCCA-3’
16	Aqp4RHAr	5’-AATAGGCCGGCCCTCAGCTGGGACAGTGTTGA-3’
17	GfaLHAf	5’-AAGCGTCGACGTCAACCCAGGCCTTTTGTA-3’
18	GfaLHAr	5’-ACAACCTAGGCGCAGAGGTGATGCGTCT-3’
19	GfaRHAf	5’-ATCACTTAAGTCCTTGTCTCGAATGACTCC-3’
20	GfaRHAr	5’-AATAGGCCGGCCCTGTGCAAAGTTGTCCCTCT-3’
21	GLFS1	5’-CTGTTTAGTTCAACCAGGCA-3’
22	GFFS1	5’-CCCCAGAGAGGACAGAGTT-3’
23	CxFS1	5’-TTTGCTGTGTTTTGTGGCTT-3’
24	ApoEFS1	5’-CCATCACAGTCCCCAAGTAA-3’
25	Aqp4FS1	5-AACTCTTTCATTGCGGGTA-3’
26	VN239	5’-CAAGGGACATCTTCCCATTC-3’
27	TK139	5’-ATTTGCCTGCATTACCGGTC-3’
28	TK141	5’-ATCAACGTTTTGTTTTCGGA-3’
29	QY74	5’-CACGCTTCAAAAGCGCACGT-3’
30	QY80	5’-ACCCAAGCGGCCGGAGAACC-3’
31	UN126	5’-CAAGGAGCCTCCTTTCTCTA-3’
32	RR189	5’-AAGCGCATGCTCCAGACTGC-3’
33	UN127	5’-CCTGCTCTACCTGGTGACTT-3’
34	VD23	5’-CGCCGACGGCACGCTGATTG-3’
35	VD24	5’-GTTTCAATATTGGCTTCATC-3’

36	AF97	5’-TCCAGACCATTGGCTTGAGTGCAGC-3’
37	AF98	5’-CTGGCGCTTCGCCAGCCATTACTGC-3’
38	CreF	5’-CCCAGGCTAAGTGCCTTCTCT-3’
39	CreR	5’-AAGCTGGATCGATAATGAGAACTTC-3’
40	beta-actinF	5’-ATCATGTTTGAGACCTTCAACAC-3’
41	beta-actinR	5’-TCTGCGCAAGTTAGGTTTTGT-3’
42	Cx30F	5’-GGTGGCGTGAACAAGCACTCT-3’
43	Cx30R	5’ CACCTTCTGCCGTTTGATGTC-3’
44	GLASTF	5’-TAAGTATCACAGCCACAGCCG-3’
45	GLASTR	5’-GAGTAGGGAGGAAAGAGGAG-3’
46	ApoEF	5’-CAGAGCTCCCAAGTCACACA-3’
47	ApoER	5’-GCGTATTTGCTGGGTCTGTT-3’
48	Aqp4F	5’-TTATGGTTCACGGGTTTGGATG-3’
49	Aqp4R	5’-AAAGCCACCATGATGCTC-3’

Table 2. Codes and sequences of primers used in this study

	LHAf	LHAr	Length of left homology arm	RHAf	RHAr	Length of right homology arm
ApoE	-241	-1	240	+45	+316	271
Aqp4	-394	-69	325	+196	+584	386
Cx30	-392	-1	391	+51	+377	326
GFAP	-362	-10	352	+64	+441	405
GLAST	-378	-13	365	+180	+498	318

Table 3. Position of 5’-ends of each primer used for the generation of homology arms and total length of homology arms. Numbers reflect relative position with regard to transcription initiation codon ATG (+1) of respective gene

Homology arms were amplified from respective purified BAC DNA by PCR using the following protocol (this was used in all subsequent PCR reactions, unless stated otherwise): PCR buffer (Sigma), 100 nM dNTP (Amersham), 0.3 mM $MgCl_2$ (Sigma), 0.75U of Taq polymerase (Sigma), 100 nM of corresponding primers in miliQ water in a final volume 25 µl. Two microliters of the respective BAC DNA (at 1 ng/µl) were added to all reactions, except for control samples, to which water or non-corresponding BAC DNA was added. The basic conditions for PCR reactions were: 1 cycle of denaturation (94°C, 5 min), 35 cycles of denaturation (94°C, 30s), annealing (55°C, 30s), elongation (72°C, 30s), followed by final

elongation (72°C, 7 min) and cooling to 4°C. Reactions were performed in a thermal cycler (GeneAmp®, PCR System 9700, Applied Biosystems). After amplification, PCR products were separated on 2% agarose gels to confirm the presence of the specific product. PCR products, which represent the homology arms, were precipitated by sodium acetate (0.3 M in 70% ethanol), spun down, washed in 70% ethanol and resuspended in miliQ water.
The plasmid pC17 (Fig. 5) is a derivative of pCre-ER^{T2}KI2Kan (Schuler et al., 2004). It contains Cre-ER^{T2} coding sequence isolated from pGS-CreER^{T2} (Indra et al., 1999) that is preceeded by a rabbit β-globin DNA segment encompassing intron 2 (β-globin intervening sequences, βGIVS). This ensures the correct open reading frame for the transcription of CreER^{T2}. Coding sequence of CreER^{T2} is followed by SV40 poly A signal to avoid transcription of regions following the CreER^{T2} coding sequence. Furthermore, there is a PGK/Tn5 promoter-driven neo selection cassette followed by polyA that is, flanked by frt sites. Finally, the plasmid contains a single SalI/AvrII site upstream of CreER^{T2} and a AflII/FseI site downstream of neo to allow for cloning of left and right homology arms, respectively.

Primer	Position	Direction	Region start	Detects	Used during
VN 239	843	counterclock	splicer	insertion of LHA	sequencing
TK 139	1438	clockwise	Cre	Cre sequence	genotyping
YM 110	1489	clockwise	Cre	Cre sequence	genotyping
SC 14	1733	counterclock	Cre	Cre sequence	genotyping
TK 140	1767	clockwise	Cre	Cre sequence	sequencing
TK 141	1768	counterclock	Cre	Cre sequence	genotyping
RJ 209	2366	clockwise	Cre	CreERT2 sequence	sequencing
TK 137	3045	clockwise	ERT2	ERT2 sequence	sequencing
OW 69	3288	counterclock	ERT2	ERT2 sequence	sequencing
QY 83	5074	clockwise	neo	neo, insertion of RHA	sequencing
QY 84	5075	counterclock	neo	neo, insertion of RHA	sequencing
QY 81	5216	clockwise	neo	neo, insertion of RHA	sequencing
TY 1	5663	counterclock	core	insertion of RHA	sequencing
RJ208	1466	counterclock	Cre	Cre sequence	in situ hybr.

Table 4. Primers used for sequencing of pC17, XXX-L, XXX-LR and for genotyping of transgenic animals. Position of annealing site, direction of sequencing, regions containing sequences recongnized by each primer are indicated

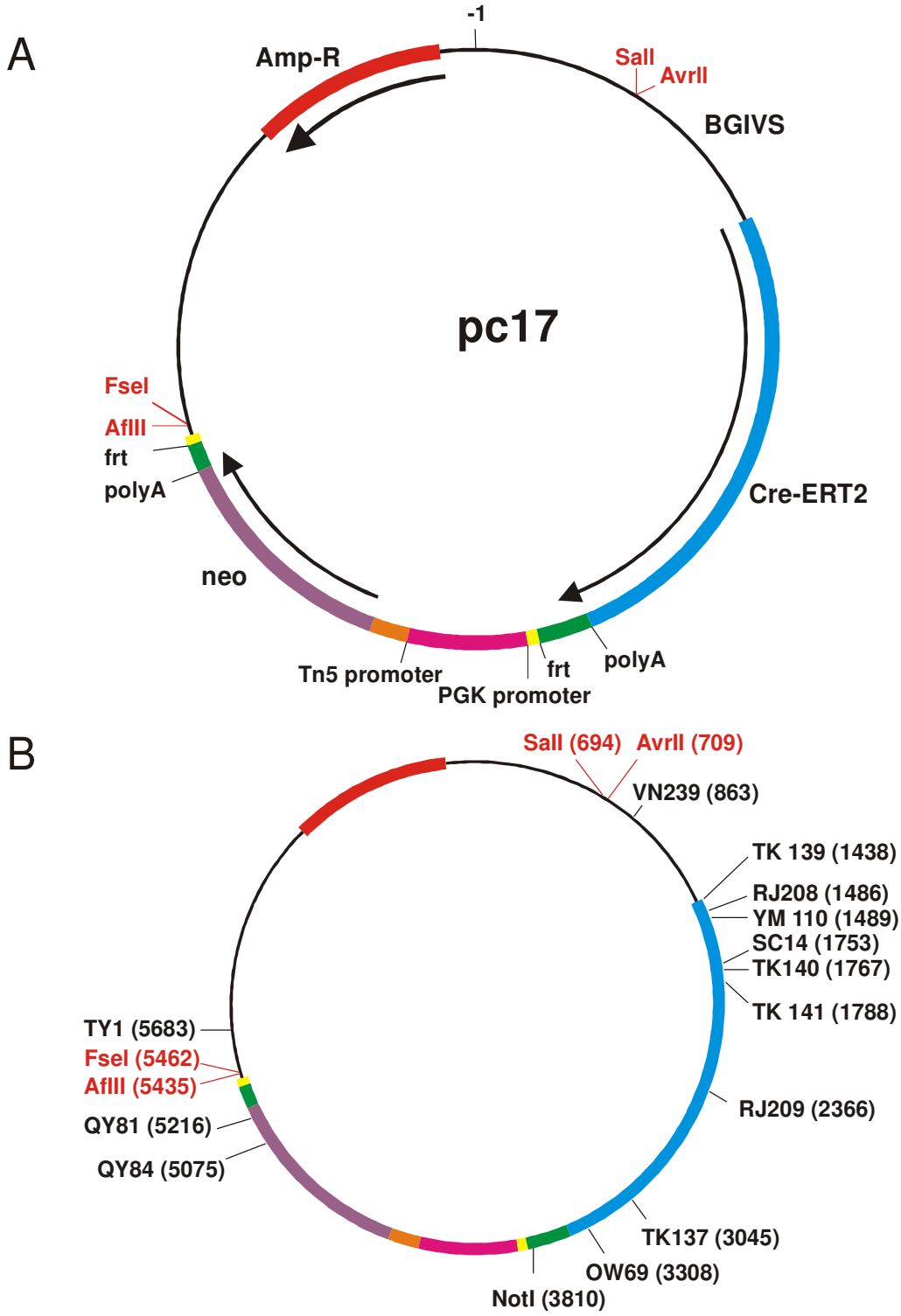

Fig. 5. Schematic representation of the CreER^{T2}-containing plasmid used for transgenesis

Localization of the most relevant components (A) and of sequences recognized by oligonucleotide probes (B) used for sequencing of the plasmid and for genotyping of transgenic lines. Numbers indicate the position of oligonucleotides in the plasmid.

Homology arms were first digested with enzymes recognizing 5'-located restriction sites (SalI for LHA, AflII for RHA) and then by enzymes recognizing 3'-located restriction sites (AvrII for LHA, FseI for RHA). The CreER^{T2} containing plasmid was digested with the same protocol. For each step, the digestion reactions contained: appropriate enzyme buffer (commercial buffers supported with respective enzyme), 5 µg of the DNA to be digested, 10U of respective enzyme and distilled water in a final reaction volume of 20 µl. After 1h of digestion at the appropriate temperature, DNA was precipitated with 0.3M sodium acetate and 70% ethanol, washed with 70% ethanol and resuspended in miliQ water. The concentration and size of digestion products was verified by running 1 µg of DNA in 2% agarose gels. Fragments were analysed using special software (Gene Construction Kit, GCK v.2.0, TextCo).

To attach homology arms to CreER^{T2} coding sequence, purified digested homology arms and plasmids were put together in the ligation reaction solution containing: ligase buffer (Epicentre), 0.4 mM ATP, 2U of ligase (Epicentre), 100 ng of digested homology arm and 20 ng of digested plasmid in a final volume of 10 µl. Ligation was performed at 16°C overnight. Reaction mixtures were then heated to 65°C to inactivate ligase. Subsequently, 1 µl of each reaction mix was electroporated to 40 µl of DH5 competent bacteria that were plated on ampicilin (20 µg/ml, Euromedex) selection plates. From positive clones, 24 were randomly selected, and 2 ml colonies were grown overnight. Then, MiniPreps were performed. Bacteria were spun down, and buffers P1 (50 mM Tris-HCl, pH 8.0; 10 mM EDTA), P2 (0.2M NaOH, 1% SDS) and P3 (3M potassium acetate) were subsequently added to perform alkaline lysis of bacteria. DNA was precipitated by 70% ethanol, washed in 70% ethanol and resuspended in 20 µl of distilled water. Insertion of the left homology arm was verified by EcoRI/PvuI digestion of pC17 and XXX-L plasmids. DNA fragments with expected size were subsequently sequenced (IGBMC Sequencing Service) using the VN239 oligonucleotide to verify correct orientation of left homology arms. Clones carrying correct plasmids were amplified and purified by MaxiPrep. One hundred ml colonies were grown overnight, spun down and DNA was extracted using the NucleoBond® PC100 Kit (Macherey-Nagel). Subsequently, XXX-L plasmids were digested with AflII, purified and digested with FseI.

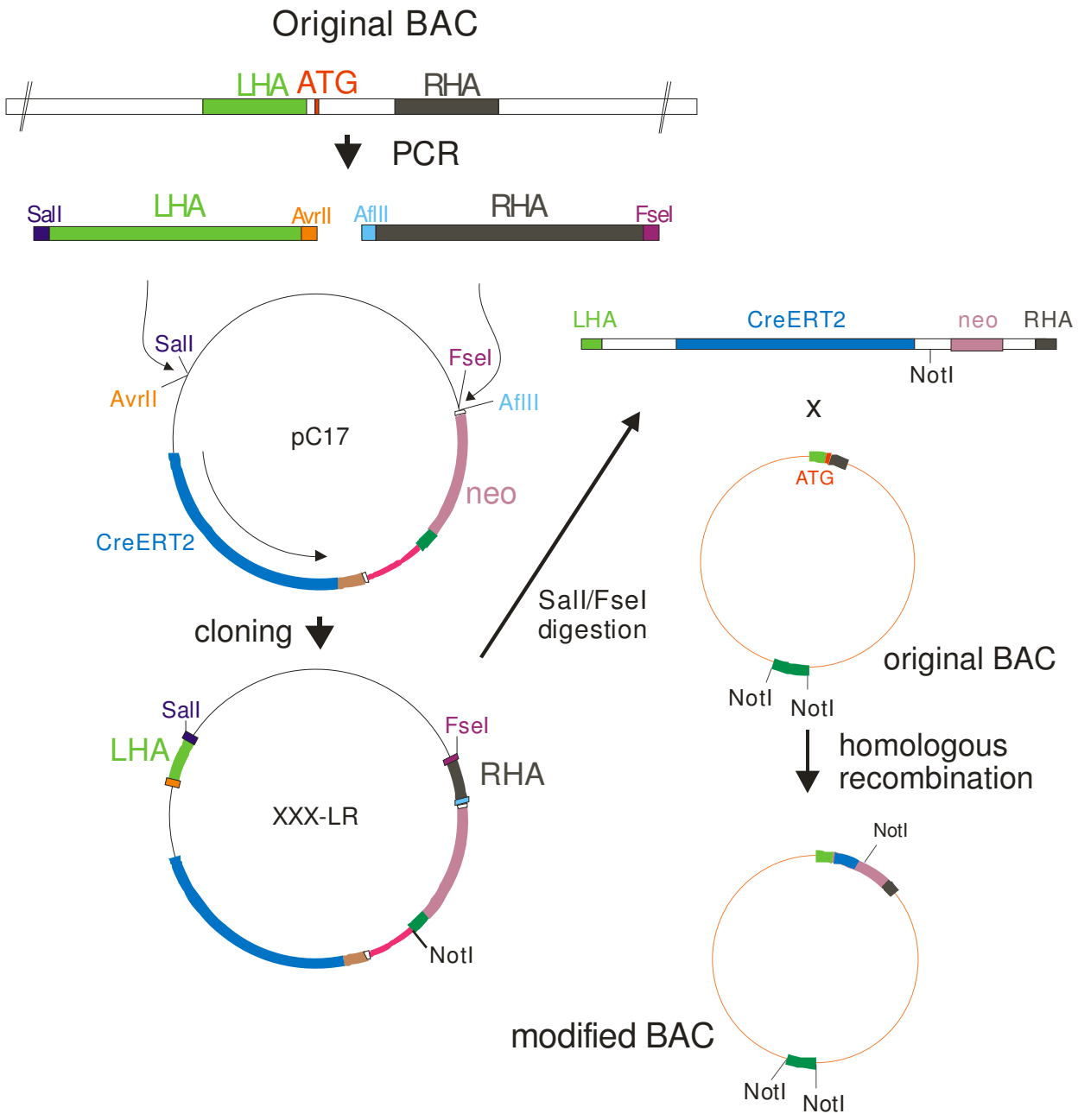

Fig.6. Generation of the BAC-based transgene constructs
Homology arms containing appropriate restriction sites were amplified from original BACs and cloned to the CreER^{T2} plasmid. After SalI/FseI digestion the CreER^{T2} cassette with attached homology arms was electroporated to DY380 bacteria containing the respective BAC. Homologous recombination resulted in modified BACs that were used for transgenesis.

After ligation with digested RHAs, the resulting XXX-LR plasmids were electroporated to DY5 competent bacteria, grown overnight, and DNA was purified as described. As with XXX-L, the insertion of RHA was verified by digestion with an appropriate restriction enzyme (SacI) and by sequencing (TY1 oligonucleotide). Clones containing correct XXX-LR plasmids were amplified by MaxiPrep, and plasmids were re-sequenced with a set of oligonucleotides (VN239, TK139, OW69, QY84, TY1; Fig.5.B, Table 4) to ensure that the integrity of plasmids was sustained throughout the clonings.

To prepare the final modified Cre expression cassette for bacterial homologous recombination, 5 µg of XXX-LR plasmids were digested with SalI, purified, digested with FseI, purified and resuspended in 50 µl of water. Correct digestion was verified by 1.5% agarose gels. The SalI/FseI fragment was extracted from the gel using NucleoSpin® Extract Kit (Macherey-Nagel). Extracted DNA was additionally purified by 0.3 M sodium acetate + 70% ethanol precipitation, washed with 70% ethanol, and resuspended in 20 µl of TE buffer.

1.2. Homologous recombination of BACs

Homologous recombination based on the DY380 E.coli strain was proven to be an efficient method to modify BACs at defined loci (Lee et al., 2001). Ten ng of purified BACs (see 1.1) were electroporated to 40 µl DY380 bacteria and plated on chloramphenicol (12.5 µg/ml, Serva) plates. Positive clones were randomly selected and 2 ml starter colonies were run overnight at 32°C. Then 50 ml colonies were initiated with ca. $8x10^8$ bacteria originating from starter colonies. They were grown until absorption at 600 nm reached 0.5 as measured by a spectrophotometer. Enzymes catalyzing homologous recombination in DY380 were induced by incubation of bacteria at 42°C for 15 min. Bacteria were then spun down, washed with cold water and resuspended in 100 µl of cold miliQ water. Purified SalI/FseI fragments containing the Cre expression cassette with the corresponding homology arms (200 ng each) were electroporated to 40 µl of recombination-competent bacteria containing the respective BAC. Immediately after electroporation, 800 µl of SOB (tryptone, 20 mg/ml, yeast extract 5 mg/ml, 0.01 M NaCl, 2.5 mM KCl, 10 mM $MgCl_2$) medium was added to ensure optimal conditions for bacterial growth. Bacteria were plated on nitrocellulose filters (PROTRAN BA85, Schleicher & Schuell) placed on LB agar (Euromedex) plates. After growing for 2h at 32°C, filters were transferred to chloramphenicol/kanamycin (15 µg/ml, Sigma) plates and were incubated overnight at 32°C. Positive clones were randomly selected and subjected to PCR with VN239 (inside the targeting fragment) and ApFS1, AqFS1, CxFS1, GFFS1 and

GLFS1 primers for ApoE-CreER^{T2}, Aqp-CreER^{T2}, Cx30-CreER^{T2} GfapCreER^{T2} and Glast-CreER^{T2} (outside the targeting fragment, Table 1), respectively. Clones delivering PCR products were subsequently amplified and modified BACs were purified with the NucleoBond® BAC 100 kit (Macherey-Nagel).

1.3. Preparation of radiactive probes

Radioactive probes for Cre (RJ208; Fig. 5B, Table 3) and for left (XXX-LF respective oligonucleotide, Table 1) and right (XXX-RR resepective oligonucleotide, Table 1) homology arms were prepared by P^{32}-based end-labelling of each primer in 10 µl kinase buffer containing 1U of T4 kinase (Biolabs), 100 ng of oligonucleotides and 0.1 mM of ATP-P^{32} (Amersham). The reaction was performed at 37°C for 1h and stopped by Tris-EDTA. To identify fragments containing left or right homology arms after NotI digestion of original and modified BACs, radioactive probes for the entire homology arms were prepared by the random-priming method. A mix of 100 ng of PCR-amplified homology arms and hexamer primers (33 ng/µl) was denaturated (100°C for 10 min) and cooled to room temperature. Then, they were added to a labelling reaction mix containing Klenow buffer (NEB), 5U of Klenow enzyme (NEB), 3 mM dNTP and 5 µl of dCTP-αP^{32} (BD Biosciences) in a final volume of 30 µl. G50 Sephadex column was prepared by placing G50 Sephadex grains in the solution to the syringe of 1 ml that was spun down at 2000 rpm for 5 min. After the labelling reaction (1h at 37°C), 150 µl of Tris-EDTA buffer was added to the reaction mix, and BAC DNA was purified on G50 Sephadex columns by spinning down at 3000 rpm for 5 min. Radioactivity of probes was verified on a scintillation counter (Beckman, LS6500).

1.4. Verification of insertion of Cre expression cassette in BACs

After amplification of clones, correct insertion of the Cre expression cassette in BACs was verified using differential restriction of original and modified BACs. Since restriction of each BAC generated numerous fragments, identification of the digestion product in the agarose gel was performed by Southern blots using radioactively-labeled probes against left or right homology arms. Each BAC (modified and original; 2 µg each) was digested with a set of restriction enzymes (KpnI, EcoRI, HindII, BamHI). DNA fragments were separated in 1.2% agarose gels, depurinated (0.2M HCl), denaturated (0.5M NaOH/1.5M NaCl), neutralized (0.5M Tris/1.5M NaCl) and transferred overnight to Hybond-N+ membranes (Amersham). DNA was fixed by UV cross-linker (STRATALINKER® 2400, Stratagene),

membranes were washed in 6 x SSC (1M NaCl, 0.1 M tri-sodium citrate) and incubated for 2h at 37°C with prehybridization buffer for end-labelled probes containing 6 x SSC, 5 x Denhardt's solution (0.1% Ficoll 400, 0.1% polyvinylpyrrolidone, 0.1% BSA), 1% SDS, 100 µg/ml of denaturated salmon sperm; for random-priming probes, 6 x SSC, 5 x Denhardt's solution, 0.5% SDS, 100 µg/ml of denaturated salmon sperm, 50% formamide. Overnight hybridization in respective prehybridization buffer was performed with P^{32}-labeled radioactive probes recognizing the left (XXX-LF) or right (XXX-RR) homology arm of respective BAC. Membranes were washed first in 2x SSC, 0.1% SDS at 42°C for 2 x 15 min, followed by 2 x 15 min washes with 0.5x SSC, 0.1% SDS at 42°C. After a check of the signal intensity with a hand-held scintillation counter (MCB 21, Eurysis Mesures), membranes were enveloped in Saran wrap and exposed to Biomax films (Kodak). The size of the digest products was estimated by analyzing the region of insertion (NCBI Sequence Viewer database; GCK software). As an additional test for correct insertion of the Cre cassette, NotI-fragments of original and modified BACs were separated on 1% agarose gels by pulse-field gel electrophoresis (PFGE), transferred to Hybond+ membranes and hybridized with end-labelled Cre probe (RJ208) or with random-labelled homology arm probes. Positive clones were sequenced using VN239 primer (Fig. 5B, Table 4) to confirm correct integration of the targeting construct in the original BAC.

1.5. Preparation of modified BACs for transgenesis

All correctly modified BACs were subsequently amplified and purified with the NucleoBond® BAC 100 Kit (Macherey-Nagel). The quality of modified BAC DNA was verified by PFGE of undigested DNA. The purification was repeated for clones of insufficient quality, i.e. displaying a significant level of degradation (such as both clones for Cx30 at Fig. 10). Finally, 2 pl of each modified BAC was injected to fertilized mouse oocytes from FVB/N females at the transgenesis facility of Institute Clinique de la Souris (ICS, Illkirch, France).

2. CHARACTERIZATION OF TRANSGENIC LINES

2.1. RNA Isolation and RT-PCR

Animals were killed by cervical dislocation, tissues were dissected and frozen in liquid nitrogen. The following steps were performed with RNAse free material. Tissues were homogenized with Ultrathurax in 0.5 ml of Trizol reagent (Sigma) and left at room temperature for 5 min. Afterwards, supernatant was transferred to a new tube and 200 µl of chlorophorm were added, mixed and spun down at 13.000 rpm for 15 min. RNA was precipitated with 70% isopropanol, washed in 70% ethanol, air-dried and resuspended in 20 µl of RNAase-free water (Invitrogen). Concentration was measured with a spectrophotometer at A260. Two micrograms of RNA were taken for cDNA synthesis using the SuperScript first-strand synthesis system (Invitrogen) following the manufacturer's protocol. PCR of cDNA was performed using the following conditions: denaturation at 94°C for 30s, followed by a number of cycles indicated below of denaturation (94°C, 30s), annealing for 30s at temperatures indicated below and elongation at 72°C for 1 min. Initially, for each pair of primers 26, 28, 30 and 32 cycles were performed to find the linear phase of amplification. Subsequent RT-PCR reactions were performed with selected cycle numbers in triplicate for each sample. Primers for Cre recombinase and for the driving genes (obtained from cited literature; Table 1) and reaction conditions were as follows: CreF, CreR: 58°C annealing temperature, 29 cycles; β-actinF, β-actinR: 60°C, 27 cycles (Dorlhiac-Llacer et al., 2001); Cx30F, Cx30R: 58°C, 27 cycles (Houghton et al., 2002); GLASTF, GLASTR: 60°C, 27 cycles (Figiel and Engele, 2000), Aqp4F, Aqp4R, 58°C, 29 cycles (Zelenin et al., 2000), ApoEF, ApoER, 60°C, 27 cycles (Usui et al., 2004). PCR products were separated on 1.5% agarose gels and the intensity of bands was measured using a ChemiGenius II unit (Syngene, Cambridge, UK).

2.2. Induction of Cre recombinase activity

To establish an efficient regime of tamoxifen (TAM) treatment, several injection protocols were tested including single injections on 5 consecutive days with 1 mg or 2 mg of TAM or with 1 mg of 4-hydroxytamoxifen (4-OHT) or two daily injections for 5 consecutive days with 1 mg of TAM. For injections, a TAM stock solution (10 mg/ml; stored at -20°C) was prepared by dissolving 100 mg of TAM (Sigma) in 1 ml of 100% ethanol, intensive vortexing and then by adding 9 ml of sunflower oil followed by intensive vortexing. Control animals were injected with a mixture (1:9) of ethanol:sunflower oil. Injections were performed using 1

ml syringes (Terumo) and sterile needles 0.5 mm diameter (Terumo). Mice were injected intraperitoneally by inserting the needle approximately 5 mm deep at the central epigastric region located below the diaphragm.

2.3. Detection of Cre activity at the DNA level

To analyze Cre-mediated recombination at the DNA level, Tg(XXX-CreER^{T2}) mice were crossed with the RXRα*af2/+* reporter line (Mascrez et al., 1998). Double-transgenic mice were identified by PCR on genomic DNA from tail biopsies using primers for Cre (TK139 and TK141), RXRα*af2/+* (UN126 and RR189). All analyses were performed on adult animals (between six and twelve weeks old).

TAM- or sham-injected mice were sacrificed by cervical dislocation 7 days after last injection. Different brain regions and selected organs/tissues were digested overnight with proteinase K (Promega) in 500 µl of proteinase K buffer (50mM Tris, 5mM EDTA, 1%SDS, 0.2M NaCl, pH=8.0) at 55°C. Then, 500 µl of phenol/chlorophorm (1:1) were added, samples were mixed and spun down at 13000 rpm for 5 min. DNA was precipitated with 70% ethanol, washed with 70% ethanol and dissolved in distilled water. PCR was run in standard conditions with primers UN126 and UN127 that identify the excised L- and wild-type alleles. One hundred ng of DNA, as determined by spectrophotometry, from each brain region or organ/tissue served as PCR template. PCR products were separated on 2% agarose gels and processed for Southern Blot, as described above. After transferring to Hybond-N+ membranes, prehybridization and overnight hybridization was performed with end-labelled radioactive probe RH199 recognizing loxP sites, and exposed to Biomax films. Blots were digitized using a flat-bed scanner.

2.4. Cytochemical detection of reporter enzymes

To detect Cre recombinase activity at the protein level, Tg(XXX-CreER^{T2}) were crossed with the R26R (Soriano, 1999) or Z/AP (Lobe et al., 1999) reporter line. Double-transgenic animals were identified by PCR on genomic DNA from tail biopsies using primers for Cre and for lacZ (VD23 and VD24) or for human placental alkaline phosphatase (hPLAP) (AF97 and AF98).

For cytochemical detection of enzymatic activity [β-galactosidase (βGal) or hPLAP], mice were killed by cervical dislocation, brains were dissected out, frozen in OCT mounting medium (Sakura, Torrance, CA) on dry ice and subsequently cut on a cryostat (Leica CM

3050) to 20 µm thick sections. Sections were immobilized on SuperFrost slides, dried and stored at -20°C. Alternatively, mice were anesthetized with a mixture of Ketamine (Virbac France SAS) and Xylazine (Bayer) and killed by transcardial perfusion with PBS (pH 7.4) followed by 4% formaldehyde in PBS. Tissues were postfixed for 2 to 4 hrs in formaldehyde, stored in 0.01% NaN_3 in PBS and cut to 50-100 µm thick sections on a vibratome.

βGal activity was detected on sections that were incubated overnight in Xgal-staining solution [1 mg/ml 5-bromo-4-chloro-3-indolyl-β-d-galactopyranoside (Euromedex), 5 mM potassium ferricyanide, 5 mM potassium ferrocyanide, 2 mM $MgCl_2$ in PBS]. For detection of hPLAP activity slides or free-floating sections were incubated first in 65°C for 30 min in PBS to inactivate endogenous alkaline phosphatase activity. After cooling to room temperature, samples were stabilized with AP-buffer (100 mM Tris pH 9.5, 100 mM NaCl, 50 mM $MgCl_2$, 0.1% Tween 20, 2 mM Levamisol). Then, sections were incubated in Xphosphate-staining buffer [AP-buffer with 0.1 mg/ml 5-bromo-4-chloro-3-indolyl-phosphate (Euromedex) and 1 mg/ml Nitro Blue tetrazolium (Euromedex)] at room temperature for 3 min (free floating sections) or overnight (slides). The reaction was stopped by adding 0.05M EDTA in PBS. Bright-field micrographs were taken on a light microscope (Leica M420) equipped with a CCD camera (Coolsnap, Photometrics).

2.5. Immunohistochemistry

For immunohistochemical staining, animals were anesthetised and perfused as described for cytochemical staining. Brains and spinal cords were taken out and cut on the vibratome at 50 µm thickness. Free-floating sections were stabilized in PBS, blocked for 1 hr at room temperature (5% normal goat serum with 0.2% Triton-X100 in PBS). Sections were then incubated overnight at 4°C with the following primary antibodies diluted in blocking solution: rabbit anti-βGal (1:1500, ICN), mouse anti-Gfap (1:500, Sigma), mouse anti-S100β (1:1000, Sigma), mouse anti-NeuN (1:500, Chemicon), mouse anti-CNPase (1:1000, Sigma). Sections were then washed 3 x 15 min in PBS and incubated for 1 hr at room temperature with secondary antibodies: anti-rabbit AlexaFluor555, anti-rabbit AlexaFluor488, anti-rabbit AlexaFluor594, anti-mouse AlexaFluor555 and anti-mouse AlexaFluor488 (all at 1:1000; Invitrogen/Molecular Probes). To detect the NeuN antibody, sections were incubated with secondary biotinylated anti-mouse antibody (1:500, VectorLabs) at room temperature for 30 min, washed 3 x 10 min in PBS and incubated with neutravidin-Oregon Green (1:500, Invitrogen/Molecular Probes). After washing with PBS, sections were mounted in Vectashield

(VectorLabs) containing the nuclear marker DAPI (10 µg/ml, Invitrogen/Molecular Probes). Immunostained sections were examined by confocal microscopy (Leica TCS SP2). Counting of cells was performed on three (CNS) 50 µm thick sections per animal using free software ImageJ (ImageJ, v1.32, Rasband, W.S., ImageJ, U.S. National Institutes of Health, Bethesda, Maryland, USA, http://rsb.info.nih.gov/ij/, 1997-2007). The number of cells double-positive for βGgal and S100β (CNS) was determined from random single planes. Photos represent z-stack reconstructions of 16 - 30 consecutive planes (5-10 µm).

RESULTS

1. GENERATION OF TRANSGENESIS CONSTRUCTS FOR CRE-ER^{T2} EXPRESSION IN ASTROCYTES

To obtain astrocyte-specific expression of CreER^{T2}, we used transgenesis constructs based on BACs that encompass mouse genes, which are expressed in astrocytes. This list included Apoe, Aqp4, Cx30, Gfap and Glast (Table 1). To drive expression of CreER^{T2} by regulatory promoter elements of each gene of interest, we replaced for each respective BAC the region containing the ATG transcription initiation codon (indicated by NCBI Gene database) with a CreER^{T2} expression cassette (Indra et al., 1999) by bacterial homologous recombination (Fig. 6; Lee et al., 2001; for details see Material and Methods). To perform homologous recombination, left and right homology arms were amplified from respective purified BAC DNA by PCR (Table 1, 2 for sequence and position of primers) and added to the CreER^{T2} expression cassette. Correct insertion was verified by diagnostic digests and by additional sequencing (Figs. 5, 7; Table 4).

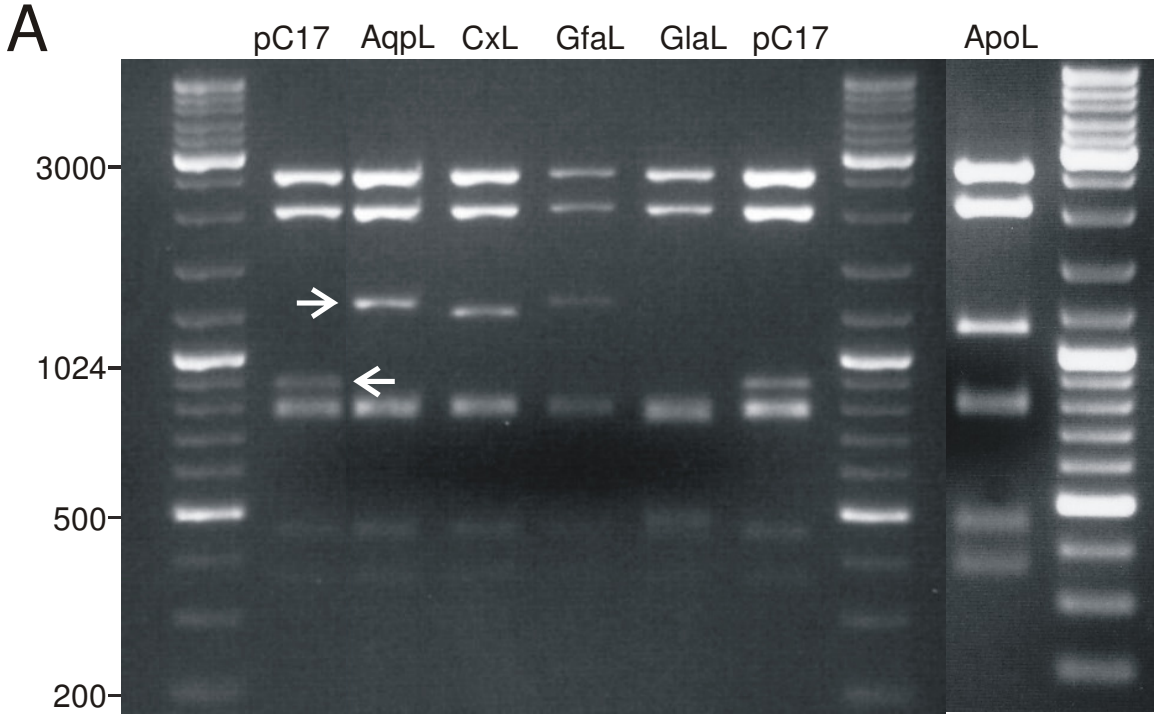

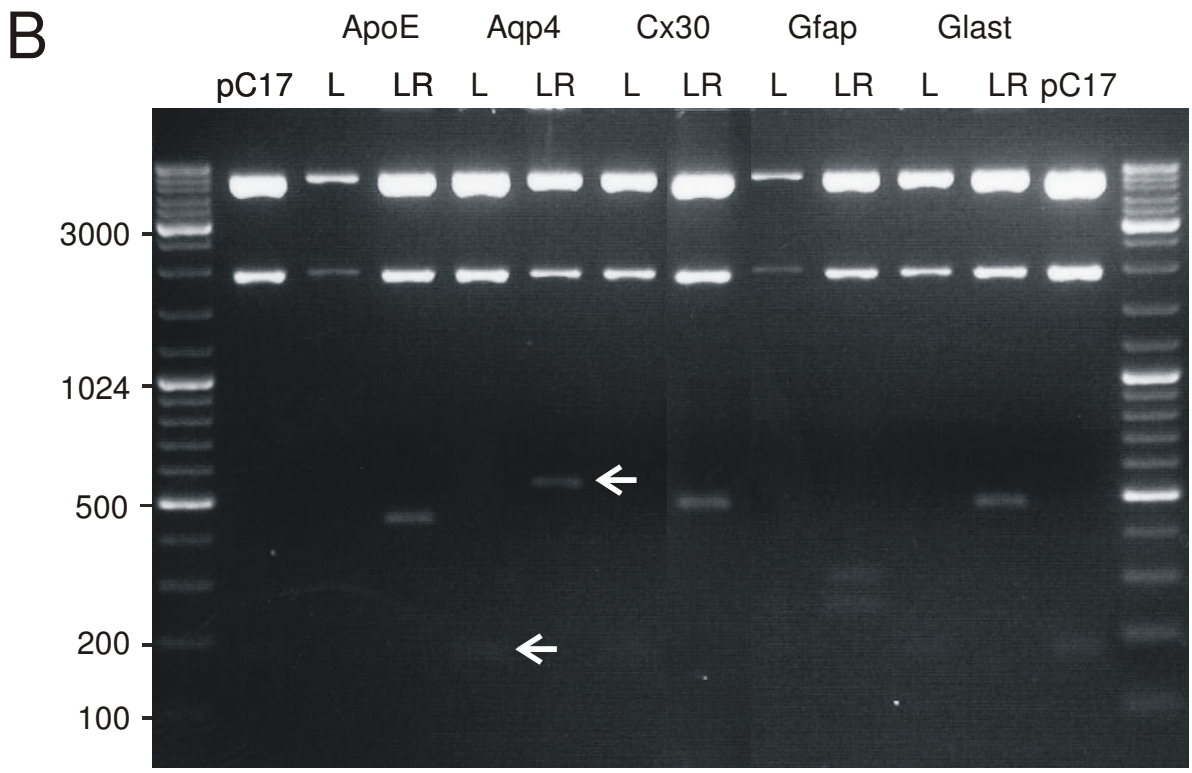

Fig.7. Insertion of homology arms in the CreER^{T2} plasmid
A, PvuI/EcoRI digestion of the CreER^{T2} plasmid in original (pc17) and modified versions (XXX-L) containing left homology arms. Note the switch of the band at ca. 870bp (arrow) in pC17 to ca. 1150bp (arrow at Aqp4-L) in XXX-L due to the insertion of left homology arm (left homology arm in Glast-L plasmid contains the EcoRI restriction site, resulting in bands at ca. 470bp and 760bp, migrating with original fragments from pC17). B, SacI digestion of pC17, XXX-L and XXX-LR plasmids. Note the switch in the band from ca. 170bp in pC17 (arrow at AqpL) and XXX-L to ca. 550bp (arrow at Aqp-LR) in XXX-LR due to the insertion of right homology arm (right homology arm of Gfap-LR contains the SacI restriction site resulting in 2 fragments at ca. 150bp and ca. 280bp).

After verification, the modified CreER^{T2} expression cassette and the BACs were subjected to homologous recombination using the DY380 strain. Correct insertion of the CreER^{T2} expression cassette was verified by two approaches. First, differential digestion by a series of restriction enzymes and subsequent Southern blots with radioactive probes for homology arms to ensure that corresponding fragments have expected size (Fig. 8).

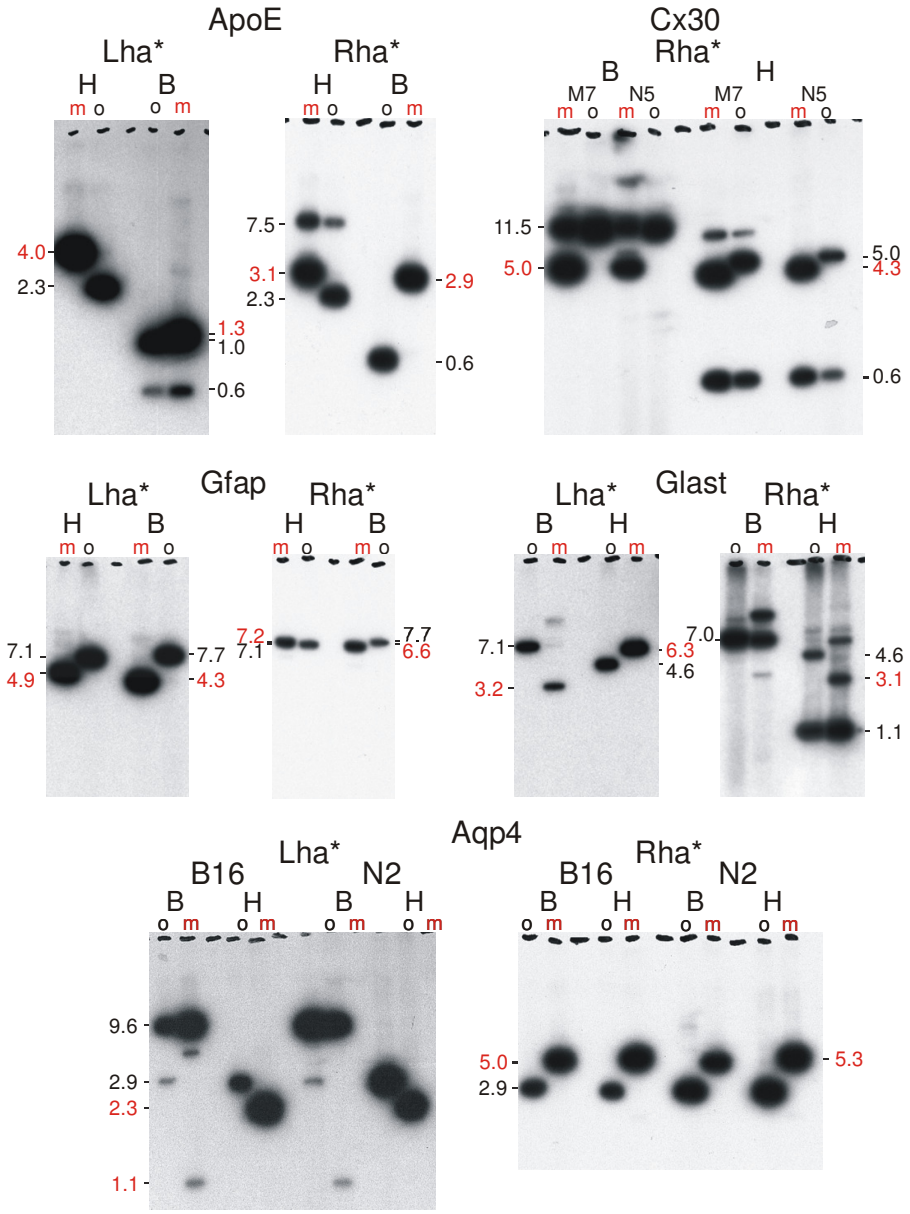

Fig. 8. Insertion of CreER^{T2} cassette in the BAC
Digestion of original (o, black) and modified (m, red) BACs with HindIII (H) or BamHI (B) followed by Southern blots and hybridization with radioactive probes recognizing either the left (Lha*) or right (Rha*) homology arm of the respective BAC. Two BACs were modified for Aqp-CreER^{T2} and Cx30-CreER^{T2} (part of original BAC code is indicated). Numbers indicate the predicted sizes of fragments in kilobase pairs.

Second, original and modified BACs were digested by NotI, whose restriction site is located in the CreER^{T2} expression cassette and in the BACs (see Fig. 5) and Southern blots were used to confirm NotI-induced separation of fragment carrying CreER^{T2} and the left homology arm from the fragment containing neo cassette and the right homology arm (Fig. 9).

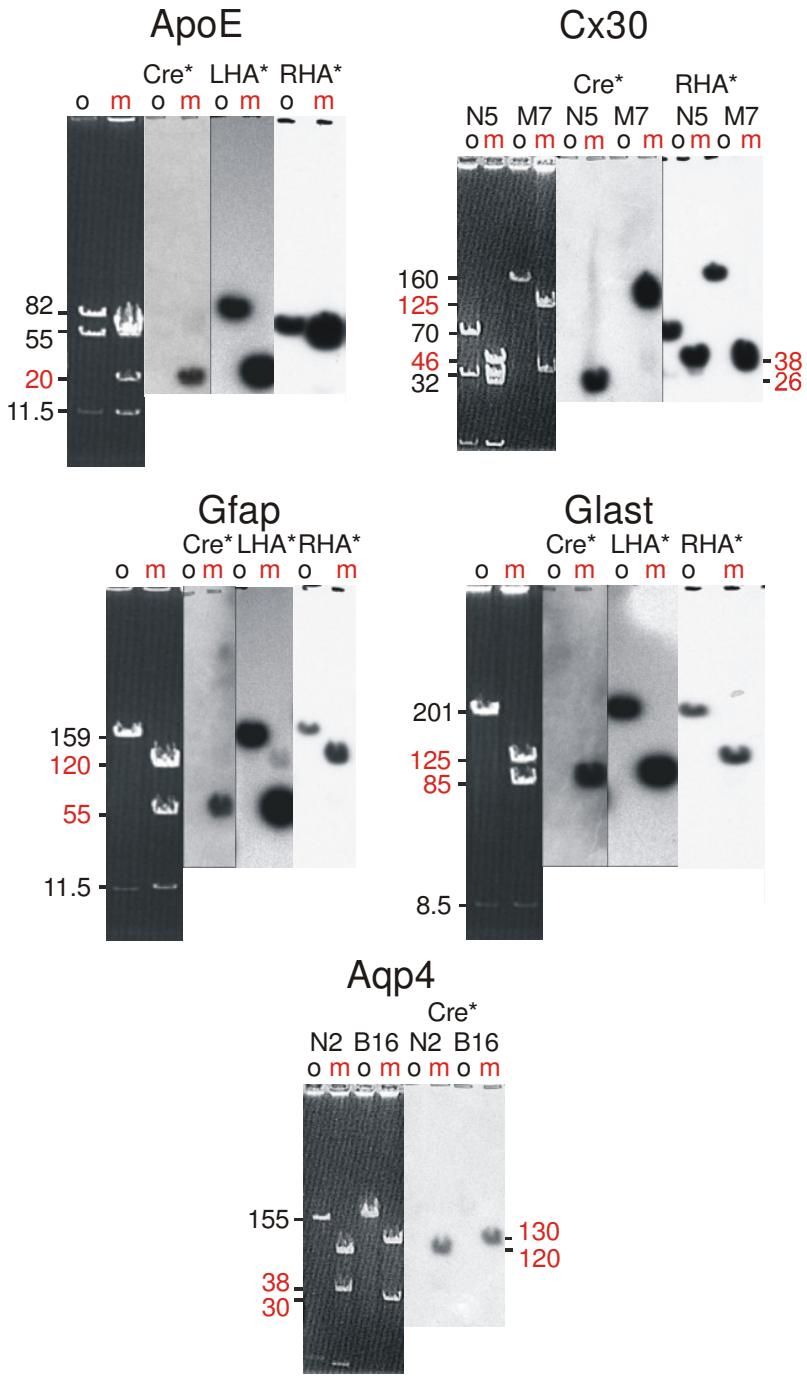

Fig. 9. Integrity of BACs after insertion of the CreER^{T2} cassette
Pulsed-field gel electrophoresis of NotI-digested original (o, black) and modified (m, red) BACs followed by Southern Blot and hybridization with radioactive probes recognizing Cre (Cre*), left (LHA*) or right (RHA*) homology arms. Numbers indicate predicted size in kilobase pairs.

Correctly modified BACs were purified (Fig. 10) and injected to fertilized mouse oocytes of FVB/N background, in order to obtain transgenic animals.

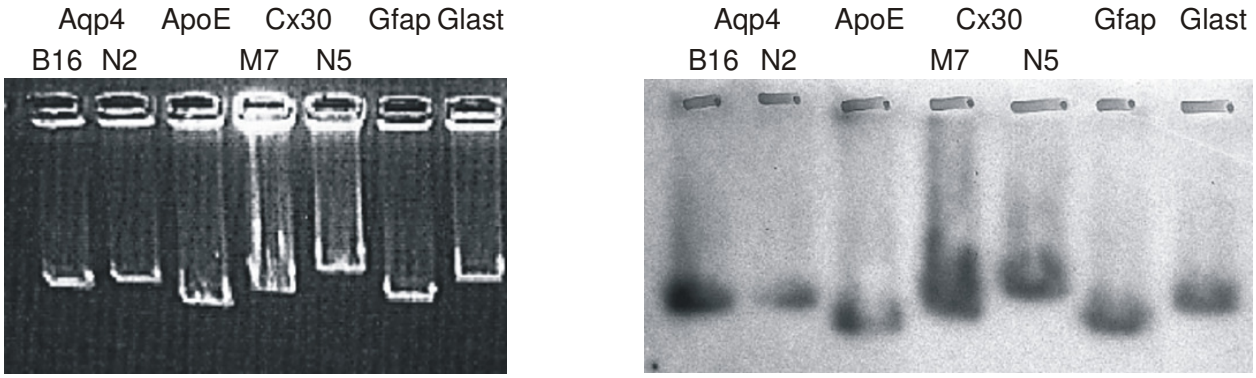

Fig. 10. Purification of modified BACs for transgenesis
Pulsed-field gel electrophoresis of modified undigested BACs (left) and subsequent hybridization with a radioactive probe recognizing Cre (right).

Microinjections of modified BACs into fertilized mouse oocytes yielded several transgenic lines for each transgene (Table 1). Founder mice were genotyped for the presence of Cre (primers TK 139 and TK 141) and neo (QY79 and QY84). Positive founders were bred to the C57Bl/6 line for 2 to 3 generations. Germ-line transmission of transgenes was observed in 2/2 lines for Tg(ApoE-CreER^{T2}), 3/3 lines for Tg(Aqp4-CreER^{T2}), 3/3 lines for Tg(Cx30-CreER^{T2}), 5/5 lines for Tg(Glast-CreER^{T2}). For unknown reasons, founders of Tg(Gfap-CreER^{T2}) did not give rise to Cre-positive litters. Therefore, this transgene was not further pursued. For two lines, Tg(ApoE-CreER^{T2})T54-44, Tg(Glast-CreER^{T2})T45-57 germ-line transmission was observed only in male litters, suggesting that the transgene was integrated to the Y chromosome.

2. SELECTION OF THE MOST EFFICIENT TRANSGENIC LINES

We first performed a series of experiments to select the lines showing the highest level of CreER^{T2}-mediated recombination for further analysis.

2.1. Comparison of transcriptional regulation by endogenous and BAC-based promoters

We first determined, whether in the different transgenic lines, the CreER^{T2} transcription pattern driven by the regulatory elements contained in respective BAC followed the activity of the respective endogenous promoter. Thus, mRNA of different brain regions and other organs was extracted and subjected to semi-quantitative RT-PCR for Cre and the transcript controlled by the endogenous promoter. The latter was also compared to the levels from wild-type animals to exclude eventual expression of respective genes contained in the BAC. In none of the transgenic lines, however, this was the case.

Comparison of two Tg(Glast-CreER^{T2}) lines revealed differences in transcript levels for Cre (Fig. 11). In most brain regions tested, the level of CreER^{T2} normalized to β-actin was much higher in Tg(Glast-CreER^{T2})T45-72 than in the Tg(Glast-CreER^{T2})T45-5 line. The Cre expression pattern in Tg(Glast-CreER^{T2})T45-72 line recapitulated the activity of the endogenous promoter, with the highest signal from cortex, cerebellum, hippocampus, midbrain, medulla and skin and with some activity in the eye and testis.

Comparison between three independent Tg(Cx30-CreER^{T2}) transgenic lines revealed that the Cre transcript level followed closely the endogenous promoter activity across all organs and tissues with highest levels of both Cx30 and Cre detected in cortex, cerebellum, midbrain, brain stem, hippocampus and in skin (Fig. 12).

Despite strong expression of ApoE in different organs and tissues tested, the Cre mRNA level was very low in Tg(ApoE-CreER^{T2})T54-29 transgenic line reaching strongest signal from cerebellum (Fig. 13). Most suprisingly, no Cre transcripts were detected in the liver, although this organ show the highest level of ApoE mRNA according to the literature (Mahley and Rall, 2001).

The level of Aqp4 mRNA in the Tg(Aqp4-CreER^{T2})T55-26 line was highest in the brain (Fig. 14) and the Cre mRNA levels followed this pattern with strong signals from cerebellum, brain stem and mesencephalon. Overall, however, transcript levels were much lower than for other transgenic lines (note the different scale of the Y axis in Fig.14).

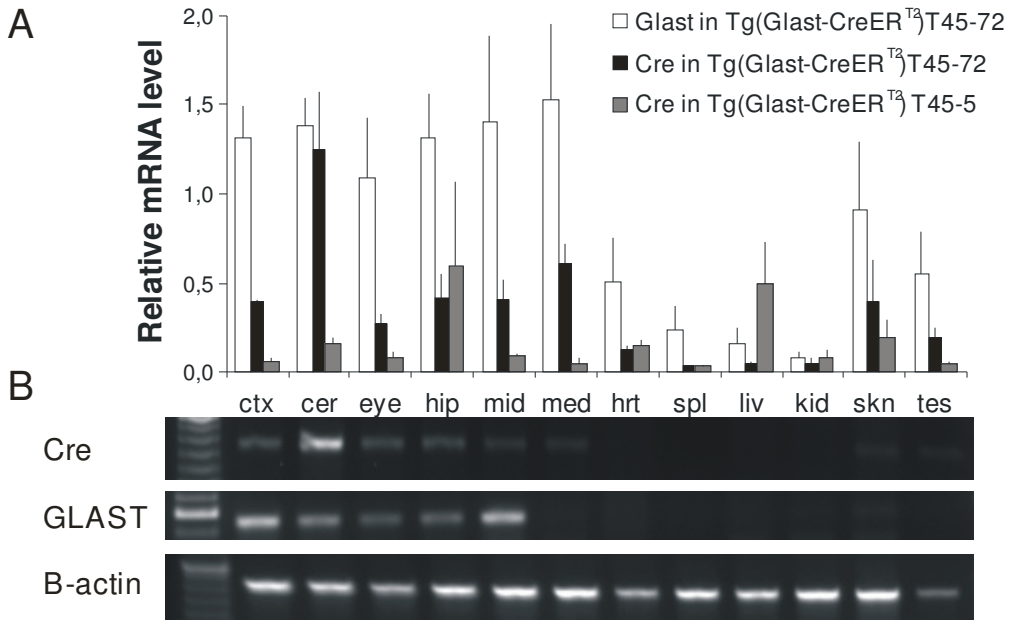

Fig. 11. Transcript levels of Cre and Glast in Tg(Glast-CreER^{T2}) lines
A, Mean levels of mRNA normalized to β-actin: Glast (white), Cre in Tg(Glast-CreER^{T2})T45-72 (black) and Tg(Glast-CreER^{T2})T45-5 (grey) lines. B, Micrograph of representative RT-PCR from Tg(Glast-CreER^{T2})T45-72 line. Whiskers indicate standard deviation [n = 2 triplicates for Tg(Glast-CreER^{T2})T45-72 and n=1 triplicate for Tg(Glast-CreER^{T2})T45-5 line].

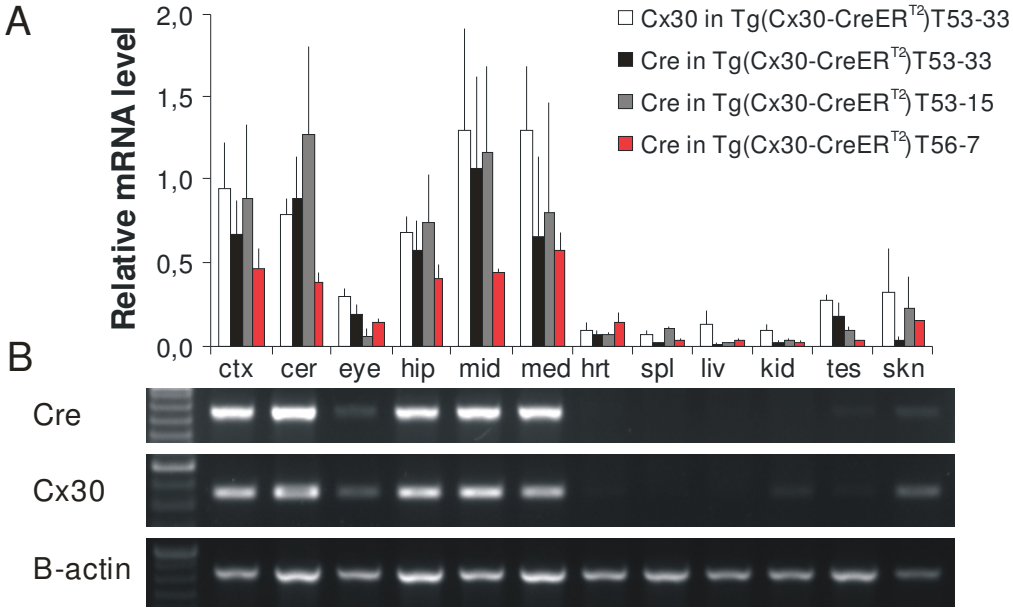

Fig. 12. Transcript levels of Cre and Cx30 in Tg(Cx30-CreER^{T2}) lines
A, Mean levels of mRNA normalized to β-actin: Cx30 (white), Cre in Tg(Cx30-CreER^{T2})T53-33 (black), Tg(Cx30-CreER^{T2})T53-15 (grey) and Tg(Cx30-CreER^{T2})T56-7 (red). B, Micrograph of representative RT-PCR from Tg(Cx30-CreER^{T2})T53-33 line. Whiskers indicate standard deviation [n = 2 triplicates for Tg(Cx30-CreER^{T2})T53-33 and n=1 triplicate for Tg(Cx30-CreER^{T2})T53-15 and Tg(Cx30-CreER^{T2})T56-7 lines].

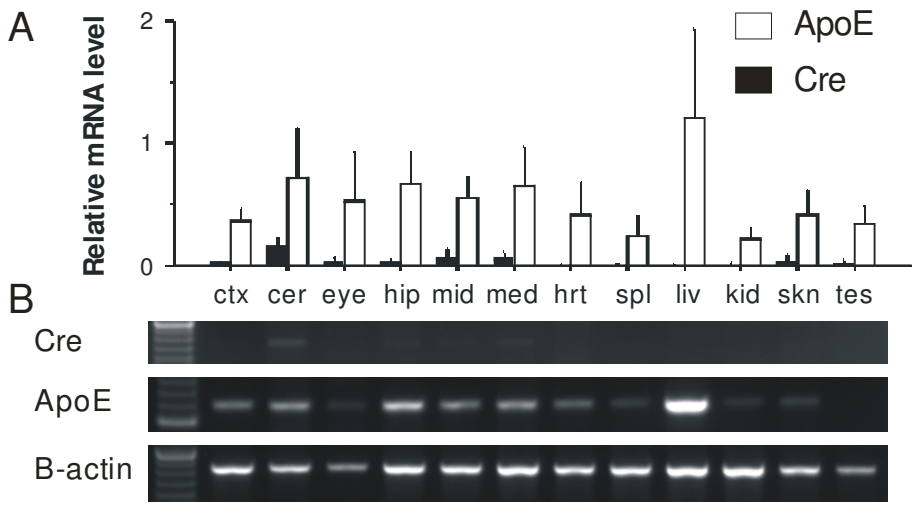

Fig. 13. Transcript levels of Cre and ApoE in Tg(ApoE-CreER^{T2})T54-29 line
A, Mean levels of mRNA to normalized to β-actin: ApoE (white) and Cre (black). B, Micrograph of representative RT-PCR for Cre, ApoE and β-actin on tissues from Tg(ApoE-CreER^{T2})T54-29 line. Whiskers indicate standard deviation (n = 2 animals, triplicate samples).

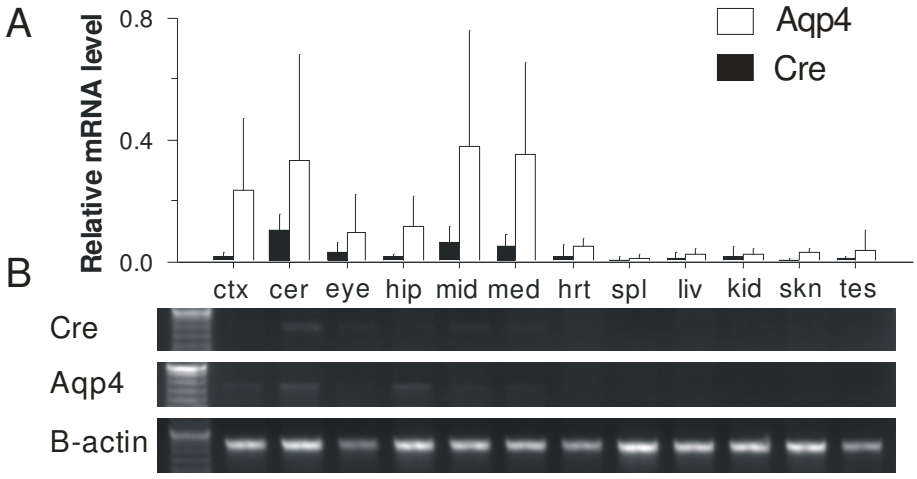

Fig. 14. Transcript levels of Cre and Aqp4 in Tg(Aqp4-CreER^{T2})T55-27 line.
A, Mean levels of mRNA to normalized to β-actin: Aqp4 (white) and Cre (black). B, Micrograph of representative RT-PCR for Cre, Aqp4 and β-actin on tissues from Tg(Aqp4-CreER^{T2})T55-27 line. Whiskers indicate standard deviation (n = 2 animals, triplicate samples).

Taken together, these results revealed a good correlation between mRNA levels of Cre and of Glast or of Cx30 in the respective transgenic lines. On the contrary, rather poor correlation was observed for transgenic lines based on the Apoe and Aqp4 promoter.

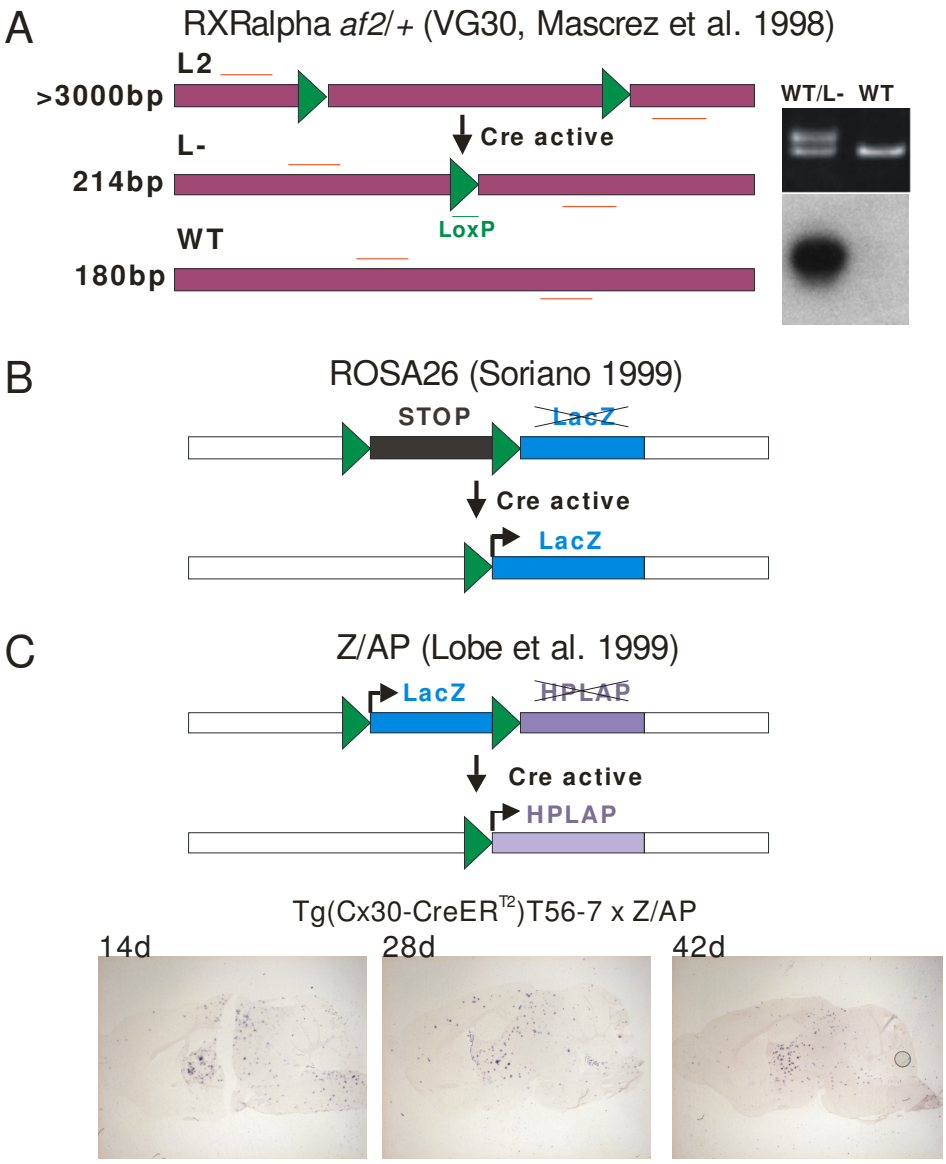

Fig. 15. Schematic presentation of reporter lines used in this study
A, In the RXRαaf2/+ reporter line, Cre excises the floxed af2 domain of the RXRα receptor that can be identified by PCR using primers (red lines) located outside of the excised sequence followed by hybridization with a loxP probe (green). Numbers indicate the size of PCR products. Insert, PCR products from wt allele and excised allele (L-) after separation on gel and after hybridization with loxP probe. B, In the ROSA26R reporter line (Soriano, 1999), Cre activity excises a floxed STOP cassette and switches on the expression of β-gal. C, In the Z/AP reporter line, Cre activity excises a constitutively expressed lacZ gene controlled by CAG promoter, and switches on the expression of hPLAP. Insert: bright field micrographs of X-phosphate stained sagital section from brains of Tg(Cx30-CreER^{T2})T56-7 x ZAP animals treated with 5x1mg of TAM and killed 14, 28 or 42 days after last injection

2.2. Characteristics of reporter lines

To select for lines with highest efficiency of Cre-mediated recombination, CreER^{T2} expressing lines were crossed with three reporter lines (Fig. 15). Cre-mediated recombination at the DNA level was tested by the RXRαaf2/+ reporter line (Mascrez et al., 1998), where Cre activity leads to excision of the floxed af2 domain of the RXRα receptor. The cellular specificity of Cre-mediated recombination was studied with reporter lines, where Cre activity induces enzymatic activities that can be detected by histochemical or immunohistochemical methods. These were ROSA 26R (Soriano, 1999) and Z/AP (Lobe et al., 1999), where Cre induces expression of β-galactosidase (β-gal) and human placental alkaline phosphatase (hPLAP), which are controlled by the ROSA locus and by the ubiquitously active CAG promoter, respectively.

For the selection of transgenic lines, a few issues were addressed including 1) the establishment of an efficient regime of tamoxifen treatment, 2) differences between lines derived from one BAC-based transgene and 3) lines that employ the same promoter, but were created using different BAC-based transgenes.

2.3. Establishment of a tamoxifen application regime and time-course of Cre-mediated recombination

At the beginning of the project, applicability of the CreER^{T2} system for recombination in the brain had not been established except for a few studies [e.g. (Weber et al., 2001)], where the protocol of TAM administration consisted of a single daily injection of 1 mg of TAM for 5 consecutive days. We compared the effects of tamoxifen and of 4-OHT, a metabolite of TAM, which was originally used to activate CreER^{T2} (Feil et al., 1997). We observed lower efficacy of 4-OHT than of TAM when adult transgenic mice were subjected to single daily intraperitoneal injections of 1 mg at five consecutive days (Fig. 16). Therefore, all further experiments were performed with TAM. Next, we aimed to establish the tamoxifen dose that induces efficient recombination without deleterious effects. We varied the concentration of TAM (1 and 2 mg) and the number of injections per day (1 or 2). Control animals were injected with vehicle. All animals in these experiments were killed either 1 week (in case of RXRαaf2/+ reporter) or 3 weeks (in case of Z/AP reporter) after the last TAM injection. In all constellations tested, higher TAM doses led to higher efficiency of Cre-mediated recombination (Figs. 16, 17, 19). Based on these results, a 5 x 2 mg injection protocol was used for all further experiments (except where indicated). Importantly, in

vehicle-injected animals we did not observed significant Cre-mediated recombination with the exception of the skin in two lines (Fig. 17). Moreover, TAM even at higher doses did not cause evident behavioural abnormalities or increase the mortality of animals.

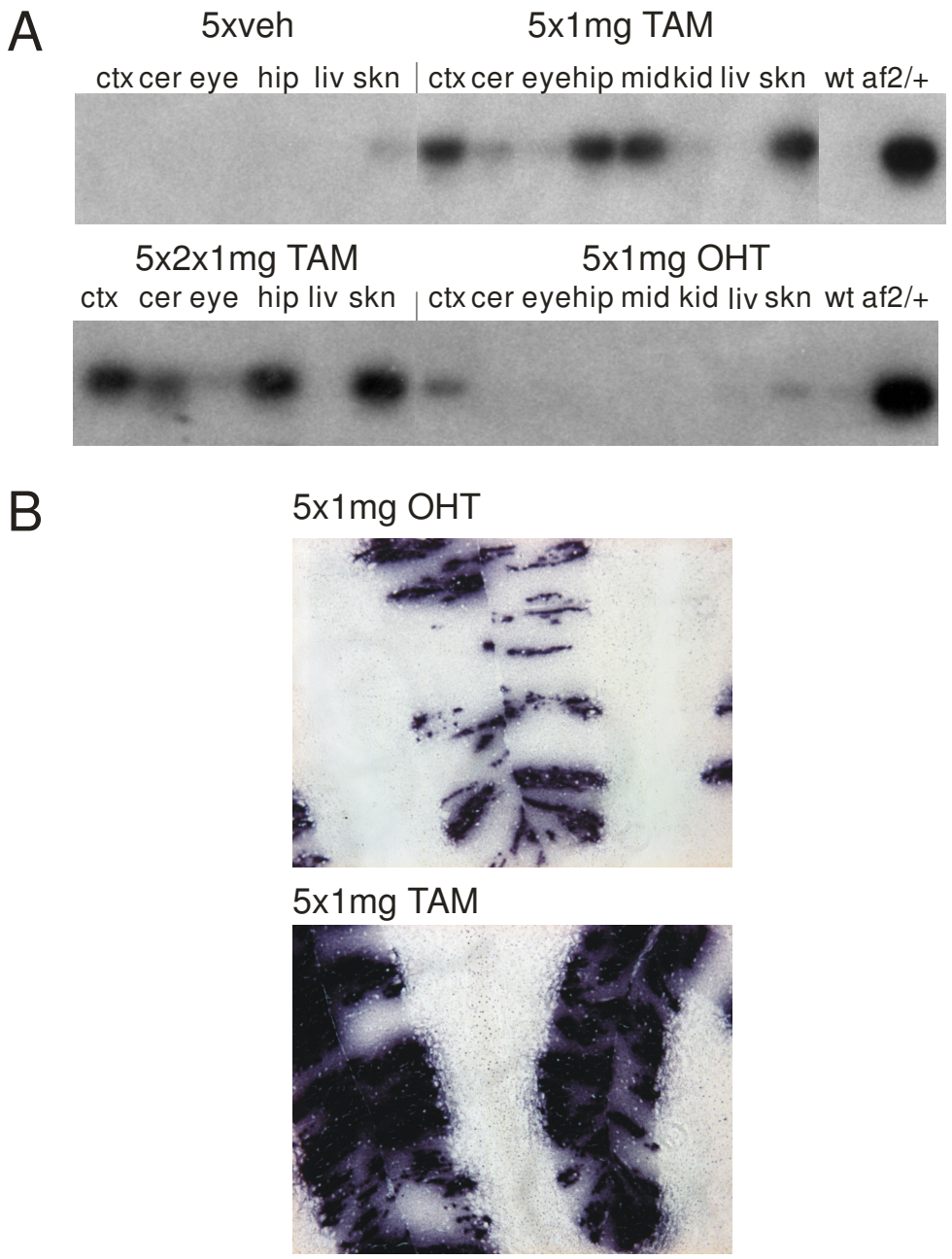

Fig. 16. Establishment of a regime for tamoxifen injections
A, Autoradiogram of Southern blots of PCR products hybridized with loxP probe. Samples are from indicated brain regions and organs/tissues extracted from adult Tg(Glast-CreER^{T2})T45-52 x RXRαaf2/+ mice that were treated with indicated doses of TAM or 4-OHT. B, Bright-field micrograph from of coronal sections from brains of Tg(Glast-CreER^{T2})T45-72 x Z/AP animals injected with TAM (top) or 4-OHT (bottom; 5 x 1 mg, each) that were processed for cytochemical detection of alkaline phosphatase activity

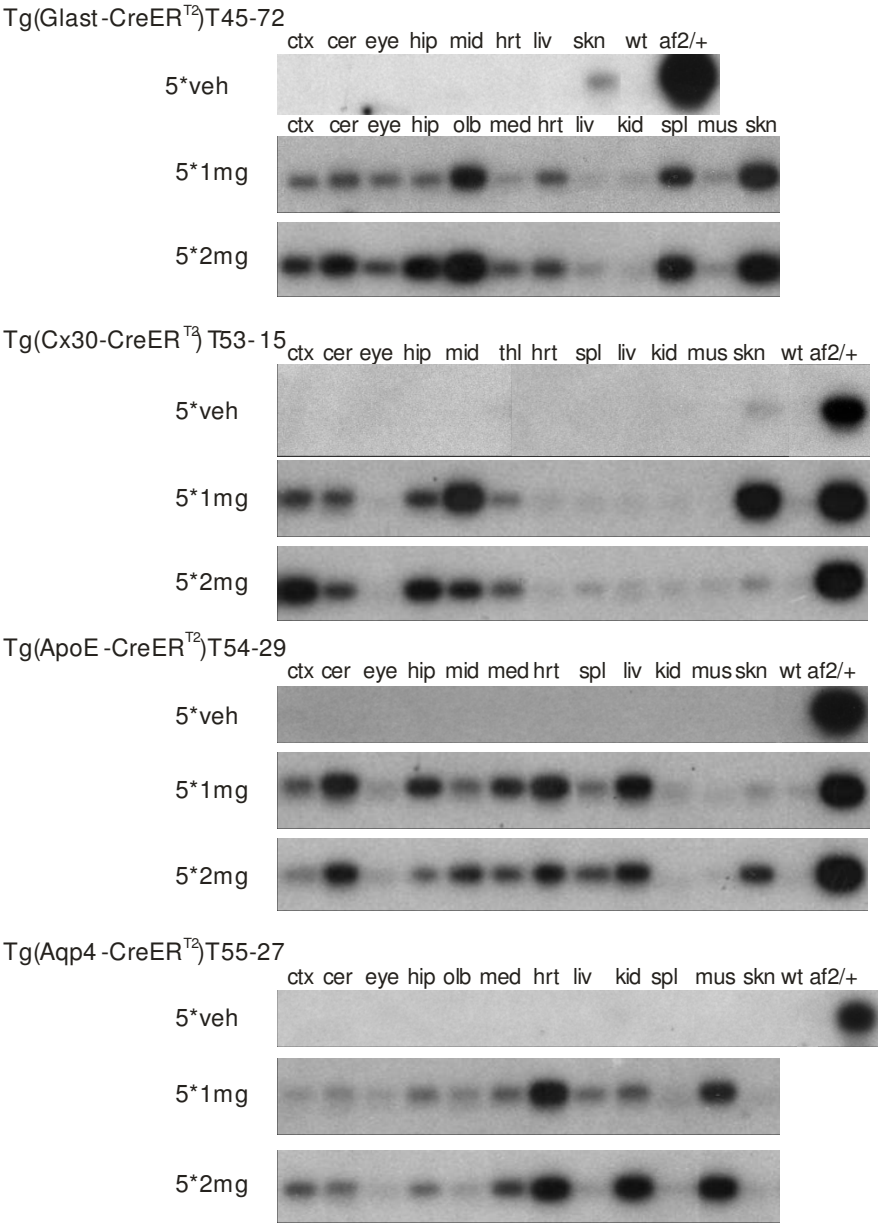

Fig. 17. TAM-induced Cre-ER^{T2} activity is dose-dependent

Autoradiograms of Southern blots of PCR products hybridized with loxP probe. Samples are from indicated brain regions and organs/tissues extracted from indicated transgenic lines crossed with the RXRαaf2/+ reporter line. Adult animals received the indicated injections and were sacrificed 1 week after the last injection.

It was reported that in the RXRαaf2/+ and the ROSA26R reporter line, the effect of Cre-mediated recombination can be detected within 24 h after the last injection, whereas in the Z/AP line, visualization of the reporter protein (hPLAP) requires at least 2 weeks until the product accumulates to a concentration sufficient for cytochemical detection (Weber et al., 2001). To test for time-dependent changes in cytochemical staining, we analyzed animals from crosses between the Tg(Cx30-CreER^{T2})T56-7 line and the Z/AP reporter. As shown in Fig. 15C no differences were observed between animals that were sacrificed 2, 4 or 6 weeks after single daily injections of 1 mg of TAM for 5 consecutive days. Therefore analysis of mice crossed on Z/AP reporter were performed between 2 and 4 weeks after the last TAM injection.

2.4. Differences between lines derived from one transgene – Glast-CreER^{T2} lines

For each transgenesis construct, we obtained two to five founders giving rise to corresponding lines. To investigate whether these lines differed, we compared the recombination efficacy of transgenc lines derived from the Glast-CreER^{T2} construct using the RXRαaf2/+ and the Z/AP reporter lines. As shown in Fig. 18, the four lines obtained for this transgene differed in the extent of Cre-mediated recombination between brain regions and organs or tissues. Based on the RXRαaf2/+ reporter, all lines showed most efficient recombination in hippocampus and olfactory bulb, with strong signal from cortex and cerebellum. In other organs including skin, kidney and bone, Cre-mediated recombination occurred in some lines. The highest efficiency of excision in the brain was displayed in Tg(Glast-CreER^{T2})T45-52 transgenic line. The same lines crossed with the Z/AP reporter line showed similar regional recombination patterns although it differed in the Cre efficacy.

In summary, these results revealed differences in the recombination efficacy between transgenic lines derived from the same BAC-based transgene. Due to its high efficiency and consistency between reporter lines the Tg(Glast-CreER^{T2})T45-72 line was chosen for further analysis.

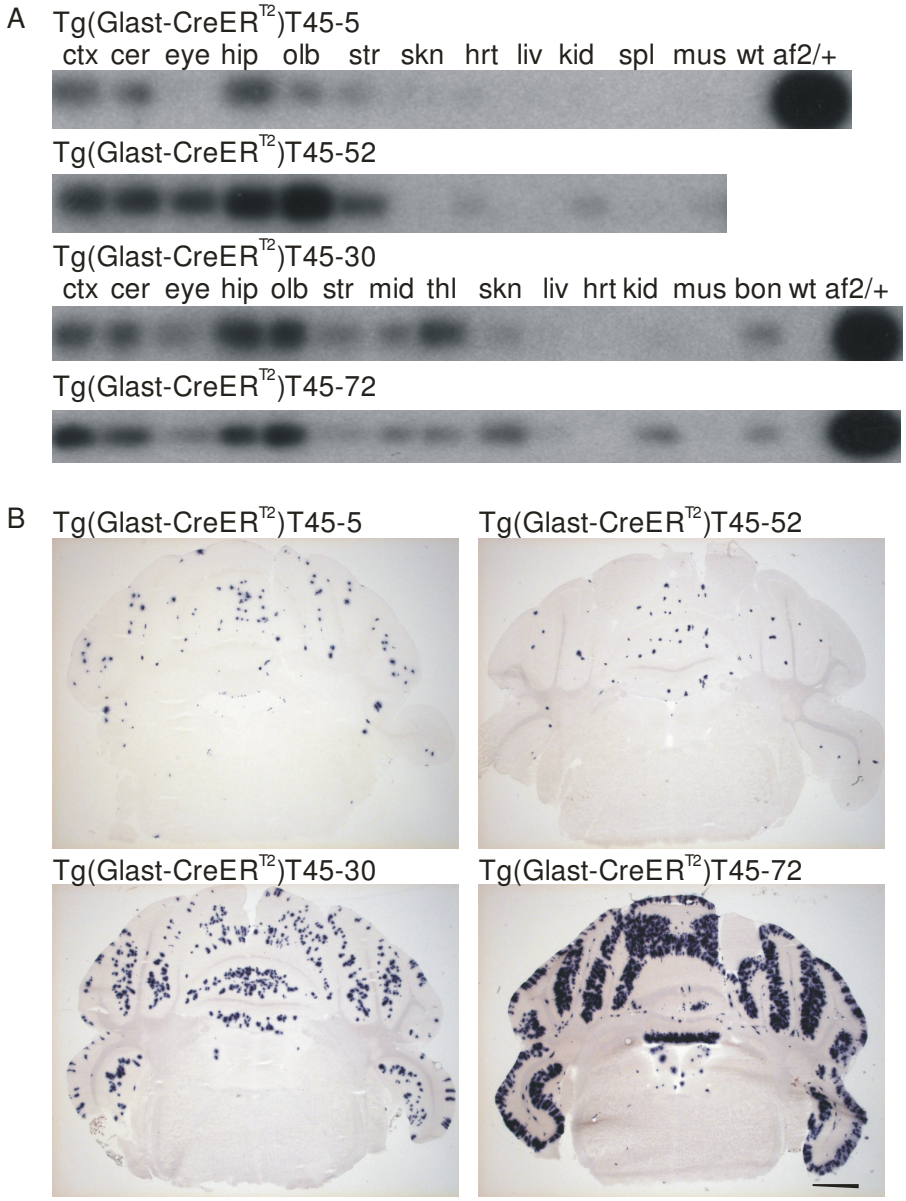

Fig. 18. Comparison of CreER^{T2} mediated recombination in different Tg(Glast-CreER^{T2}) lines derived from the same transgenesis construct

A, Autoradiograms of Southern blots of PCR products followed by hybridization with a loxP probe. Samples from indicated brain regions and organs/tissues from indicated transgenic lines crossed with the RXRαaf2/+ reporter line. B, Bright-field micrographs of coronal sections from brains of indicated transgenic lines crossed with the Z/AP reporter line that were processed for cytochemical detection of alkaline phosphatase activity. For these experiments, adult animals received single daily injections of TAM (1 mg) on five consecutive days and were sacrificed 1 (A) or 3 (B) weeks after the last TAM injection. Scale bar, 1mm.

2.5. Comparison of transgenic lines derived from different BACs for the same promoter – Cx30-CreER^{T2} lines

Next, we compared the recombination pattern in transgenesis constructs based on two different BACs to explore possible BAC-specific differences. Two lines [Tg(Cx30-CreER^{T2})T53-15 and Tg(Cx30-CreER^{T2})T53-33] were obtained from BAC RP24-368M7 and one [Tg(Cx30-CreER^{T2})T56-7] from BAC RP23-213N5. The two BACs differ in size, mainly due to the larger sequence upstream of the ATG starting codon in RP24-368M7 (see Table 1). Comparison of Cre activity at the DNA level using RXRαaf2/+ reporter line revealed that all Tg(Cx30-CreER^{T2}) lines displayed similar patterns and intensities of CreER^{T2} activity in the organs tested (Fig 17, 19A). For all lines, the strongest Cre activity was detected in cortex, cerebellum, hippocampus and mesencephalon, as well as in the skin extracted from animals injected with TAM. Vehicle-treated animals did not show recombination, apart from the skin. The similarity between lines was confirmed when Cre-mediated recombination was analysed with the Z/AP reporter line (Fig. 19B). hPLAP-positive cells were most numerous in thalamus, brain stem, cortex with some activity in hippocampus and cerebellar Bergamnn glia.

Taken together, these results suggested that both BACs used to generate transgenic lines contain regulatory sequences sufficient for robust expression of the Cx30-CreER^{T2} transgene in different brain regions. The Tg(Cx30-CreER^{T2})T53-33 line showed the highest efficacy among all other lines and was therefore selected for further characterization.

2.6. Characterization of Tg(ApoE-CreER^{T2}) and Tg(Aqp4-CreER^{T2}) transgenic lines

RT-PCR analysis revealed very low levels of Cre mRNA in the brain and in other organs of ApoE- or Aqp4-based transgenic animals (Fig. 13, 14). However, when tested with with the RXRαaf2/+, substantial CreER^{T2}-mediated excision was observed at the DNA level in the cerebellum and in other organs like liver extracted from the Tg(ApoE-CreER^{T2})T54-29 line. Vehicle did not induce any recombination (Fig. 18). In the Tg(Aqp4-CreER^{T2})T55-27 line, most efficient excision was observed in heart, spleen and muscle, while the efficiency of recombination in the brain was much lower. To test for the regional distribution of CreER^{T2} activity in the brain, we crossed these transgenic lines with the Z/AP reporter. In brains of Tg(ApoE-CreER^{T2}) x Z/AP animals Bergmann glia and cells at the border of the mesencephalon displayed hPLAP expression, but Tg(Aqp4-CreER^{T2}) x Z/AP line showed only very few hPLAP-positive cells (Fig. 20 A,B).

Taken together, the transgenic animals based on the Apoe and Aqp4 promoters showed low transcript levels of Cre. Since CreER^{T2} activity in the brain of these animals lower than in the Cx30- and Glast lines and on the other hand quite substantial in other organs, we did not investigate these lines further.

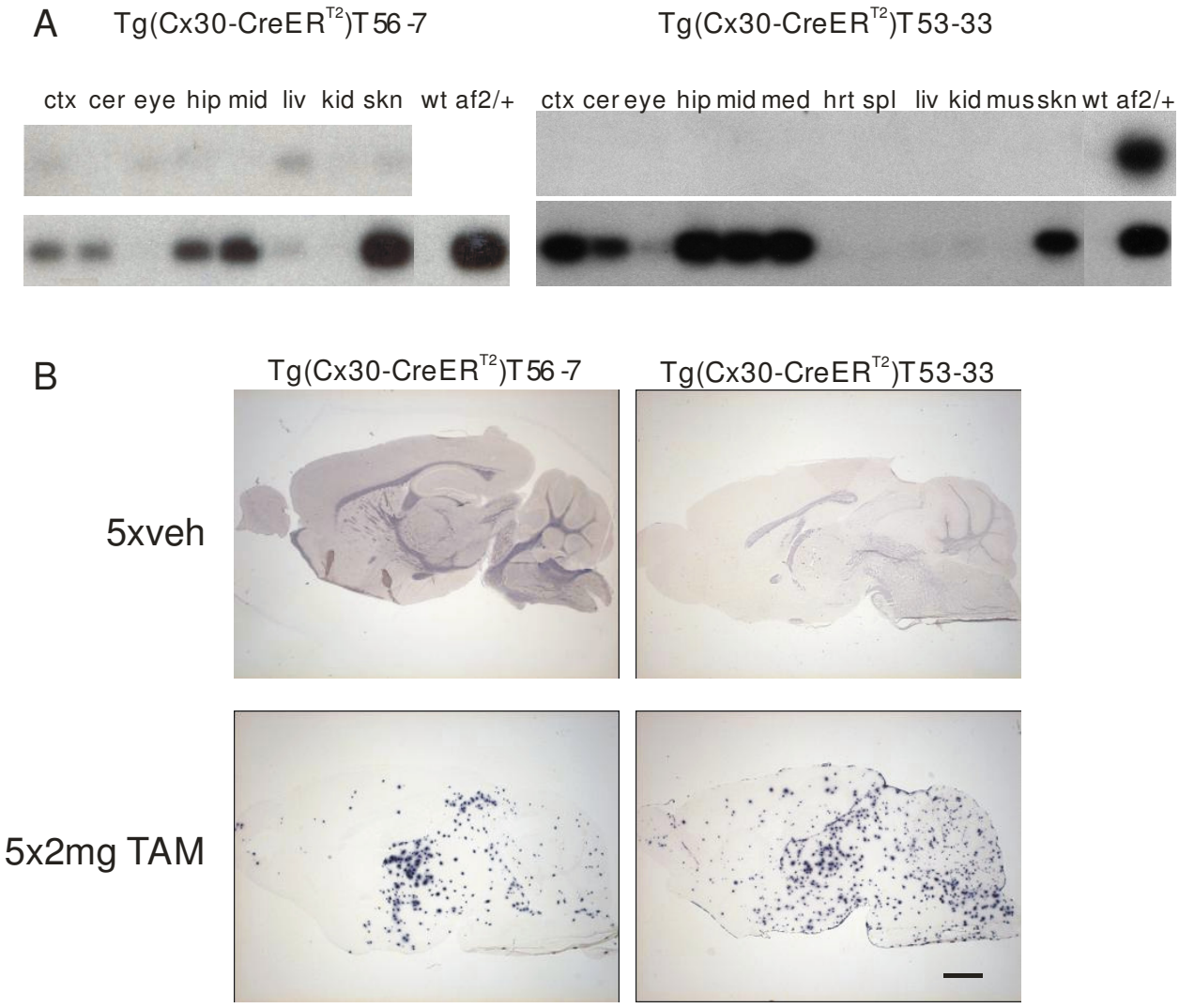

Fig. 19. Comparison of transgenic lines derived from different BACs for the Cx30 promoter
A, Autoradiograms of Southern blots of PCR products followed by hybridization with a loxP probe. Samples from indicated brain regions and organs/tissues from indicated transgenic lines crossed with the RXRαaf2/+ reporter line. Adult animals were subjected to vehicle (upper graphs) or TAM (lower graphs) treatment. B, Bright-field micrographs of sagittal sections from brains of indicated transgenic lines crossed with the Z/AP reporter line that were processed for cytochemical detection of alkaline phosphatase activity. Scale bar, 1mm.

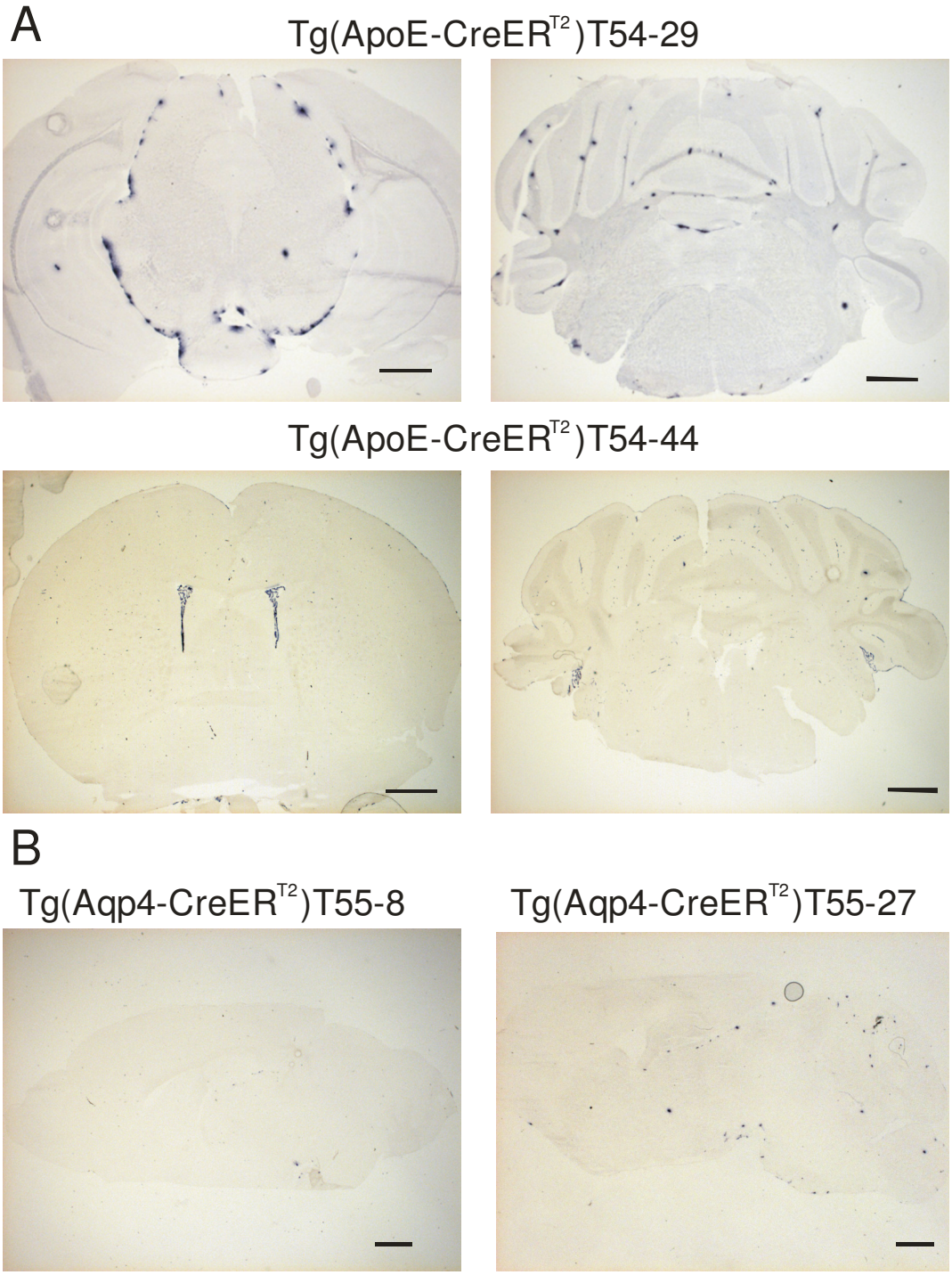

Fig. 20. Distribution of CreER^{T2}-mediated recombination in ApoE- and Aqp4-based transgenic lines
Bright-field micrographs of sagittal sections from brains of Tg(ApoE-CreER^{T2}) (A) or Tg(Aqp4-CreER^{T2}) (B) crossed with the Z/AP reporter line that received 5x1mg of TAM and were sacrificed 3 weeks after the last TAM injection. Sections were processed for cytochemical detection of alkaline phosphatase activity. Scale bar, 1mm.

3. DETAILED CHARACTERIZATION OF SELECTED TRANSGENIC LINES

To explore the potential of the selected transgenic lines for inducible, astrocyte-specific gene manipulation, we characterized the regional distribution and cellular specificity of Cre activity and quantified its efficiency in selected brain areas. For these experiments, mice received single daily injections of either vehicle or 2 mg of TAM for 5 consecutive days (Fig. 22-30) and were sacrificed within 1 (ROSA26R) or 4 (Z/AP) weeks after the last injection.

3.1. Characterization of Tg(Glast-CreER^{T2})T45-72 transgenic line

To determine the distribution of cells displaying CreER^{T2} activity we first analysed mice from crosses of Tg(Glast-CreER^{T2})T45-72 with the Z/AP or with the ROSA26R reporter line. No expression of β-gal was observed in brains from vehicle-injected animals (Fig. 22A). In brains from TAM-treated animals, cells expressing reporter enzymes were most numerous in the molecular layer of the cerebellum. Other regions with significant numbers of β-gal/hPLAP-positive cells were hypothalamus, cortex and hippocampus. Analysis at higher magnification revealed the cellular morphology of hPLAP-expressing cells (Fig. 21). Cells in the cerebellar molecular layer showed a radial morphology and closely resembled Bergmann glia (Fig. 22B). In cortex (Fig. 22 E), hippocampus (Fig. 22F) and hypothalamus (Fig. 22H) hPLAP-positive cells had small somata and stellate morphology and thus resembled astrocytes. Numerous hPLAP-positive cells were also observed in the subgranular layer of dentate gyrus, where they displayed radial morphology (Fig. 22 F, 24C) and in the lateral wall of lateral ventricles (Fig. 22). Only very few cells showing recombination were detected in thalamus (Fig. 22G), medulla oblongata (Fig 22 C), midbrain (Fig. 22D) or cerebellar white matter (Fig 22B). In the retina, radial cells resembling Muller glia expressed hPLAP (Fig. 24).

We studied the identity of cells undergoing CreER^{T2}-mediated recombination in mice from the Tg(Glast-CreER^{T2})T45-72 x ROSA26R line. Double immunohistochemical staining was performed on brain sections from these animals with antibodies directed against β-gal and against cellular markers: S100β, Gfap for astrocytes or NeuN for neurons. Analysis of stained sections by confocal microscopy revealed that cells expressing β-gal were positive for the astrocyte marker, but did not colocalize with the neuronal marker (Fig. 23).

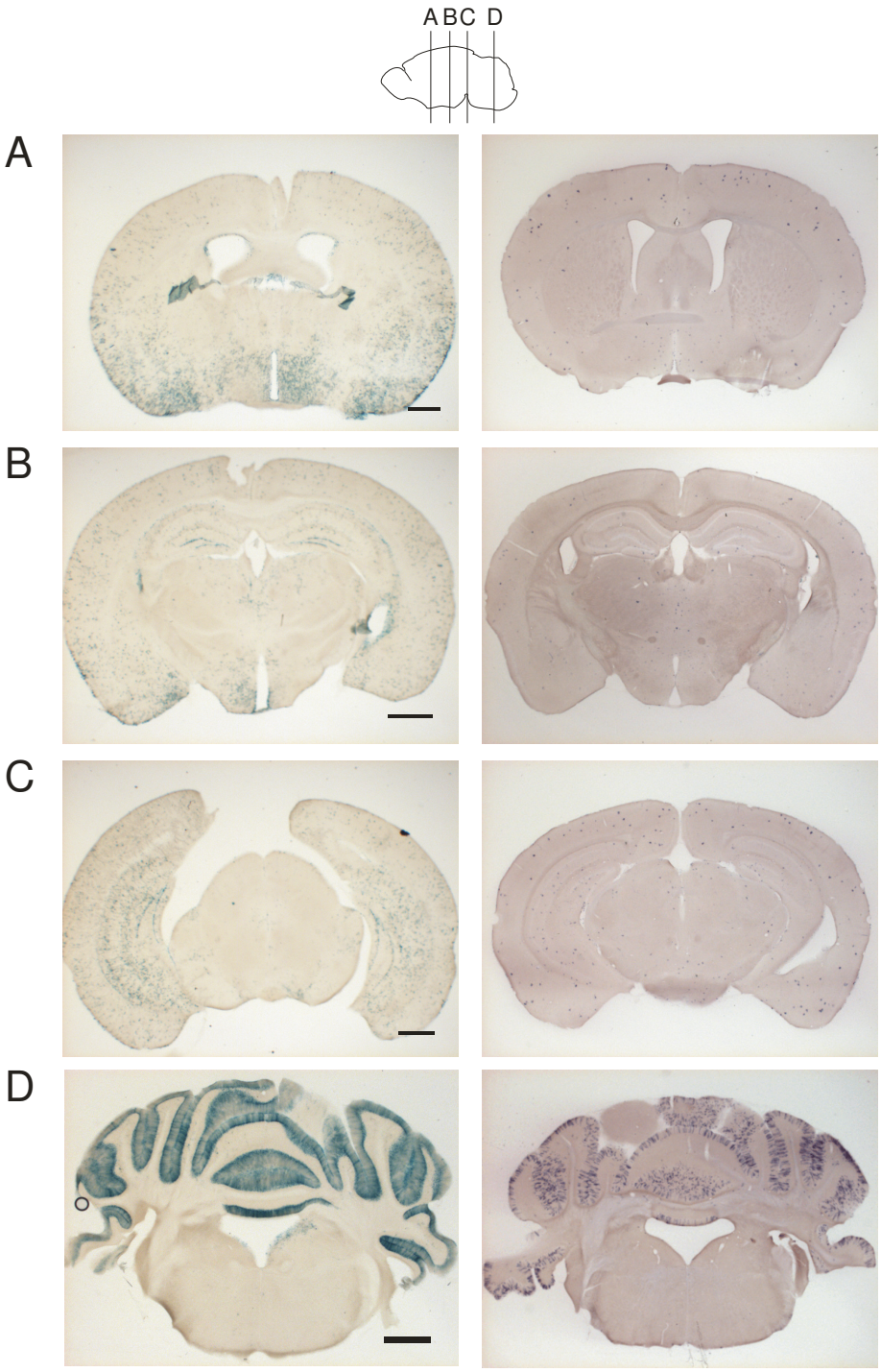

Fig. 21. Regional distribution of CreER^{T2}-mediated recombination in the Tg(Glast-CreER^{T2})T45-72 line
Bright field micrographs of X-gal (left column) and X-phosphate (right column) stained coronal sections of brains from adult animals from crosses of Tg(Glast-CreERT2)T45-72 with the ROSA26R (left) or Z/AP (right) reporter line, respectively. Adult mice were injected with 5 x 2 mg of TAM and sacrificed 1(ROSA) or 3 (Z/AP) weeks after last injection. Scale bars, 1 mm.

Fig. 22. Sub-regional distribution of CreER^{T2}-mediated recombination in Tg(Glast-CreER^{T2})T45-72 line

Bright field micrographs of X-gal (left, right A) or X-phosphate (right, except A) coronal brain sections from adult animals from Tg(Glast-CreER^{T2})T45-72 crossed with ROSA26R (left, right A) or Z/AP (right, except A) injected with vehicle (A) or 5x2mg of TAM (B-H) and sacrificed 1 week after last injection. A. Cerebellum/hippocampus B. Cerebellum, C. Medulla oblongata, D. Midbrain, E. Cortex, F. Hippocampus, G. Thalamus, H. Hypothalamus. Scale bars, 0.2 mm (A, B, E-H), 0.5 mm (C, D).

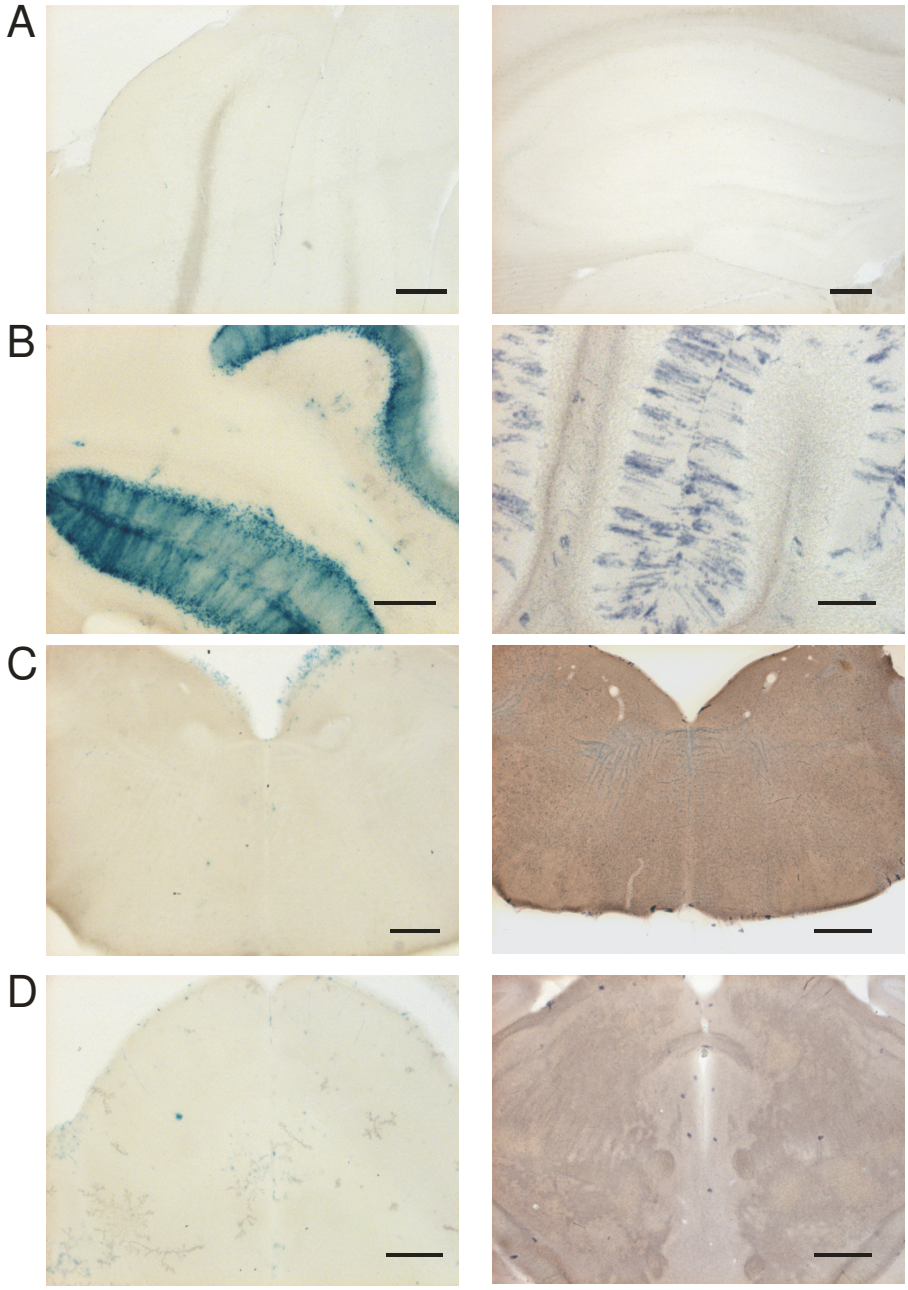

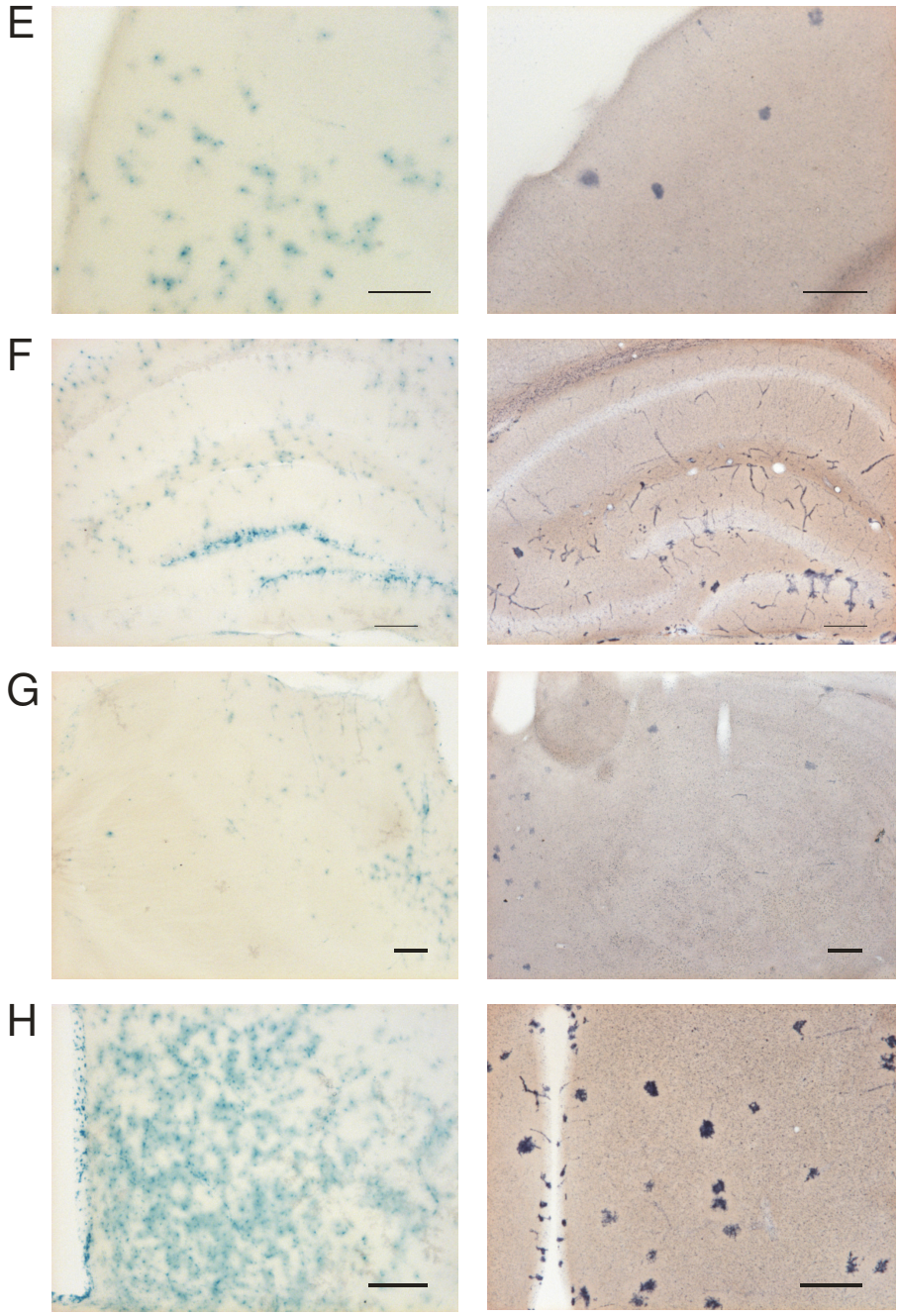
E
F
G
H

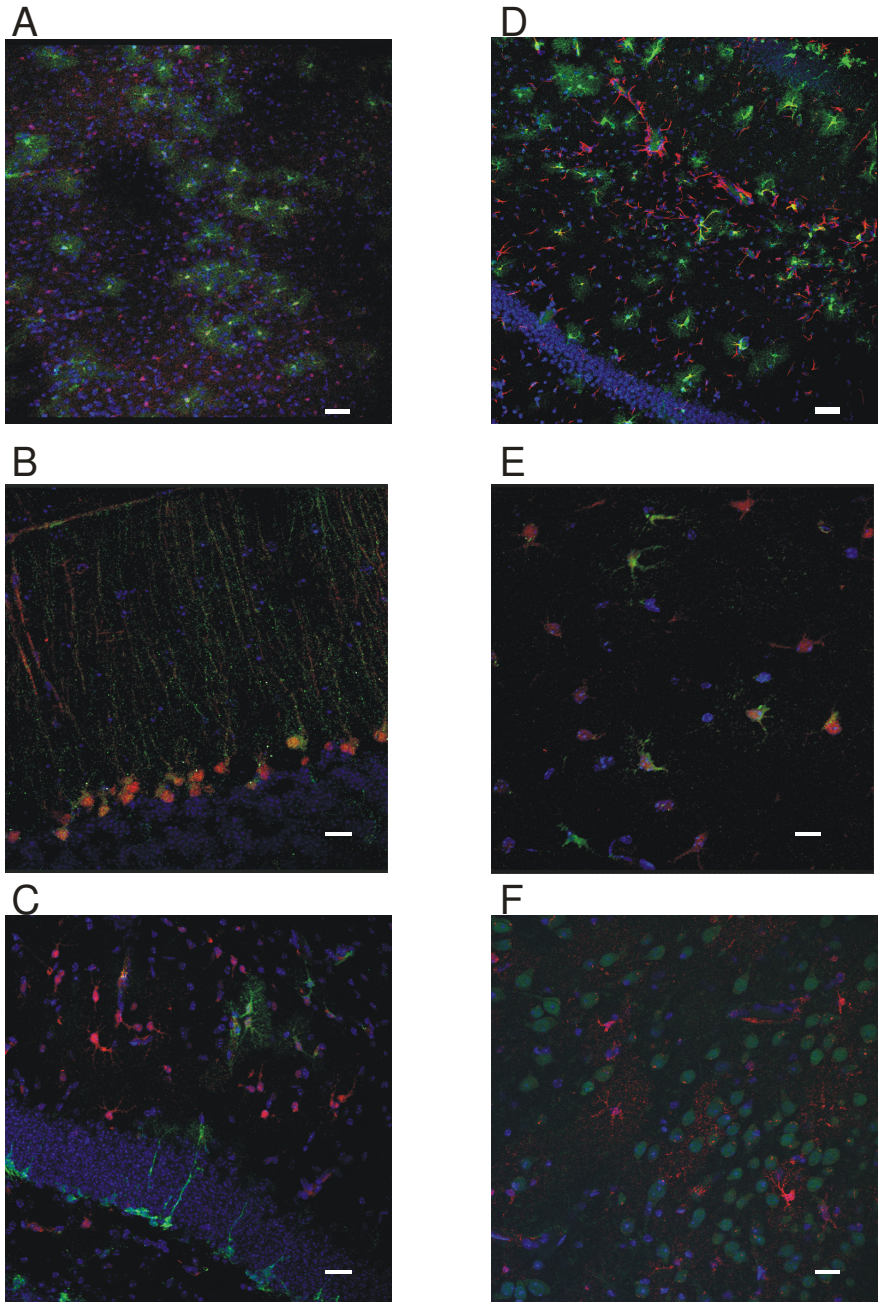

Fig. 23. Cellular specificity of CreER^{T2}-mediated recombination in Tg(Glast-CreER^{T2})T45-72 transgenic line

Confocal fluorescence micrographs (merged z-stacks) of coronal brain sections that were immunolabeled for β-gal (green) and cellular markers – S100β (A-C, E), Gfap (D) and NeuN (F) and labelled by the nuclear marker DAPI (blue). Adult transgenic mice crossed with the ROSAR26 reporter line were injected with 5 x 2 mg TAM and sacrificed 5 days after the last injection. A, F, cortex; B, cerebellum; C, D, E, hippocampus. Scale bars, 50 µm (A,D), 20 µm (B, C, E, F).

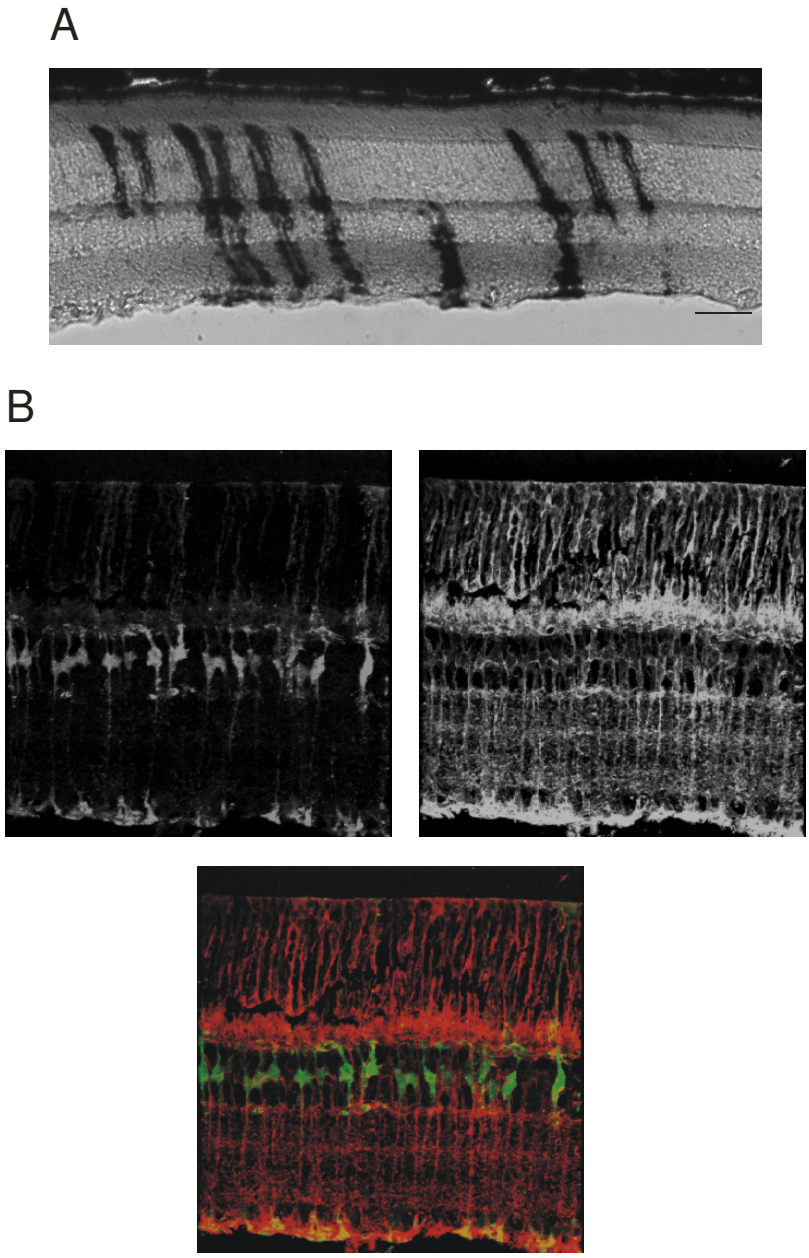

Fig. 24. CreER^{T2}-mediated recombination in retinae of the Tg(Glast-CreER^{T2}) line
A, Bright field micrographs of X-phosphate stained retinal sections from adult TAM-injected Tg(Glast-CreERT2) x Z/AP animals. B, Confocal fluorescence micrographs (merged z-stack) of retinal sections that were immunolabelled for β-Gal (top, left) and Glast (top right). Adult Tg(Glast-CreERT2) x ROSA26R animals were injected with 5x2 mg TAM and sacrificed 5 days after the last injection. Bottom, merged image. Scale bars, 50 µm (A), 20 µm (B).

In retinae of bigenic mice, β-gal-positive cells were identified as Muller glia, since – apart from their characteristic morphology – they expressed Glast as shown by immunohistochemical staining (Fig. 24), which was performed by A. Niemiec. In cooperation with V. Prevot (INSERM UR816, Lille, France) β-gal-positive radial cells lying at the wall of the third ventricle were identified as tanycytes. In cooperation with C. Goritz and J. Frisen (Karolinska Institute, Sweden), β-gal expressing radial cells in the subgranular layer of dentate gyrus were identified as neural stem/progenitor cells based on their localization, morphology and expression of Gfap. Additionally, in brain sections obtained from animals sacrificed two weeks after the last TAM injection (19 days after the first TAM injection), β-gal-positive cells expressing doublecortin (marker of immature neurons) and NeuN were identified in the hippocampus and olfactory bulb. This indicated that Tg(Glast-CreER^{T2})T45-72 can be used to target neuronal stem cells.

To estimate the efficiency of astrocyte-specific, Cre-mediated recombination we examined sections from the Tg(Glast-CreER^{T2})T45-72 X ROSA26R line, since the ROSA26R reporter line displayed generally higher numbers of reporter protein-positive cells than Z/AP (Fig. 21, 22). Since there is currently no marker that would label all astrocytes, we selected S100β among the various proteins for which astrocyte-specific expression was reported, namely Gfap, Glast, Glt-1, glutamine synthetase, connexin 30 or 43 or aquaporin 4. S100β is expressed by a majority of astrocytes and its distribution throughout the brain is rather ubiquitous (Ogata and Kosaka, 2002). However, the activity of S100β promoter was also observed in neurons (Vives et al., 2003) and oligodendrocytes (Hachem et al. 2005). For cell counts, S100β-positive cells with morphology that clearly did not resemble astrocytes were excluded. We determined two fractions of cells (Table 5), namely the percentage of cells that were β-Gal and S100β positive among all S100β+ cells and the fraction of cells that were positive for β-gal, but not for S100β. The first fraction was highest in Bergmann glia, where virtually all S100β-positive cells displayed β-gal activity (Fig. 23). The fraction of cells that were β-gal-positive, but did not stain for S100β was very low reaching maximally 1% in cortex and cerebellum and 5% in the hippocampus. Taken together, these data showed that the Tg(Glast-CreER^{T2})T45-72 line allows to target distinct populations of astrocytes in the cortex, hippocampus, cerebellum and the retina of adult mice with efficacies of up to 90%. Notably, this line also allows to target adult neuronal stem cells in neurogenic regions.

	Ganat et al., (2006) (Gfap/β-gal)	Mori et al. (2006)	Tg(Glast-CreER^{T2})T45-72	Tg(Cx30-CreER^{T2})T53-33
Cortex	62%	81%	>99%	~92%
Bergmann glia	82%	98%	>99%	>99%
Hippocampus			~98%	~92%
	(Hirrlinger et al. 2006)	Mori et al., (2006)	Tg(Glast-CreER^{T2})T45-72	Tg(Cx30-CreER^{T2})T53-33
Cortex	26%	30%	15 +/- 5%	36 +/- 3%
Cerebellum - Bergmann glia	88%	86%	97 +/- 4%	86 +/- 4%
Thalamus	49%		3 +/- 2%	65 +/- 15%
Hippocampus	32%		15 +/- 5%	32 +/- 6%
Medulla	41%		1 +/- 1%	52 +/- 3%
Cerebellum – granule cell layer + white matter			12 +/- 6%	35 +/- 16%
Retina (β-gal+/Glast+)			27 ± 5% (n = 4)	0
Hypothalamus			53 +/- 13%	54 +/- 6%
Striatum			8 +/- 6%	33 +/- 9%

Table 5. Comparison of the specificity and efficiency of CreER^{T2}-mediated recombination between Tg(Glast-CreER^{T2})T45-72 and Tg(Cx30-CreER^{T2})T53-33, Tg(hGfap-CreER^{T2}) (Ganat et al., 2006; Hirrlinger et al., 2006) and Tg(Glast-CreER^{T2}) (Mori et al, 2006).

Upper part: Approximate fraction of cells expressing marker protein Gfap or S100β among reporter protein-positive cells. Lower part: approximate values of fraction of reporter protein positive cells among the S100β positive cells (n=3 section/animal, 3 animals).

3.2. Characterization of Tg(Cx30-CreER^{T2})T53-33 line

The line based on the Cx30 promoter was characterized in a similar fashion as described for the Glast line. The regional distribution of cells displaying CreER^{T2} activity was determined using the Z/AP reporter line. In vehicle-treated mice, no cells showing CreER^{T2}-mediated recombination were detected (Fig. 19B). In brains from TAM-treated animals, hPLAP-positive cells were numerous throughout the cortex, striatum, corpus callosum, hippocampus, thalamus, hypothalamus, midbrain, brain stem and in the cerebellum (Fig. 25, 26). Higher magnification revealed that hPLAP-positive cells were small and displayed stellate morphology closely resembling astrocytes in all brain regions examined including cortex (Fig. 26E), hippocampus (Fig. 26F), thalamus (Fig. 26G), hypothalamus (Fig. 26H), medulla oblongata (Fig. 26B), midbrain (Fig. 26C), grey matter of spinal cord (Fig. 26D) and white matter in cerebellum (Fig. 26A). Similar as in the Glast-line, cells in the molecular layer of the cerebellum showed a radial morphology typical of Bergmann glia (Fig. 26A). However, in contrast to the Glast line, no Cre -mediated recombination was observed in the neural retina.

To confirm the identity of cells showing Cre activity, double immunohistochemical stainings were performed on sections obtained from Tg(Cx30-CreER^{T2})T53-33 x ROSA26R animals (Fig. 27, 28) using the same antibodies as described above. The presence of β-gal positive cells in white matter (Figs. 25, 26A) prompted additional stainings with antibodies against the oligodendrocyte marker CNPase (Fig. 28D). As shown by confocal microscopy, β-gal colocalized with astrocytic markers (Fig. 28A, B), but not with the neuronal (Fig. 28C) or oligodendrocyte marker (Fig. 28D) indicating that the Cx30 promoter drives Cre expression exclusively in astrocytes.

To estimate the efficiency of Cre-mediated recombination, we stained sections for S100β and β-Gal and determined the fractions as described above. The highest efficiency of recombination was estimated in Bergmann glia, as well as in astrocytes from thalamus, medulla, hippocampus and cortex (Table 4). The number of β-gal-positive, but S100β-negative cells was also low reaching 8% in cortex and hippocampus, 1% in thalamus and less than 1% in cerebellum and medulla oblongata.

Taken together these results showed that the Tg(Cx30-CreER^{T2})T53-33 line allows for inducible genetic manipulation in astrocytes residing in cortex, hippocampus, thalamus, midbrain, medulla oblongata, white matter and cerebellar Bergmann glia.

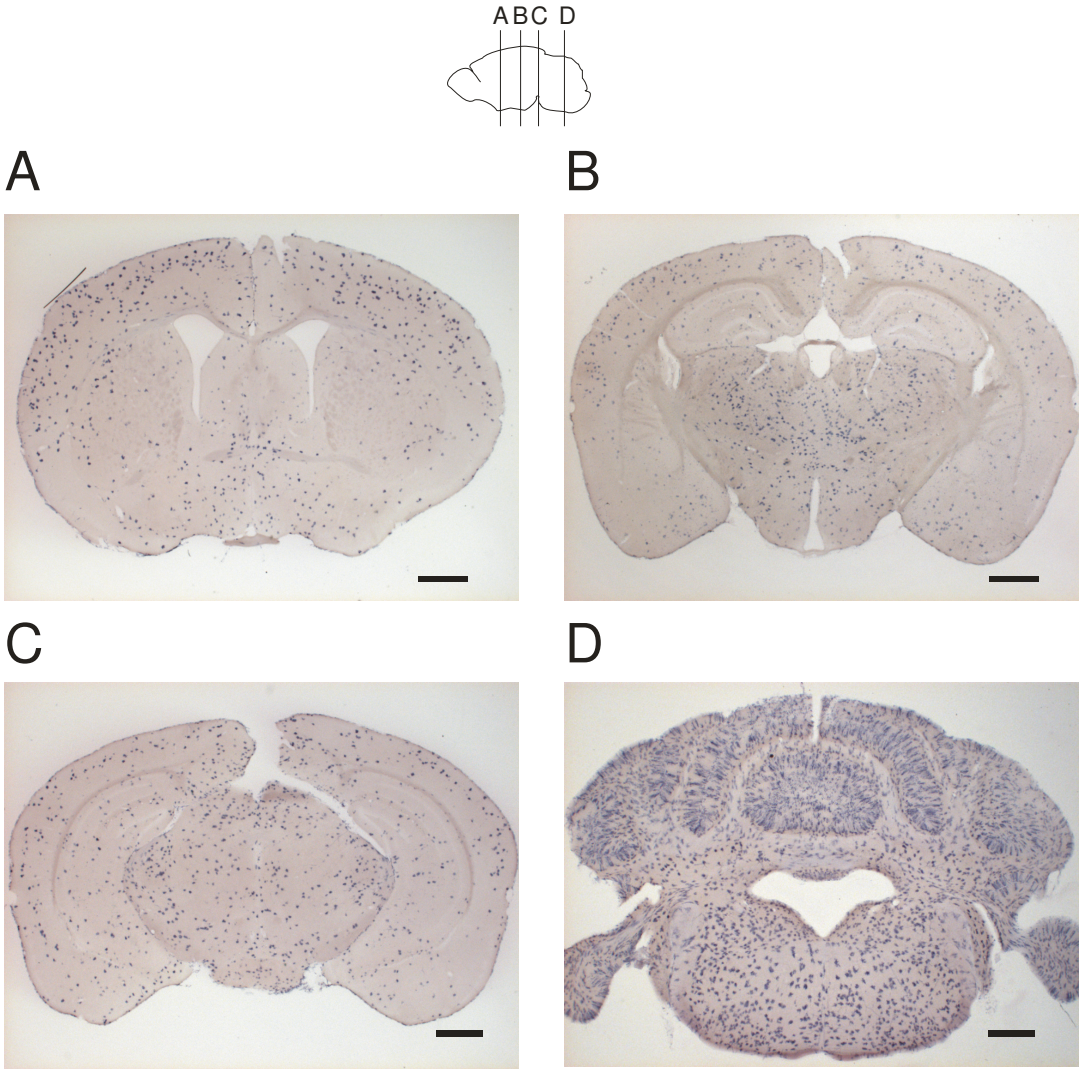

Fig. 25. Regional distribution of CreER^{T2}-mediated recombination in Tg(Cx30-CreER^{T2})T53-33 transgenic line
Bright field images of X-phosphate stained coronal sections of brains from adult animals from Tg(Cx30-CreER^{T2})T53-33 x Z/AP injected with TAM and sacrificed 3 weeks after last injection. Scale bars, 1 mm.

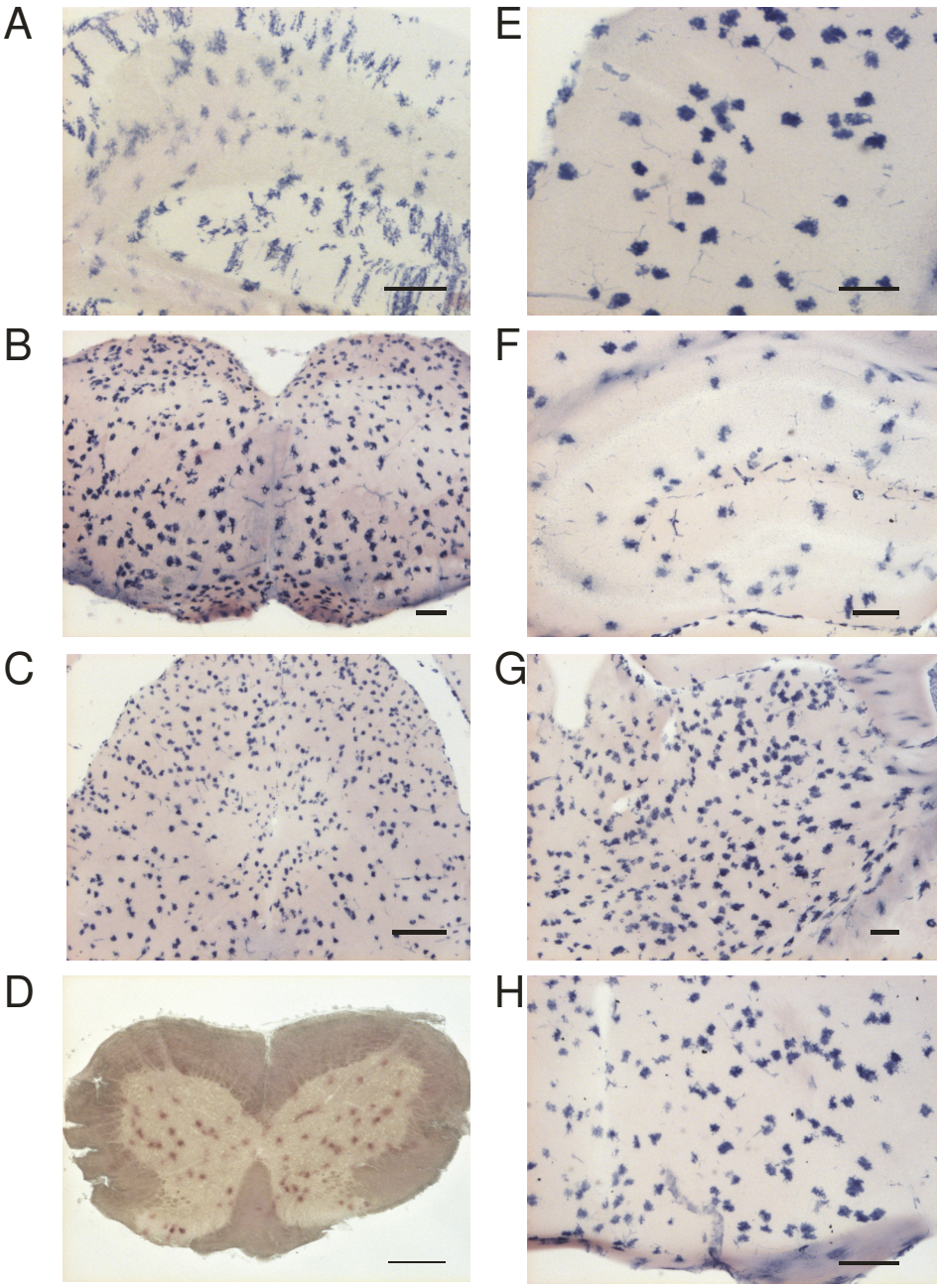

Fig. 27. Subregional distribution of CreER^{T2}-mediated recombination in Tg(Cx30-CreER^{T2})T53-33 transgenic line
Bright field images of X-phosphate stained coronal sections of brains from adult animals from Tg(Cx30-CreER^{T2})T53-33 x Z/AP injected with TAM and sacrificed 3 weeks after last injection. A. Cerebellum, B. Medulla oblongata, C. Midbrain, D. Spinal cord, E. Cortex, F. Hippocampus, G. Thalamus, H. Hypothalamus. Scale bars, 0.2 mm (A, B, E, F, G) and 0.5 mm (C, D).

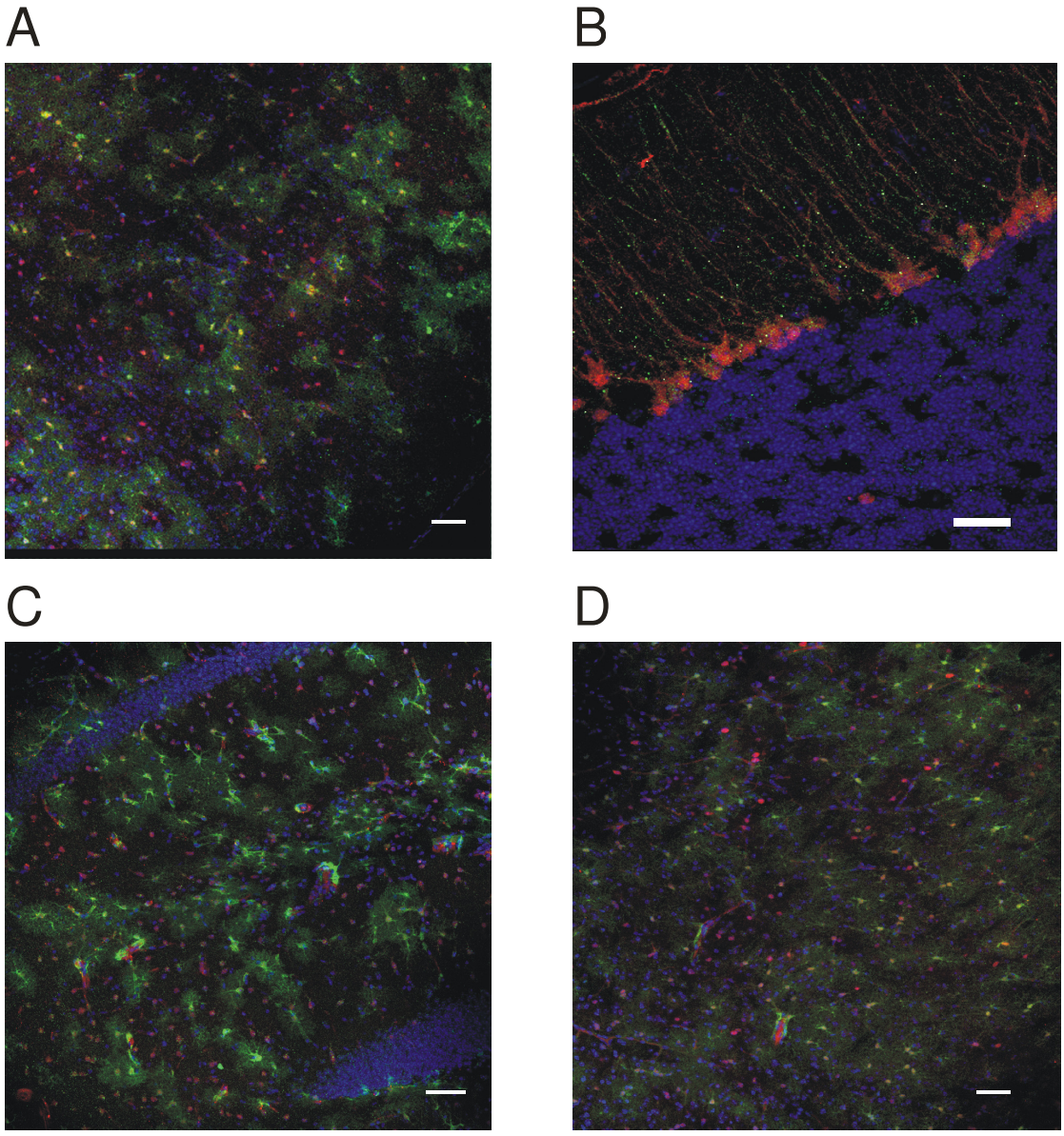

Fig. 28. Cellular specificity of CreERT2-mediated recombination in Tg(Cx30-CreERT2)T53-33 transgenic line
Confocal fluorescence micrographs (merged z-stack) of coronal sections of brains from adult Tg(Cx30-CreER^{T2})T53-33 x ROSA animals that were injected with TAM and sacrificed 5 days after the last injection. Sections were immunolabelled for β-gal (green) and S100β (red) and labelled with the nuclear marker DAPI (blue). A. Cortex, B. Cerebellum, C. Hippocampus, D. Thalamus Scale bar, 50 µm (A, C, D), 20 µm (B).

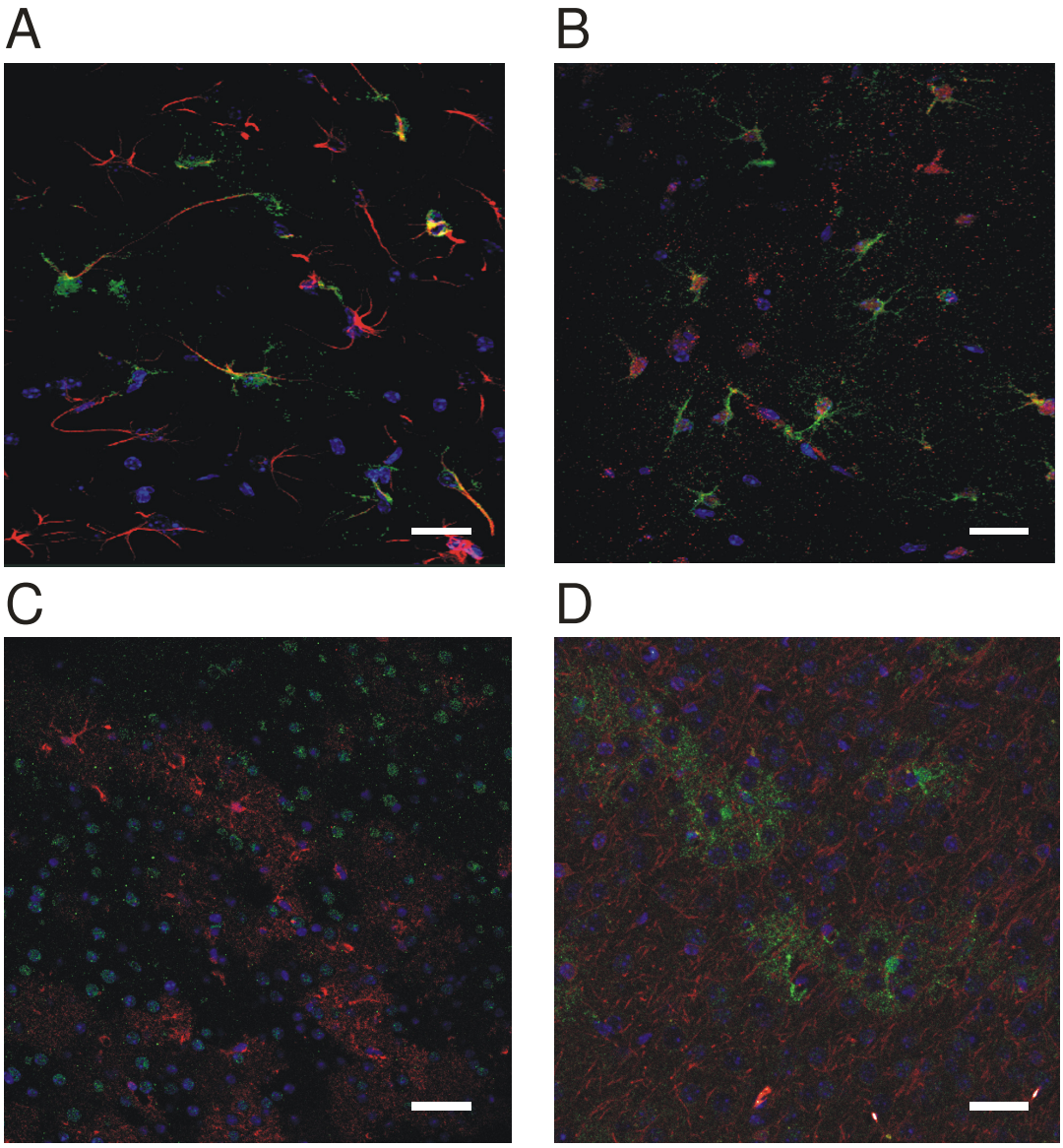

Fig. 28. Cellular specificity of CreERT2-mediated recombination in Tg(Cx30-CreERT2)T53-33 transgenic line

Confocal fluorescence micrographs (merged z-stack) of coronal sections of brains from adult Tg(Cx30-CreER^{T2})T53-33 x ROSA animals that were injected with TAM and sacrificed 5 days after the last injection. Sections were immunolabelled for β-gal (green, red in C) and cellular markers (red, green in C): Gfap(A), S100β (B), , NeuN (C) and CNPase (D), and labelled with the nuclear marker DAPI (blue). A, B, Cortex, C, D, Hippocampus. Scale bar, 20 µm (A, B, D), 50 µm (C).

DISCUSSION

1. COMPARISON OF NEWLY GENERATED TRANSGENIC MICE WITH EXISTING *IN VIVO* MODELS TO STUDY ASTROCYTES

In this project new transgenic mouse models for inducible gene ablation in astrocytes have been generated. Two of these lines, which are based on the Glast and Cx30 promoter, allow for efficient excision of loxP-flanked genes by CreER^{T2} recombinase and should therefore complement the range of existing animal models to study astrocyte function *in vivo* .

To enable astrocyte-specific, inducible gene ablation a set of transgenic lines taking advantage of inducible CreER^{T2} recombinase system were recently reported using different approaches. Three independent groups (Casper et al. 2007; Ganat et al. 2006; Hirrlinger et al. 2006) used conventional transgenesis engaging the 2.2 kb hGfap promoter to drive CreER^{T2} recombinase. Aditionally, knock-in approaches were used to drive the expression of CreER^{T} recombinase from the Cx43 locus (Eckardt et al., 2004) and of CreER^{T2} from the Glast locus (Mori et al., 2006). In case of Tg(Cx43-CreER^{T}) line, astrocyte-specific expression was not proven, since this line was used for inducible deletion of Cx43 in the heart to overcome lethality due to the cardiac dysfunction (Eckardt et al., 2004).

Our transgenic lines showed Cre activity in selected peripheral organs. In the Tg(Glast-CreER^{T2})T45-72 line Cre-mediated activity at the DNA level was detected in heart, spleen and skin, whereas in the Tg(Cx30-CreER^{T2})T53-33 line peripheral Cre activity was limited to the skin. In none of the other studies cited above the activity of CreER^{T2} outside the brain was studied, apart from Tg(Cx43-CreER^{T}), where Cre-mediated recombination was detected in lung, heart and muscles. Therefore it is not possible to compare Cre activity in peripheral organs of transgenic lines generated in this project with other transgenic lines. This information is however important, since gene ablation in peripheral organs may confound phenotypes that would falsely be attributed to astrocyte-specific defects.

In the Tg(Glast-CreER^{T2})T45-72 line Cre-mediated recombination was observed in cortical and hippocampal astrocytes, as well as in tanycytes, Muller glia and Bergmann glia, whereas in Tg(Cx30-CreER^{T2})T53-33 it was limited to astrocytes throughout the brain. The comparison of our data with those from other studies (Table 5, upper part) confirms the high percentage of astrocyte marker positive cells among the reporter protein-positive cells. On the other hand very low or absent colocalization of reporter protein with neuronal or oligodendroglial markers were noticed in all lines. Altogether these data point to the very high degree of specificity of targeting astrocytes using hGfap, Glast or Cx30 promoter in the adult brain.

So far, the molecular and physiological characteristics of the astrocytes that are targeted by the Glast- and Cx30 promoters have not been investigated. However, since GluT cells were reported to display high activity of hGfap promoter (Matthias et al., 2003), to express glutamate transporters (Matthias et al., 2003; Zhou and Kimelberg, 2006) and to be coupled via gap junctions (Wallraff et al., 2004), it seems probable that all transgenic lines mentioned here target the GluT subpopulation. Systematic investigation of coexpression of various astrocytic markers reported that Glast is expressed by all Gfap-positive cells in the hippocampus and in a fraction of Gfap-negative astrocytes (Zhou and Kimelberg, 2006). Indeed, although not quantitatively estimated, the expression of β-gal displayed excellent overlap with Gfap in Tg(Glast-CreER^{T2})T45-72 and Tg(Cx30- CreER^{T2})T53-33 lines. To further elucidate the issue of identity of targeted cells electrophysiological studies would be necessary. It appears, however, that astrocytes may constitute a very heterogeneous population of cells (Kimelberg 2004; Walz 2000). In fact, a recent study described a high degree of diversity of these cells at the molecular and morphological level and suggested a regional specification of astrocytes (Emsley and Macklis, 2006). Further studies are now necessary to better define the diversity of astrocytes and these are feasible now with the new transgenic mouse models.

A high level of CreER^{T2} activity was observed in neuronal stem cells in lines based on the Glast (Mori et al., 2006; this study), hGfap (Ganat et al. 2006) and the nestin promoter (Imayoshi et al., 2006); Forni et al., 2006; Burns et al., 2007). These lines constitute new models for investigations of adult neurogenesis. Interestingly, a potential interest in the Tg(Cx30-CreER^{T2})T53-33 line arises from the fact that no signs of recombination in neuronal stem cells were observed . Since neuronal progenitors in the adult brain share most of the molecular phenotype with astrocytes, this transgenic line may serve as a unique tool to target astrocytes without affecting adult progenitor cells.

The highest efficiency of Cre-mediated recombination in both lines was observed in Bergmann glia, with additional high efficiency in Tg(Cx30-CreER^{T2})T53-33 throughout the brain. Similarly to our approach, Mori et al. (2006) and Hirrlinger et al. (2006) performed a quantitative estimation of efficiency of CreER^{T2} mediated recombination by counting reporter protein positive cells among the S100β-positive cells, which allows for a direct comparison with our results. Concerning the Glast line, there is a remarkable similarity between the efficacies reported by Mori et al. (2006) and our data. On the other hand, our approach allows to estimate the efficiency of targeting S100β-positive cells. The actual efficiency of Cre-

mediated recombination in subpopulation expressing CreER^{T2} (i.e. Glast- OR Cx30-positive cells) may be higher than reported here. It was estimated that Glast is expressed in 60-70% of S100β-positive astrocytes (Mori et al., 2006), unfortunately, no data exist on the co-expression of Cx30 and S100β. Taking into account the observation that S100β labels both GluT and GluR subpopulation of astrocytes, that are roughly equal (Matthias et al., 2003) it may be concluded that our lines target GluT cells with higher efficiency than described here.

2. DETERMINANTS OF EFFICIENT CRE-ER^{T2} MEDIATED RECOMBINATION

The quality of transgenic lines engaging CreER^{T2} activity depends crucially on parameters like germ-line transmission, high expression of Cre transcript and an efficient regime for ligand administration.

In this study, the efficacy at which founders were obtained from microinjected oocytes was around 5% and thus similar to traditional transgenesis with short constructs (Houdebine, 2005). The efficiency of germ-line transmission of the transgene reached was very high and reached almost 90%, as it was observed in 13/15 cases. Similarly high rates have been observed in previous studies that used BAC-based transgenesis (Yang et al., 1997; Antoch et al., 1997) underlining the efficacy of this approach. The reason, why none of the lines derived from the Gfap-containing BAC showed germ line transmission is unclear. One explanation could be that the transgene insertion disrupted genes that are necessary for reproduction. Alternatively, the transgenesis construct itself may have interfered with reproduction possibly due to overexpression of unwanted sequences from the BAC.

Transgenesis with short constructs often results in a high variability between lines derived from a given transgene. The reason for this is that transgene expression depends on its insertion site in the genomic DNA (Hatada et al., 1999) and may be affected by position effect variegation (Heaney and Bronson, 2006). To avoid the influence of neighboring DNA, the use of insulators was shown to greatly increase the efficiency of transgene expression (Giraldo et al., 2003), and the 5' and 3' regions on the BAC beyond the promoter regions of interest may act as such insulator sequences and enhance the efficiency of transgene expression (Lee et al., 2001). This was confirmed by our study, since all transgenic lines showed expression of active CreER^{T2} protein.

A crucial determinant for the efficiency of CreER^{T2} is its level of expression. This is supported by two observations. First, a significant difference between Tg(Glast-CreER^{T2})T45-

72 line and Tg(Glast-CreER^{T2})T45-5 line in terms of CreER^{T2} transcript levels was mirrored by the level of Cre-mediated recombination as indicated by different reporter lines. Second, in all Tg(Cx30-CreER^{T2}) lines high levels of Cre mRNA resulted in efficient recombination in respective brain regions, whereas conversely low mRNA levels of Tg(ApoE-CreER^{T2}) and Tg(Aqp4-CreER^{T2}) resulted in low Cre activity.

Transcription of CreER^{T2} was driven by regulatory sequences of respective genes contained in the BACs, which were reported to ensure faithful and efficient expression of transgenes (Heintz 2001). Indeed, in case of Tg(Glast-CreER^{T2})T45-72 and Tg(Cx30-CreER^{T2}) lines, the expression pattern of Cre mRNA followed the activity of endogenous promoter as indicated by previous studies (Glast: Berger and Hediger 2006; Schmitt et al. 1997; Torp et al. 1994; Cx30: Dahl et al., 1996; Kunzelmann et al., 1999). No differences were observed between transgenic lines derived from two different BACs in case of Tg(Cx30-CreER^{T2}) lines suggesting that both contain regulatory sequences for specific and efficient expression of the transgene from Cx30 locus.

The suitability of BACs as transgene carriers is further supported by a high similarity in terms of Cre activity between Tg(Glast-CreER^{T2})T45-72 generated in this study with the knock-in of CreER^{T2} to the Glast locus published recently (Mori et al., 2006). Both approaches resulted in efficient astrocyte-specific CreER^{T2} mediated recombination, although different protocols of TAM injections were used [5x2x1 mg of TAM in Mori et al., (2006), 5x2 mg TAM in this study]. However, Mori et al. (2006) did not report eventual differences between generated transgenic lines. In our study, differences in Cre mRNA levels were observed between two Tg(Glast-CreER^{T2}) originating from the same BAC. This observation may suggest that although BACs are reported to be independent of the site of insertion to genomic DNA (Giraldo and Montoliu, 2001), it may not be true in all cases. Alternatively, there may have been a difference in the number of copies of the Glast-CreER^{T2} transgene, since BACs allow for copy number-dependent transgene delivery (Antoch et al., 1997). This issue, as well as other possible causes like disintegration of the BAC after transgenesis (Kaufman et al., 1999) cannot be excluded.

Unfortunately, our results so far indicate that the Apoe-based construct did not recapitulate the natural gene expression pattern. This may have been due to different reasons. The first arises from the fact that the cellular specificity of ApoE expression is regulated by cell-specific enhancers located few kilobase pairs downstream of the gene (Grehan et al., 2001). It is possible that the insertion of the CreER^{T2} coding cassette changed the local DNA structure and impaired efficient transcription from this region. Alternatively, since Cre mRNA

was detected at a certain level, the activity of the Apoe promoter contained in BAC may be weak under normal conditions. A recent study on new transgenic mice, where the expression of a fluorescent protein was driven by the endogenous Apoe promoter, revealed the activity of the latter in discrete populations of astrocytes and endothelial cells (Xu et al., 2006). In our study Cre activity visualized by the Z/AP reporter line appeared in undefined cells in the mesencephalon as well as in cells from the choroid plexus. This suggested that only those cells with very strong promoter activity show Cre-mediated recombination. A similar correlation was observed for other transgenic lines. A high level of Cre-mediated recombination in Tg(Glast-CreER^{T2})T45-72 was observed in cerebellar Bergmann glia, but not in astrocytes from the granule cell layer or from white matter and such a pattern of endogenous promoter acitivity was reported in an earlier study on Glast expression (Chaudhry et al., 1995).

Similar to the Apoe-based transgenic mice, levels of Cre mRNA in Tg(Aqp4-CreER^{T2}) were very low. This appeared not surprising given that the natural expression level of Aqp4 is also low. However, this resulted in very low levels of recombination in the brain, while high recombination efficiency was observed in heart, kidney and skeletal muscles. The Aqp4 promoter may be too weak to drive Cre expression in the brain, at least to a level that can be detected by the reporter lines. Another possible explanation for the low expression is that the region for CreER^{T2} insertion was based on the NCBI database. A comparison of the sequence data at the beginning of the project (2003) with a most recent version reveals an inconsistency that may have led us to choose the wrong ATG codon. We decided to target the transcription isoform Aqp4.M23X (Zelenin et al., 2000), which is identical to MIWC3 (Ma et al., 1996) that was reported to be expressed in the brain (Zelenin et al., 2000). At the time of the project, the ATG initiation codon of Aqp4 was located at the same position as ATG of M23X isoform. In the current version of the database, the initiation codon of Aqp4 has changed its position and is located now a few hundred bps upstream of the region targeted in our project, and corresponds to Aqp4.M1 isoform (Umenishi et al. 1996). Currently, it is unknown whether the locus that we targeted drives initiation of expression. A possible explanation why our mice show Cre-mediated recombination in peripheral tissues is that the CreER^{T2} in Tg(Aqp4-CreER^{T2}) lines is in fact under the control of regulatory sequences of M1 isoform of Aqp4 (Nielsen et al., 1997; Umenishi et al., 1996), which drives expression outside the brain.

During this project a single daily injection of 2 mg of TAM for five consecutive days was chosen as an efficient regime of TAM administration. Notably, in all cases, CreER^{T2} was

strictly dependent on the presence of ligand, since signs of leaky baseline expression age were occasional or absent. Parallel studies employed similar adminstration paradigms using TAM (Mori et al., 2006, Hirrlinger et al., 2006, Casper et al., 2007) or 4-OHT (Ganat et al., 2006) for efficient recombination in the brain. These data indicate that the CreER^{T2} system in conjunction with tamoxifen can be used for gene ablation in the brain. Accumulation in the brain of both, TAM and OHT, was reported to peak 6h after intraperitoneal injection and to decrease within 24h (Ganat et al., 2006; Lien et al., 1991; Zervas et al., 2004; Ganat et al. 2006). These kinetics suggest that TAM exerts its action within 24h after administration. Such a fast effect was confirmed both at the DNA (Weber et al., 2001) and at the protein level (Hirrlinger et al., 2006). Notably, Mori et al. (2006) used oral administration of TAM to pregnant females to follow the fate of progenitors born during embryonic development (Mori et al., 2006).

We noticed that the different reporter lines gave divergent results concerning the efficacies of recombination in astrocytes, first between the DNA and enzyme-based lines and also among the latter. For example, the Tg(Glast-CreER^{T2})T45-52 line showed high efficiency of recombination in the brain at the DNA level, but very little with the Z/AP reporter line. The Tg(Glast-CreER^{T2})T45-72 line showed recombination at the DNA level in thalamus, midbrain or medulla oblongata, but this was not indicated by the enzyme-based reporter lines. Moreover, crosses of Tg(Glast-CreER^{T2})T45-72 with ROSA26R showed much more numerous cells with CreER^{T2} activity than crosses with the Z/AP reporter. This was also observed by Ganat et al. (2006), where astrocytes expressing the reporter protein in ROSA26R outnumbered by ten-fold those indicated by the Z/EG reporter line, which uses the same promoter, but EGFP instead of hPLAP. This may be due to different accessibility of the floxed locus for Cre recombinase, since the local DNA structure may differ between reporter lines. Alternatively, this may be due to the differences in regulatory sequences of reporter protein constructs used for transgenesis. Overall, there is also evidence that reporter lines underestimate systematically the number of cells showing Cre-mediated recombination (Nagy, 2000).

During the course of this project, the generation of astrocyte-specific reporter lines was reported. These transgenic lines carry the reporter protein under the control of connexin-43 (Theis et al., 2001a; Theis et al., 2001b) or Gfap promoter (Casper and McCarthy, 2006). The advantage of these lines is that one can estimate the efficiency of CreER^{T2} mediated recombination in Gfap-expressing cells and their progeny, without problems related to the use of reporter lines employing ubiquitous promoters. For example, in case of hGfap-Cre

(Malatesta et al., 2003), BLBP-Cre (Anthony et al., 2004) or mGfap-Cre (Casper and McCarthy, 2006) lines, very few astrocytes expressed reporter protein in the adult brain when ROSA26R or Z/AP reporters were used. On the other hand, the use of astrocyte-specific reporter lines imposes limitations. First, it allows only to estimate the efficiency of recombination in Cx43- or Gfap-positive astrocytes, leaving no access to Cx43- or Gfap-negative subpopulation of this cell type, which constitute a significant fraction (Matthias et al., 2003; Wallraff et al., 2004; Walz, 2000).

CONCLUSIONS AND PERSPECTIVES

My work led to the generation of at least two new transgenic mouse models that allow to target astrocytes genetically. BAC-based transgenesis proved to be efficient given that 90% of founders displayed germ-line transmission. Aditionally, in all lines tested, TAM induced recombination, at least at the DNA level.

The two most efficient lines target different subpopulations of astrocytes and astroglial cells. The regional differences in CreER^{T2} mediated recombination in the two lines described in this project allow for comparative studies on astrocytes. The Tg(Cx30-CreER^{T2})T53-33 line allows for inducible, astrocyte-specific ablation of floxed genes in the cerebellum, thalamus, midbrain, medulla oblongata, grey matter of spinal cord, cortex and hippocampus. The Tg(Glast-CreER^{T2})T45-72 targets astrocytes in hippocampus and cortex, as well as Bergmann glia in the cerebellum, Muller glia in the retina, hypothalamic tanycytes and adult neuronal progenitors of subventricular zone and subgranular layer of dentate dyrus. Tg(ApoE-CreER^{T2}) and Tg(Aqp4-CreER^{T2}) transgenic lines generated during this project do not show efficient CreER^{T2} mediated gene recombination in the brain. These new models allow to study effects of cell-autonomous gene loss in astrocytes at defined stages of development and in the adult. Transgenic lines generated during this project broaden the set of models enabling such investigations and meet therefore an urgent need of genetic tools to study the function of these cells *in vivo* .

REFERENCES

Amiry-Moghaddam M, Otsuka T, Hurn PD, Traystman RJ, Haug FM, Froehner SC, Adams ME, Neely JD, Agre P, Ottersen OP, Bhardwaj A (2003) An alpha-syntrophin-dependent pool of AQP4 in astroglial end-feet confers bidirectional water flow between blood and brain. Proc Natl Acad Sci U S A 100:2106-2111.

Angulo MC, Kozlov AS, Charpak S, Audinat E (2004) Glutamate released from glial cells synchronizes neuronal activity in the hippocampus. J Neurosci 24:6920-6927.

Anthony TE, Klein C, Fishell G, Heintz N (2004) Radial glia serve as neuronal progenitors in all regions of the central nervous system. Neuron 41:881-890.

Antoch MP, Song EJ, Chang AM, Vitaterna MH, Zhao Y, Wilsbacher LD, Sangoram AM, King DP, Pinto LH, Takahashi JS (1997) Functional identification of the mouse circadian Clock gene by transgenic BAC rescue. Cell 89:655-667.

Araque A, Parpura V, Sanzgiri RP, Haydon PG (1998a) Glutamate-dependent astrocyte modulation of synaptic transmission between cultured hippocampal neurons. Eur J Neurosci 10:2129-2142.

Araque A, Sanzgiri RP, Parpura V, Haydon PG (1998b) Calcium elevation in astrocytes causes an NMDA receptor-dependent increase in the frequency of miniature synaptic currents in cultured hippocampal neurons. J Neurosci 18:6822-6829.

Araque A, Martin ED, Perea G, Arellano JI, Buno W (2002) Synaptically released acetylcholine evokes Ca2+ elevations in astrocytes in hippocampal slices. J Neurosci 22:2443-2450.

Attwell D, Laughlin SB (2001) An energy budget for signaling in the grey matter of the brain. J Cereb Blood Flow Metab 21:1133-1145.

Bajenaru ML, Zhu Y, Hedrick NM, Donahoe J, Parada LF, Gutmann DH (2002) Astrocyte-specific inactivation of the neurofibromatosis 1 gene (NF1) is insufficient for astrocytoma formation. Mol Cell Biol 22:5100-5113.

Barres BA, Chun LL, Corey DP (1988) Ion channel expression by white matter glia: I. Type 2 astrocytes and oligodendrocytes. Glia 1:10-30.

Barres BA, Koroshetz WJ, Chun LL, Corey DP (1990) Ion channel expression by white matter glia: the type-1 astrocyte. Neuron 5:527-544.

Basarsky TA, Duffy SN, Andrew RD, MacVicar BA (1998) Imaging spreading depression and associated intracellular calcium waves in brain slices. J Neurosci 18:7189-7199.

Beattie EC, Stellwagen D, Morishita W, Bresnahan JC, Ha BK, Von Zastrow M, Beattie MS, Malenka RC (2002) Control of synaptic strength by glial TNFalpha. Science 295:2282-2285.

Bechmann I, Galea I, Perry VH (2007) What is the blood-brain barrier (not)? Trends Immunol 28:5-11.

Beierlein M, Regehr WG (2006) Brief bursts of parallel fiber activity trigger calcium signals in bergmann glia. J Neurosci 26:6958-6967.

Benediktsson AM, Schachtele SJ, Green SH, Dailey ME (2005) Ballistic labeling and dynamic imaging of astrocytes in organotypic hippocampal slice cultures. J Neurosci Methods 141:41-53.

Berger UV, Hediger MA (2006) Distribution of the glutamate transporters GLT-1 (SLC1A2) and GLAST (SLC1A3) in peripheral organs. Anat Embryol (Berl) 211:595-606.

Bergles DE, Jahr CE (1998) Glial contribution to glutamate uptake at Schaffer collateral-commissural synapses in the hippocampus. J Neurosci 18:7709-7716.

Bezzi P, Gundersen V, Galbete JL, Seifert G, Steinhauser C, Pilati E, Volterra A (2004) Astrocytes contain a vesicular compartment that is competent for regulated exocytosis of glutamate. Nat Neurosci 7:613-620.

Bezzi P, Carmignoto G, Pasti L, Vesce S, Rossi D, Rizzini BL, Pozzan T, Volterra A (1998) Prostaglandins stimulate calcium-dependent glutamate release in astrocytes. Nature 391:281-285.

Brenner M, Kisseberth WC, Su Y, Besnard F, Messing A (1994) GFAP promoter directs astrocyte-specific expression in transgenic mice. J Neurosci 14:1030-1037.

Broer A, Deitmer JW, Broer S (2004) Astroglial glutamine transport by system N is upregulated by glutamate. Glia 48:298-310.

Burns KA, Ayoub AE, Breunig JJ, Adhami F, Weng WL, Colbert MC, Rakic P, Kuan CY (2007) Nestin-CreER Mice Reveal DNA Synthesis by Nonapoptotic Neurons following Cerebral Ischemia-Hypoxia. Cereb Cortex.

Bushong EA, Martone ME, Jones YZ, Ellisman MH (2002) Protoplasmic astrocytes in CA1 stratum radiatum occupy separate anatomical domains. J Neurosci 22:183-192.

Butt AM, Kiff J, Hubbard P, Berry M (2002) Synantocytes: new functions for novel NG2 expressing glia. J Neurocytol 31:551-565.

Cai J, Chen Y, Cai WH, Hurlock EC, Wu H, Kernie SG, Parada LF, Lu QR (2007) A crucial role for Olig2 in white matter astrocyte development. Development 134:1887-1899.

Casper KB, McCarthy KD (2006) GFAP-positive progenitor cells produce neurons and oligodendrocytes throughout the CNS. Mol Cell Neurosci 31:676-684.

Casper KB, Jones K, McCarthy KD (2007) Characterization of astrocyte-specific conditional knockouts. Genesis 45:292-299.

Chaudhry FA, Lehre KP, van Lookeren Campagne M, Ottersen OP, Danbolt NC, Storm-Mathisen J (1995) Glutamate transporters in glial plasma membranes: highly differentiated localizations revealed by quantitative ultrastructural immunocytochemistry. Neuron 15:711-720.

Christopherson KS, Ullian EM, Stokes CC, Mullowney CE, Hell JW, Agah A, Lawler J, Mosher DF, Bornstein P, Barres BA (2005) Thrombospondins are astrocyte-secreted proteins that promote CNS synaptogenesis. Cell 120:421-433.

Coco S, Calegari F, Pravettoni E, Pozzi D, Taverna E, Rosa P, Matteoli M, Verderio C (2003) Storage and release of ATP from astrocytes in culture. J Biol Chem 278:1354-1362.

Cornell-Bell AH, Finkbeiner SM, Cooper MS, Smith SJ (1990) Glutamate induces calcium waves in cultured astrocytes: long-range glial signaling. Science 247:470-473.

Cotrina ML, Lin JH, Alves-Rodrigues A, Liu S, Li J, Azmi-Ghadimi H, Kang J, Naus CC, Nedergaard M (1998) Connexins regulate calcium signaling by controlling ATP release. Proc Natl Acad Sci U S A 95:15735-15740.

D'Ambrosio R, Gordon DS, Winn HR (2002) Differential role of KIR channel and Na(+)/K(+)-pump in the regulation of extracellular K(+) in rat hippocampus. J Neurophysiol 87:87-102.

D'Ambrosio R, Wenzel J, Schwartzkroin PA, McKhann GM, 2nd, Janigro D (1998) Functional specialization and topographic segregation of hippocampal astrocytes. J Neurosci 18:4425-4438.

D'Ascenzo M, Fellin T, Terunuma M, Revilla-Sanchez R, Meaney DF, Auberson YP, Moss SJ, Haydon PG (2007) mGluR5 stimulates gliotransmission in the nucleus accumbens. Proc Natl Acad Sci U S A 104:1995-2000.

Dahl E, Manthey D, Chen Y, Schwarz HJ, Chang YS, Lalley PA, Nicholson BJ, Willecke K (1996) Molecular cloning and functional expression of mouse connexin-30,a gap junction gene highly expressed in adult brain and skin. J Biol Chem 271:17903-17910.

Daikhin Y, Yudkoff M (2000) Compartmentation of brain glutamate metabolism in neurons and glia. J Nutr 130:1026S-1031S.

Danbolt NC (2001) Glutamate uptake. Prog Neurobiol 65:1-105.

Dani JW, Chernjavsky A, Smith SJ (1992) Neuronal activity triggers calcium waves in hippocampal astrocyte networks. Neuron 8:429-440.

Davies AM (1998) Developmental changes in the neurotrophic factor survival requirements of peripheral nervous system neurons. Prog Brain Res 117:47-56.

de Lima AD, Voigt T (1999) Astroglia inhibit the proliferation of neocortical cells and prevent the generation of small GABAergic neurons *in vitro* . Eur J Neurosci 11:3845-3856.

Denis-Donini S, Glowinski J, Prochiantz A (1984) Glial heterogeneity may define the three-dimensional shape of mouse mesencephalic dopaminergic neurones. Nature 307:641-643.

Derouiche A, Rauen T (1995) Coincidence of L-glutamate/L-aspartate transporter (GLAST) and glutamine synthetase (GS) immunoreactions in retinal glia: evidence for coupling of GLAST and GS in transmitter clearance. J Neurosci Res 42:131-143.

Diamond JS, Bergles DE, Jahr CE (1998) Glutamate release monitored with astrocyte transporter currents during LTP. Neuron 21:425-433.

Dorlhiac-Llacer PE, Marquezini MV, Toffoletto O, Carneiro RC, Maranhao RC, Chamone DA (2001) *In vitro* cytotoxicity of the LDE: daunorubicin complex in acute myelogenous leukemia blast cells. Braz J Med Biol Res 34:1257-1263.

Duan S, Anderson CM, Keung EC, Chen Y, Chen Y, Swanson RA (2003) P2X7 receptor-mediated release of excitatory amino acids from astrocytes. J Neurosci 23:1320-1328.

Dymecki SM (1996) Flp recombinase promotes site-specific DNA recombination in embryonic stem cells and transgenic mice. Proc Natl Acad Sci U S A 93:6191-6196.

Eckardt D, Theis M, Degen J, Ott T, van Rijen HV, Kirchhoff S, Kim JS, de Bakker JM, Willecke K (2004) Functional role of connexin43 gap junction channels in adult mouse heart assessed by inducible gene deletion. J Mol Cell Cardiol 36:101-110.

Elmariah SB, Oh EJ, Hughes EG, Balice-Gordon RJ (2005) Astrocytes regulate inhibitory synapse formation via Trk-mediated modulation of postsynaptic GABAA receptors. J Neurosci 25:3638-3650.

Emmi A, Wenzel HJ, Schwartzkroin PA, Taglialatela M, Castaldo P, Bianchi L, Nerbonne J, Robertson GA, Janigro D (2000) Do glia have heart? Expression and functional role for ether-a-go-go currents in hippocampal astrocytes. J Neurosci 20:3915-3925.

Emsley JG, Macklis JD (2006) Astroglial heterogeneity closely reflects the neuronal-defined anatomy of the adult murine CNS. Neuron Glia Biol 2:175-186.

Eng LF, Ghirnikar RS, Lee YL (2000) Glial fibrillary acidic protein: GFAP-thirty-one years (1969-2000). Neurochem Res 25:1439-1451.

Feil R, Wagner J, Metzger D, Chambon P (1997) Regulation of Cre recombinase activity by mutated estrogen receptor ligand-binding domains. Biochem Biophys Res Commun 237:752-757.

Feil R, Brocard J, Mascrez B, LeMeur M, Metzger D, Chambon P (1996) Ligand-activated site-specific recombination in mice. Proc Natl Acad Sci U S A 93:10887-10890.

Fellin T, Pascual O, Haydon PG (2006a) Astrocytes coordinate synaptic networks: balanced excitation and inhibition. Physiology (Bethesda) 21:208-215.

Fellin T, Gomez-Gonzalo M, Gobbo S, Carmignoto G, Haydon PG (2006b) Astrocytic glutamate is not necessary for the generation of epileptiform neuronal activity in hippocampal slices. J Neurosci 26:9312-9322.

Fellin T, Pascual O, Gobbo S, Pozzan T, Haydon PG, Carmignoto G (2004) Neuronal synchrony mediated by astrocytic glutamate through activation of extrasynaptic NMDA receptors. Neuron 43:729-743.

Fiacco TA, McCarthy KD (2004) Intracellular astrocyte calcium waves in situ increase the frequency of spontaneous AMPA receptor currents in CA1 pyramidal neurons. J Neurosci 24:722-732.

Fiacco TA, McCarthy KD (2006) Astrocyte calcium elevations: properties, propagation, and effects on brain signaling. Glia 54:676-690.

Fiacco TA, Agulhon C, Taves SR, Petravicz J, Casper KB, Dong X, Chen J, McCarthy KD (2007) Selective stimulation of astrocyte calcium in situ does not affect neuronal excitatory synaptic activity. Neuron 54:611-626.

Figiel M, Engele J (2000) Pituitary adenylate cyclase-activating polypeptide (PACAP), a neuron-derived peptide regulating glial glutamate transport and metabolism. J Neurosci 20:3596-3605.

Fok-Seang J, Miller RH (1992) Astrocyte precursors in neonatal rat spinal cord cultures. J Neurosci 12:2751-2764.

Forni PE, Scuoppo C, Imayoshi I, Taulli R, Dastru W, Sala V, Betz UA, Muzzi P, Martinuzzi D, Vercelli AE, Kageyama R, Ponzetto C (2006) High levels of Cre expression in neuronal progenitors cause defects in brain development leading to microencephaly and hydrocephaly. J Neurosci 26:9593-9602.

Freeman MR (2006) Sculpting the nervous system: glial control of neuronal development. Curr Opin Neurobiol 16:119-125.

Furuta A, Rothstein JD, Martin LJ (1997) Glutamate transporter protein subtypes are expressed differentially during rat CNS development. J Neurosci 17:8363-8375.

Ganat YM, Silbereis J, Cave C, Ngu H, Anderson GM, Ohkubo Y, Ment LR, Vaccarino FM (2006) Early postnatal astroglial cells produce multilineage precursors and neural stem cells *in vivo* . J Neurosci 26:8609-8621.

Garcia AD, Doan NB, Imura T, Bush TG, Sofroniew MV (2004) GFAP-expressing progenitors are the principal source of constitutive neurogenesis in adult mouse forebrain. Nat Neurosci 7:1233-1241.

Giangrande A (1995) Proneural genes influence gliogenesis in Drosophila. Development 121:429-438.

Giaume C, McCarthy KD (1996) Control of gap-junctional communication in astrocytic networks. Trends Neurosci 19:319-325.

Giraldo P, Montoliu L (2001) Size matters: use of YACs, BACs and PACs in transgenic animals. Transgenic Res 10:83-103.

Giraldo P, Rival-Gervier S, Houdebine LM, Montoliu L (2003) The potential benefits of insulators on heterologous constructs in transgenic animals. Transgenic Res 12:751-755.

Goritz C, Mauch D, Pfrieger FW (2005) Multiple mechanisms mediate cholesterol-induced synaptogenesis in a CNS neuron. Mol Cell Neurosci. 29(2):190-201.

Grehan S, Tse E, Taylor JM (2001) Two distal downstream enhancers direct expression of the human apolipoprotein E gene to astrocytes in the brain. J Neurosci 21:812-822.

Grosche J, Matyash V, Moller T, Verkhratsky A, Reichenbach A, Kettenmann H (1999) Microdomains for neuron-glia interaction: parallel fiber signaling to Bergmann glial cells. Nat Neurosci 2:139-143.

Gu H, Marth JD, Orban PC, Mossmann H, Rajewsky K (1994) Deletion of a DNA polymerase beta gene segment in T cells using cell type-specific gene targeting. Science 265:103-106.

Guthrie PB, Knappenberger J, Segal M, Bennett MV, Charles AC, Kater SB (1999) ATP released from astrocytes mediates glial calcium waves. J Neurosci 19:520-528.

Haber M, Zhou L, Murai KK (2006) Cooperative astrocyte and dendritic spine dynamics at hippocampal excitatory synapses. J Neurosci 26:8881-8891.

Hachem S, Aguirre A, Vives V, Marks A, Gallo V, Legraverend C (2005) Spatial and temporal expression of S100B in cells of oligodendrocyte lineage. Glia 51:81-97.

Hama H, Hara C, Yamaguchi K, Miyawaki A (2004) PKC signaling mediates global enhancement of excitatory synaptogenesis in neurons triggered by local contact with astrocytes. Neuron 41:405-415.

Hans G, Moonen G, Rigo JM (2002) Modulation of neuronal survival and excitability by an astroglia-derived factor. J Physiol Paris 96:323-328.

Hassinger TD, Guthrie PB, Atkinson PB, Bennett MV, Kater SB (1996) An extracellular signaling component in propagation of astrocytic calcium waves. Proc Natl Acad Sci U S A 93:13268-13273.

Hassinger TD, Atkinson PB, Strecker GJ, Whalen LR, Dudek FE, Kossel AH, Kater SB (1995) Evidence for glutamate-mediated activation of hippocampal neurons by glial calcium waves. J Neurobiol 28:159-170.

Hatada S, Kuziel W, Smithies O, Maeda N (1999) The influence of chromosomal location on the expression of two transgenes in mice. J Biol Chem 274:948-955.

Haydon PG (2001) GLIA: listening and talking to the synapse. Nat Rev Neurosci 2:185-193.

He F, Ge W, Martinowich K, Becker-Catania S, Coskun V, Zhu W, Wu H, Castro D, Guillemot F, Fan G, de Vellis J, Sun YE (2005) A positive autoregulatory loop of Jak-STAT signaling controls the onset of astrogliogenesis. Nat Neurosci 8:616-625.

Heaney JD, Bronson SK (2006) Artificial chromosome-based transgenes in the study of genome function. Mamm Genome 17:791-807.

Heim N, Garaschuk O, Friedrich MW, Mank M, Milos RI, Kovalchuk Y, Konnerth A, Griesbeck O (2007) Improved calcium imaging in transgenic mice expressing a troponin C-based biosensor. Nat Methods 4:127-129.

Heintz N (2001) BAC to the future: the use of bac transgenic mice for neuroscience research. Nat Rev Neurosci 2:861-870.

Hertz L, Zielke HR (2004) Astrocytic control of glutamatergic activity: astrocytes as stars of the show. Trends Neurosci 27:735-743.

Hirrlinger J, Hulsmann S, Kirchhoff F (2004) Astroglial processes show spontaneous motility at active synaptic terminals in situ. Eur J Neurosci 20:2235-2239.

Hirrlinger PG, Scheller A, Braun C, Hirrlinger J, Kirchhoff F (2006) Temporal control of gene recombination in astrocytes by transgenic expression of the tamoxifen-inducible DNA recombinase variant CreERT2. Glia 54:11-20.

Holthoff K, Witte OW (2000) Directed spatial potassium redistribution in rat neocortex. Glia 29:288-292.

Hosoya T, Takizawa K, Nitta K, Hotta Y (1995) glial cells missing: a binary switch between neuronal and glial determination in Drosophila. Cell 82:1025-1036.

Houdebine LM (2005) Relations between animal transgenesis and reproduction. Reprod Nutr Dev 45:363-376.

Houghton FD, Barr KJ, Walter G, Gabriel HD, Grummer R, Traub O, Leese HJ, Winterhager E, Kidder GM (2002) Functional significance of gap junctional coupling in preimplantation development. Biol Reprod 66:1403-1412.

Hu R, Cai WQ, Wu XG, Yang Z (2007) Astrocyte-derived estrogen enhances synapse formation and synaptic transmission between cultured neonatal rat cortical neurons. Neuroscience 144:1229-1240.

Imayoshi I, Ohtsuka T, Metzger D, Chambon P, Kageyama R (2006) Temporal regulation of Cre recombinase activity in neural stem cells. Genesis 44:233-238.

Indra AK, Warot X, Brocard J, Bornert JM, Xiao JH, Chambon P, Metzger D (1999) Temporally-controlled site-specific mutagenesis in the basal layer of the epidermis: comparison of the recombinase activity of the tamoxifen-inducible Cre-ER(T) and Cre-ER(T2) recombinases. Nucleic Acids Res 27:4324-4327.

Jones BW, Fetter RD, Tear G, Goodman CS (1995) glial cells missing: a genetic switch that controls glial versus neuronal fate. Cell 82:1013-1023.

Jourdain P, Bergersen LH, Bhaukaurally K, Bezzi P, Santello M, Domercq M, Matute C, Tonello F, Gundersen V, Volterra A (2007) Glutamate exocytosis from astrocytes controls synaptic strength. Nat Neurosci 10:331-339.

Kandel ER, Schwartz JH, Jessell TM (2000) Principles of neural science, 4th Edition. New York: McGraw-Hill, Health Professions Division.

Kang J, Jiang L, Goldman SA, Nedergaard M (1998) Astrocyte-mediated potentiation of inhibitory synaptic transmission. Nat Neurosci 1:683-692.

Kang N, Xu J, Xu Q, Nedergaard M, Kang J (2005) Astrocytic glutamate release-induced transient depolarization and epileptiform discharges in hippocampal CA1 pyramidal neurons. J Neurophysiol 94:4121-4130.

Kasischke KA, Vishwasrao HD, Fisher PJ, Zipfel WR, Webb WW (2004) Neural activity triggers neuronal oxidative metabolism followed by astrocytic glycolysis. Science 305:99-103.

Kaufman RM, Pham CT, Ley TJ (1999) Transgenic analysis of a 100-kb human beta-globin cluster-containing DNA fragment propagated as a bacterial artificial chromosome. Blood 94:3178-3184.

Kellendonk C, Tronche F, Monaghan AP, Angrand PO, Stewart F, Schutz G (1996) Regulation of Cre recombinase activity by the synthetic steroid RU 486. Nucleic Acids Res 24:1404-1411.

Kempermann G, Jessberger S, Steiner B, Kronenberg G (2004) Milestones of neuronal development in the adult hippocampus. Trends Neurosci 27:447-452.

Kettenmann H, Ransom BR, eds (2004) Neuroglia. New York: Oxford University Press.

Kimelberg HK (2004) The problem of astrocyte identity. Neurochem Int 45:191-202.

Kofuji P, Newman EA (2004) Potassium buffering in the central nervous system. Neuroscience 129:1045-1056.

Kofuji P, Ceelen P, Zahs KR, Surbeck LW, Lester HA, Newman EA (2000) Genetic inactivation of an inwardly rectifying potassium channel (Kir4.1 subunit) in mice: phenotypic impact in retina. J Neurosci 20:5733-5740.

Kozlov AS, Angulo MC, Audinat E, Charpak S (2006) Target cell-specific modulation of neuronal activity by astrocytes. Proc Natl Acad Sci U S A 103:10058-10063.

Kunzelmann P, Schroder W, Traub O, Steinhauser C, Dermietzel R, Willecke K (1999) Late onset and increasing expression of the gap junction protein connexin30 in adult murine brain and long-term cultured astrocytes. Glia 25:111-119.

Lakso M, Sauer B, Mosinger B, Jr., Lee EJ, Manning RW, Yu SH, Mulder KL, Westphal H (1992) Targeted oncogene activation by site-specific recombination in transgenic mice. Proc Natl Acad Sci U S A 89:6232-6236.

Lazebnik Y (2002) Can a biologist fix a radio?--Or, what I learned while studying apoptosis. Cancer Cell 2:179-182.

Leavitt BR, Hernit-Grant CS, Macklis JD (1999) Mature astrocytes transform into transitional radial glia within adult mouse neocortex that supports directed migration of transplanted immature neurons. Exp Neurol 157:43-57.

Lee EC, Yu D, Martinez de Velasco J, Tessarollo L, Swing DA, Court DL, Jenkins NA, Copeland NG (2001) A highly efficient Escherichia coli-based chromosome engineering system adapted for recombinogenic targeting and subcloning of BAC DNA. Genomics 73:56-65.

Liang SL, Carlson GC, Coulter DA (2006) Dynamic regulation of synaptic GABA release by the glutamate-glutamine cycle in hippocampal area CA1. J Neurosci 26:8537-8548.

Lien EA, Solheim E, Ueland PM (1991) Distribution of tamoxifen and its metabolites in rat and human tissues during steady-state treatment. Cancer Res 51:4837-4844.

Lim DA, Alvarez-Buylla A (1999) Interaction between astrocytes and adult subventricular zone precursors stimulates neurogenesis. Proc Natl Acad Sci U S A 96:7526-7531.

Lin TN, Wang Q, Simonyi A, Chen JJ, Cheung WM, He YY, Xu J, Sun AY, Hsu CY, Sun GY (2004) Induction of secretory phospholipase A2 in reactive astrocytes in response to transient focal cerebral ischemia in the rat brain. J Neurochem 90:637-645.

Liu QS, Xu Q, Arcuino G, Kang J, Nedergaard M (2004) Astrocyte-mediated activation of neuronal kainate receptors. Proc Natl Acad Sci U S A 101:3172-3177.

Liu Y, Rao MS (2004) Glial progenitors in the CNS and possible lineage relationships among them. Biol Cell 96:279-290.

Loaiza A, Porras OH, Barros LF (2003) Glutamate triggers rapid glucose transport stimulation in astrocytes as evidenced by real-time confocal microscopy. J Neurosci 23:7337-7342.

Lobe CG, Koop KE, Kreppner W, Lomeli H, Gertsenstein M, Nagy A (1999) Z/AP, a double reporter for cre-mediated recombination. Dev Biol 208:281-292.

Lu QR, Sun T, Zhu Z, Ma N, Garcia M, Stiles CD, Rowitch DH (2002) Common developmental requirement for Olig function indicates a motor neuron/oligodendrocyte connection. Cell 109:75-86.

Ma T, Yang B, Verkman AS (1996) Gene structure, cDNA cloning, and expression of a mouse mercurial-insensitive water channel. Genomics 33:382-388.

MacVicar BA, Feighan D, Brown A, Ransom B (2002) Intrinsic optical signals in the rat optic nerve: role for K(+) uptake via NKCC1 and swelling of astrocytes. Glia 37:114-123.

Magistretti PJ (2006) Neuron-glia metabolic coupling and plasticity. J Exp Biol 209:2304-2311.

Magistretti PJ, Pellerin L (1999) Cellular mechanisms of brain energy metabolism and their relevance to functional brain imaging. Philos Trans R Soc Lond B Biol Sci 354:1155-1163.

Mahley RW, Rall SCJ (2001) Apolipoprotein E: far more than a lipid transport protein. . Annu Rev Genomics Human Genet 1:507-537.

Malatesta P, Hack MA, Hartfuss E, Kettenmann H, Klinkert W, Kirchhoff F, Gotz M (2003) Neuronal or glial progeny: regional differences in radial glia fate. Neuron 37:751-764.

Mandelbrot BB (1982) The fractal geometry of nature. San Francisco: W.H. Freeman.

Manzoni OJ, Manabe T, Nicoll RA (1994) Release of adenosine by activation of NMDA receptors in the hippocampus. Science 265:2098-2101.

Maragakis NJ, Rothstein JD (2006) Mechanisms of Disease: astrocytes in neurodegenerative disease. Nat Clin Pract Neurol 2:679-689.

Marino S, Vooijs M, van Der Gulden H, Jonkers J, Berns A (2000) Induction of medulloblastomas in p53-null mutant mice by somatic inactivation of Rb in the external granular layer cells of the cerebellum. Genes Dev 14:994-1004.

Masahira N, Takebayashi H, Ono K, Watanabe K, Ding L, Furusho M, Ogawa Y, Nabeshima Y, Alvarez-Buylla A, Shimizu K, Ikenaka K (2006) Olig2-positive progenitors in the embryonic spinal cord give rise not only to motoneurons and oligodendrocytes, but also to a subset of astrocytes and ependymal cells. Dev Biol 293:358-369.

Mascrez B, Mark M, Dierich A, Ghyselinck NB, Kastner P, Chambon P (1998) The RXRalpha ligand-dependent activation function 2 (AF-2) is important for mouse development. Development 125:4691-4707.

Matthias K, Kirchhoff F, Seifert G, Huttmann K, Matyash M, Kettenmann H, Steinhauser C (2003) Segregated expression of AMPA-type glutamate receptors and glutamate transporters defines distinct astrocyte populations in the mouse hippocampus. J Neurosci 23:1750-1758.

Mauch DH, Nagler K, Schumacher S, Goritz C, Muller EC, Otto A, Pfrieger FW (2001) CNS synaptogenesis promoted by glia-derived cholesterol. Science 294:1354-1357.

McKhann GM, 2nd, D'Ambrosio R, Janigro D (1997) Heterogeneity of astrocyte resting membrane potentials and intercellular coupling revealed by whole-cell and gramicidin-perforated patch recordings from cultured neocortical and hippocampal slice astrocytes. J Neurosci 17:6850-6863.

Medina JM, Tabernero A (2002) Astrocyte-synthesized oleic acid behaves as a neurotrophic factor for neurons. J Physiol Paris 96:265-271.

Metzger D, Clifford J, Chiba H, Chambon P (1995) Conditional site-specific recombination in mammalian cells using a ligand-dependent chimeric Cre recombinase. Proc Natl Acad Sci U S A 92:6991-6995.

Mi H, Barres BA (1999) Purification and characterization of astrocyte precursor cells in the developing rat optic nerve. J Neurosci 19:1049-1061.

Michel G, Mosser J, Olle J (1984) Pharmacokinetics and tissue localization of doxycycline polyphosphate and doxycycline hydrochloride in the rat. Eur J Drug Metab Pharmacokinet 9:149-153.

Miyawaki A, Griesbeck O, Heim R, Tsien RY (1999) Dynamic and quantitative Ca2+ measurements using improved cameleons. Proc Natl Acad Sci U S A 96:2135-2140.

Montana V, Ni Y, Sunjara V, Hua X, Parpura V (2004) Vesicular glutamate transporter-dependent glutamate release from astrocytes. J Neurosci 24:2633-2642.

Mori T, Tanaka K, Buffo A, Wurst W, Kuhn R, Gotz M (2006) Inducible gene deletion in astroglia and radial glia--a valuable tool for functional and lineage analysis. Glia 54:21-34.

Mothet JP, Pollegioni L, Ouanounou G, Martineau M, Fossier P, Baux G (2005) Glutamate receptor activation triggers a calcium-dependent and SNARE protein-dependent release of the gliotransmitter D-serine. Proc Natl Acad Sci U S A 102:5606-5611.

Mothet JP, Parent AT, Wolosker H, Brady RO, Jr., Linden DJ, Ferris CD, Rogawski MA, Snyder SH (2000) D-serine is an endogenous ligand for the glycine site of the N-methyl-D-aspartate receptor. Proc Natl Acad Sci U S A 97:4926-4931.

Mucke L, Oldstone MB, Morris JC, Nerenberg MI (1991) Rapid activation of astrocyte-specific expression of GFAP-lacZ transgene by focal injury. New Biol 3:465-474.

Mulligan SJ, MacVicar BA (2004) Calcium transients in astrocyte endfeet cause cerebrovascular constrictions. Nature 431:195-199.

Muyrers JP, Zhang Y, Testa G, Stewart AF (1999) Rapid modification of bacterial artificial chromosomes by ET-recombination. Nucleic Acids Res 27:1555-1557.

Nagler K, Mauch DH, Pfrieger FW (2001) Glia-derived signals induce synapse formation in neurones of the rat central nervous system. J Physiol 533:665-679.

Nagy A (2000) Cre recombinase: the universal reagent for genome tailoring. Genesis 26(2):99-109.

Nakashima K, Yanagisawa M, Arakawa H, Taga T (1999) Astrocyte differentiation mediated by LIF in cooperation with BMP2. FEBS Lett 457:43-46.

Nakashima K, Takizawa T, Ochiai W, Yanagisawa M, Hisatsune T, Nakafuku M, Miyazono K, Kishimoto T, Kageyama R, Taga T (2001) BMP2-mediated alteration in the

developmental pathway of fetal mouse brain cells from neurogenesis to astrocytogenesis. Proc Natl Acad Sci U S A 98:5868-5873.

Nedergaard M (1994) Direct signaling from astrocytes to neurons in cultures of mammalian brain cells. Science 263:1768-1771.

Newman EA (2004) Glial modulation of synaptic transmission in the retina. Glia 47:268-274.

Newman EA (2005) Calcium increases in retinal glial cells evoked by light-induced neuronal activity. J Neurosci 25:5502-5510.

Newman EA, Zahs KR (1997) Calcium waves in retinal glial cells. Science 275:844-847.

Newman EA, Frambach DA, Odette LL (1984) Control of extracellular potassium levels by retinal glial cell K+ siphoning. Science 225:1174-1175.

Nielsen S, Nagelhus EA, Amiry-Moghaddam M, Bourque C, Agre P, Ottersen OP (1997) Specialized membrane domains for water transport in glial cells: high-resolution immunogold cytochemistry of aquaporin-4 in rat brain. J Neurosci 17:171-180.

Nimmerjahn A, Kirchhoff F, Kerr JN, Helmchen F (2004) Sulforhodamine 101 as a specific marker of astroglia in the neocortex *in vivo* . Nat Methods 1:31-37.

Nishida H, Okabe S (2007) Direct astrocytic contacts regulate local maturation of dendritic spines. J Neurosci 27:331-340.

Nishiyama A (2007) Polydendrocytes: NG2 cells with many roles in development and repair of the CNS. Neuroscientist 13:62-76.

Nixdorf-Bergweiler BE, Albrecht D, Heinemann U (1994) Developmental changes in the number, size, and orientation of GFAP-positive cells in the CA1 region of rat hippocampus. Glia 12:180-195.

Nolte C, Matyash M, Pivneva T, Schipke CG, Ohlemeyer C, Hanisch UK, Kirchhoff F, Kettenmann H (2001) GFAP promoter-controlled EGFP-expressing transgenic mice: a tool to visualize astrocytes and astrogliosis in living brain tissue. Glia 33:72-86.

Ogata K, Kosaka T (2002) Structural and quantitative analysis of astrocytes in the mouse hippocampus. Neuroscience 113:221-233.

Orban PC, Chui D, Marth JD (1992) Tissue- and site-specific DNA recombination in transgenic mice. Proc Natl Acad Sci U S A 89:6861-6865.

Panatier A, Theodosis DT, Mothet JP, Touquet B, Pollegioni L, Poulain DA, Oliet SH (2006) Glia-derived D-serine controls NMDA receptor activity and synaptic memory. Cell 125:775-784.

Parpura V, Fang Y, Basarsky T, Jahn R, Haydon PG (1995) Expression of synaptobrevin II, cellubrevin and syntaxin but not SNAP-25 in cultured astrocytes. FEBS Lett 377:489-492.

Parpura V, Basarsky TA, Liu F, Jeftinija K, Jeftinija S, Haydon PG (1994) Glutamate-mediated astrocyte-neuron signalling. Nature 369:744-747.

Parri HR, Gould TM, Crunelli V (2001) Spontaneous astrocytic Ca2+ oscillations in situ drive NMDAR-mediated neuronal excitation. Nat Neurosci 4:803-812.

Pascual O, Casper KB, Kubera C, Zhang J, Revilla-Sanchez R, Sul JY, Takano H, Moss SJ, McCarthy K, Haydon PG (2005) Astrocytic purinergic signaling coordinates synaptic networks. Science 310:113-116.

Pasti L, Volterra A, Pozzan T, Carmignoto G (1997) Intracellular calcium oscillations in astrocytes: a highly plastic, bidirectional form of communication between neurons and astrocytes in situ. J Neurosci 17:7817-7830.

Pellerin L, Magistretti PJ (1994) Glutamate uptake into astrocytes stimulates aerobic glycolysis: a mechanism coupling neuronal activity to glucose utilization. Proc Natl Acad Sci U S A 91:10625-10629.

Perea G, Araque A (2005) Properties of synaptically evoked astrocyte calcium signal reveal synaptic information processing by astrocytes. J Neurosci 25:2192-2203.

Pfrieger FW, Barres BA (1996) New views on synapse-glia interactions. Curr Opin Neurobiol 6:615-621.

Pfrieger FW, Barres BA (1997) Synaptic efficacy enhanced by glial cells *in vitro* . Science 277:1684-1687.

Piet R, Jahr CE (2007) Glutamatergic and purinergic receptor-mediated calcium transients in Bergmann glial cells. J Neurosci 27:4027-4035.

Pines G, Danbolt NC, Bjoras M, Zhang Y, Bendahan A, Eide L, Koepsell H, Storm-Mathisen J, Seeberg E, Kanner BI (1992) Cloning and expression of a rat brain L-glutamate transporter. Nature 360:464-467.

Porter JT, McCarthy KD (1996) Hippocampal astrocytes in situ respond to glutamate released from synaptic terminals. J Neurosci 16:5073-5081.

Porter JT, McCarthy KD (1997) Astrocytic neurotransmitter receptors in situ and *in vivo* . Prog Neurobiol 51:439-455.

Raff MC, Miller RH, Noble M (1983) A glial progenitor cell that develops *in vitro* into an astrocyte or an oligodendrocyte depending on culture medium. Nature 303:390-396.

Raichle ME (1998) Behind the scenes of functional brain imaging: a historical and physiological perspective. Proc Natl Acad Sci U S A 95:765-772.

Rao MS, Noble M, Mayer-Proschel M (1998) A tripotential glial precursor cell is present in the developing spinal cord. Proc Natl Acad Sci U S A 95:3996-4001.

Rash JE, Yasumura T, Dudek FE, Nagy JI (2001a) Cell-specific expression of connexins and evidence of restricted gap junctional coupling between glial cells and between neurons. J Neurosci 21:1983-2000.

Rash JE, Yasumura T, Hudson CS, Agre P, Nielsen S (1998) Direct immunogold labeling of aquaporin-4 in square arrays of astrocyte and ependymocyte plasma membranes in rat brain and spinal cord. Proc Natl Acad Sci U S A 95:11981-11986.

Rash JE, Yasumura T, Davidson KG, Furman CS, Dudek FE, Nagy JI (2001b) Identification of cells expressing Cx43, Cx30, Cx26, Cx32 and Cx36 in gap junctions of rat brain and spinal cord. Cell Commun Adhes 8:315-320.

Reichenbach A, Siegel A, Senitz D, Smith TG, Jr. (1992) A comparative fractal analysis of various mammalian astroglial cell types. Neuroimage 1:69-77.

Rietze R, Poulin P, Weiss S (2000) Mitotically active cells that generate neurons and astrocytes are present in multiple regions of the adult mouse hippocampus. J Comp Neurol 424:397-408.

Rothstein JD, Martin L, Levey AI, Dykes-Hoberg M, Jin L, Wu D, Nash N, Kuncl RW (1994) Localization of neuronal and glial glutamate transporters. Neuron 13:713-725.

Rothstein JD, Dykes-Hoberg M, Pardo CA, Bristol LA, Jin L, Kuncl RW, Kanai Y, Hediger MA, Wang Y, Schielke JP, Welty DF (1996) Knockout of glutamate transporters reveals a major role for astroglial transport in excitotoxicity and clearance of glutamate. Neuron 16:675-686.

Rozen S, Skaletsky H (2000) Primer3 on the WWW for general users and for biologist programmers. Methods Mol Biol 132:365-386.

Sadowski PD (1995) The Flp recombinase of the 2-microns plasmid of Saccharomyces cerevisiae. Prog Nucleic Acid Res Mol Biol 51:53-91.

Sauer B, Henderson N (1988) Site-specific DNA recombination in mammalian cells by the Cre recombinase of bacteriophage P1. Proc Natl Acad Sci U S A 85:5166-5170.

Scemes E (2000) Components of astrocytic intercellular calcium signaling. Mol Neurobiol 22:167-179.

Schiavo G, Benfenati F, Poulain B, Rossetto O, Polverino de Laureto P, DasGupta BR, Montecucco C (1992) Tetanus and botulinum-B neurotoxins block neurotransmitter release by proteolytic cleavage of synaptobrevin. Nature 359:832-835.

Schmitt A, Asan E, Puschel B, Kugler P (1997) Cellular and regional distribution of the glutamate transporter GLAST in the CNS of rats: nonradioactive in situ hybridization and comparative immunocytochemistry. J Neurosci 17:1-10.

Schuler M, Dierich A, Chambon P, Metzger D (2004) Efficient temporally controlled targeted somatic mutagenesis in hepatocytes of the mouse. Genesis 39:167-172.

Seidman KJ, Teng AL, Rosenkopf R, Spilotro P, Weyhenmeyer JA (1997) Isolation, cloning and characterization of a putative type-1 astrocyte cell line. Brain Res 753:18-26.

Seki Y, Feustel PJ, Keller RW, Jr., Tranmer BI, Kimelberg HK (1999) Inhibition of ischemia-induced glutamate release in rat striatum by dihydrokinate and an anion channel blocker. Stroke 30:433-440.

Serrano A, Haddjeri N, Lacaille JC, Robitaille R (2006) GABAergic network activation of glial cells underlies hippocampal heterosynaptic depression. J Neurosci 26:5370-5382.

Shimshek DR, Kim J, Hubner MR, Spergel DJ, Buchholz F, Casanova E, Stewart AF, Seeburg PH, Sprengel R (2002) Codon-improved Cre recombinase (iCre) expression in the mouse. Genesis 32:19-26.

Shizuya H, Birren B, Kim UJ, Mancino V, Slepak T, Tachiiri Y, Simon M (1992) Cloning and stable maintenance of 300-kilobase-pair fragments of human DNA in Escherichia coli using an F-factor-based vector. Proc Natl Acad Sci U S A 89:8794-8797.

Sibilia M, Steinbach JP, Stingl L, Aguzzi A, Wagner EF (1998) A strain-independent postnatal neurodegeneration in mice lacking the EGF receptor. Embo J 17:719-731.

Simard M, Arcuino G, Takano T, Liu QS, Nedergaard M (2003) Signaling at the gliovascular interface. J Neurosci 23:9254-9262.

Slezak M, Pfrieger FW (2003) New roles for astrocytes: regulation of CNS synaptogenesis. Trends Neurosci 26:531-535.

Slezak M, Pfrieger FW, Soltys Z (2006) Synaptic plasticity, astrocytes and morphological homeostasis. J Physiol Paris 99:84-91.

Song H, Stevens CF, Gage FH (2002a) Astroglia induce neurogenesis from adult neural stem cells. Nature 417:39-44.

Song HJ, Stevens CF, Gage FH (2002b) Neural stem cells from adult hippocampus develop essential properties of functional CNS neurons. Nat Neurosci 5:438-445.

Sonnewald U, Westergaard N, Petersen SB, Unsgard G, Schousboe A (1993) Metabolism of [U-13C]glutamate in astrocytes studied by 13C NMR spectroscopy: incorporation of more label into lactate than into glutamine demonstrates the importance of the tricarboxylic acid cycle. J Neurochem 61:1179-1182.

Soriano P (1999) Generalized lacZ expression with the ROSA26 Cre reporter strain. Nat Genet 21:70-71.

Soustelle L, Trousse F, Jacques C, Ceron J, Cochard P, Soula C, Giangrande A (2007) Neurogenic role of Gcm transcription factors is conserved in chicken spinal cord. Development 134:625-634.

Steindler DA (1993) Glial boundaries in the developing nervous system. Annu Rev Neurosci 16:445-470.

Steiner B, Kronenberg G, Jessberger S, Brandt MD, Reuter K, Kempermann G (2004) Differential regulation of gliogenesis in the context of adult hippocampal neurogenesis in mice. Glia 46:41-52.

Steinhauser C, Berger T, Frotscher M, Kettenmann H (1992) Heterogeneity in the Membrane Current Pattern of Identified Glial Cells in the Hippocampal Slice. Eur J Neurosci 4:472-484.

Steinmetz CC, Buard I, Claudepierre T, Nagler K, Pfrieger FW (2006) Regional variations in the glial influence on synapse development in the mouse CNS. J Physiol 577:249-261.

Stellwagen D, Malenka RC (2006) Synaptic scaling mediated by glial TNF-alpha. Nature 440:1054-1059.

Stevens ER, Esguerra M, Kim PM, Newman EA, Snyder SH, Zahs KR, Miller RF (2003) D-serine and serine racemase are present in the vertebrate retina and contribute to the physiological activation of NMDA receptors. Proc Natl Acad Sci U S A 100:6789-6794.

Storck T, Schulte S, Hofmann K, Stoffel W (1992) Structure, expression, and functional analysis of a Na(+)-dependent glutamate/aspartate transporter from rat brain. Proc Natl Acad Sci U S A 89:10955-10959.

Su M, Hu H, Lee Y, d'Azzo A, Messing A, Brenner M (2004) Expression specificity of GFAP transgenes. Neurochem Res 29:2075-2093.

Suadicani SO, Brosnan CF, Scemes E (2006) P2X7 receptors mediate ATP release and amplification of astrocytic intercellular Ca2+ signaling. J Neurosci 26:1378-1385.

Sul JY, Orosz G, Givens RS, Haydon PG (2004) Astrocytic connectivity in the hippocampus. Neuron Glia Biology 1:3-11.

Sun Y, Nadal-Vicens M, Misono S, Lin MZ, Zubiaga A, Hua X, Fan G, Greenberg ME (2001) Neurogenin promotes neurogenesis and inhibits glial differentiation by independent mechanisms. Cell 104:365-376.

Takahashi T, Misson JP, Caviness VS, Jr. (1990) Glial process elongation and branching in the developing murine neocortex: a qualitative and quantitative immunohistochemical analysis. J Comp Neurol 302:15-28.

Takano T, Tian GF, Peng W, Lou N, Libionka W, Han X, Nedergaard M (2006) Astrocyte-mediated control of cerebral blood flow. Nat Neurosci 9:260-267.

Takano T, Kang J, Jaiswal JK, Simon SM, Lin JH, Yu Y, Li Y, Yang J, Dienel G, Zielke HR, Nedergaard M (2005) Receptor-mediated glutamate release from volume sensitive channels in astrocytes. Proc Natl Acad Sci U S A 102:16466-16471.

Tanaka K, Watase K, Manabe T, Yamada K, Watanabe M, Takahashi K, Iwama H, Nishikawa T, Ichihara N, Kikuchi T, Okuyama S, Kawashima N, Hori S, Takimoto M,

Wada K (1997) Epilepsy and exacerbation of brain injury in mice lacking the glutamate transporter GLT-1. Science 276:1699-1702.

Theis M, Mas C, Doring B, Kruger O, Herrera P, Meda P, Willecke K (2001) General and conditional replacement of connexin43-coding DNA by a lacZ reporter gene for cell-autonomous analysis of expression. Cell Commun Adhes 8:383-386.

Torp R, Danbolt NC, Babaie E, Bjoras M, Seeberg E, Storm-Mathisen J, Ottersen OP (1994) Differential expression of two glial glutamate transporters in the rat brain: an in situ hybridization study. Eur J Neurosci 6:936-942.

Tran MD, Neary JT (2006) Purinergic signaling induces thrombospondin-1 expression in astrocytes. Proc Natl Acad Sci U S A 103:9321-9326.

Ueki T, Tanaka M, Yamashita K, Mikawa S, Qiu Z, Maragakis NJ, Hevner RF, Miura N, Sugimura H, Sato K (2003) A novel secretory factor, Neurogenesin-1, provides neurogenic environmental cues for neural stem cells in the adult hippocampus. J Neurosci 23:11732-11740.

Uhlmann EJ, Wong M, Baldwin RL, Bajenaru ML, Onda H, Kwiatkowski DJ, Yamada K, Gutmann DH (2002) Astrocyte-specific TSC1 conditional knockout mice exhibit abnormal neuronal organization and seizures. Ann Neurol 52:285-296.

Ullian EM, Sapperstein SK, Christopherson KS, Barres BA (2001) Control of synapse number by glia. Science 291:657-661.

Umenishi F, Verkman AS, Gropper MA (1996) Quantitative analysis of aquaporin mRNA expression in rat tissues by RNase protection assay. DNA Cell Biol 15:475-480.

Usui T, Yamagami S, Yokoo S, Mimura T, Ono K, Amano S (2004) Gene expression profile in corneal neovascularization identified by immunology related macroarray. Mol Vis 10:832-836.

Vaccarino FM, Schwartz ML, Raballo R, Nilsen J, Rhee J, Zhou M, Doetschman T, Coffin JD, Wyland JJ, Hung YT (1999) Changes in cerebral cortex size are governed by fibroblast growth factor during embryogenesis. Nat Neurosci 2:246-253.

Van Duyne GD (2001) A structural view of cre-loxp site-specific recombination. Annu Rev Biophys Biomol Struct 30:87-104.

Venance L, Piomelli D, Glowinski J, Giaume C (1995) Inhibition by anandamide of gap junctions and intercellular calcium signalling in striatal astrocytes. Nature 376:590-594.

Ventura R, Harris KM (1999) Three-dimensional relationships between hippocampal synapses and astrocytes. J Neurosci 19:6897-6906.

Verkhratsky A (2006) Patching the glia reveals the functional organisation of the brain. Pflugers Arch 453:411-420.

Verkhratsky A, Orkand RK, Kettenmann H (1998) Glial calcium: homeostasis and signaling function. Physiol Rev 78:99-141.

Verrou C, Zhang Y, Zurn C, Schamel WW, Reth M (1999) Comparison of the tamoxifen regulated chimeric Cre recombinases MerCreMer and CreMer. Biol Chem 380:1435-1438.

Vives V, Alonso G, Solal AC, Joubert D, Legraverend C (2003) Visualization of S100B-positive neurons and glia in the central nervous system of EGFP transgenic mice. J Comp Neurol 457:404-419.

Voutsinos-Porche B, Knott G, Tanaka K, Quairiaux C, Welker E, Bonvento G (2003a) Glial glutamate transporters and maturation of the mouse somatosensory cortex. Cereb Cortex 13:1110-1121.

Voutsinos-Porche B, Bonvento G, Tanaka K, Steiner P, Welker E, Chatton JY, Magistretti PJ, Pellerin L (2003b) Glial glutamate transporters mediate a functional metabolic crosstalk between neurons and astrocytes in the mouse developing cortex. Neuron 37:275-286.

Waagepetersen HS, Qu H, Schousboe A, Sonnewald U (2001) Elucidation of the quantitative significance of pyruvate carboxylation in cultured cerebellar neurons and astrocytes. J Neurosci Res 66:763-770.

Wallraff A, Odermatt B, Willecke K, Steinhauser C (2004) Distinct types of astroglial cells in the hippocampus differ in gap junction coupling. Glia 48:36-43.

Walz W (2000) Controversy surrounding the existence of discrete functional classes of astrocytes in adult gray matter. Glia 31:95-103.

Wang X, Lou N, Xu Q, Tian GF, Peng WG, Han X, Kang J, Takano T, Nedergaard M (2006) Astrocytic Ca2+ signaling evoked by sensory stimulation *in vivo* . Nat Neurosci 9:816-823.

Weber P, Metzger D, Chambon P (2001) Temporally controlled targeted somatic mutagenesis in the mouse brain. Eur J Neurosci 14:1777-1783.

Witcher MR, Kirov SA, Harris KM (2007) Plasticity of perisynaptic astroglia during synaptogenesis in the mature rat hippocampus. Glia 55:13-23.

Wolff JR, Chao TI (2004) Cytoarchitectonics of non-neuronal cells in the central nervous system. Advances in Molecular and Cell Biology 31:1-51.

Wolosker H, Blackshaw S, Snyder SH (1999) Serine racemase: a glial enzyme synthesizing D-serine to regulate glutamate-N-methyl-D-aspartate neurotransmission. Proc Natl Acad Sci U S A 96:13409-13414.

Wu S, Wu Y, Capecchi MR (2006) Motoneurons and oligodendrocytes are sequentially generated from neural stem cells but do not appear to share common lineage-restricted progenitors *in vivo* . Development 133:581-590.

Wunderlich FT, Wildner H, Rajewsky K, Edenhofer F (2001) New variants of inducible Cre recombinase: a novel mutant of Cre-PR fusion protein exhibits enhanced sensitivity and an expanded range of inducibility. Nucleic Acids Res 29:E47.

Xu PT, Li YJ, Qin XJ, Scherzer CR, Xu H, Schmechel DE, Hulette CM, Ervin J, Gullans SR, Haines J, Pericak-Vance MA, Gilbert JR (2006) Differences in apolipoprotein E3/3 and E4/4 allele-specific gene expression in hippocampus in Alzheimer disease. Neurobiol Dis 21:256-275.

Yang XW, Model P, Heintz N (1997) Homologous recombination based modification in Escherichia coli and germline transmission in transgenic mice of a bacterial artificial chromosome. Nat Biotechnol 15:859-865.

Yang Y, Ge W, Chen Y, Zhang Z, Shen W, Wu C, Poo M, Duan S (2003) Contribution of astrocytes to hippocampal long-term potentiation through release of D-serine. Proc Natl Acad Sci U S A 100:15194-15199.

Ye P, Popken GJ, Kemper A, McCarthy K, Popko B, D'Ercole AJ (2004) Astrocyte-specific overexpression of insulin-like growth factor-I promotes brain overgrowth and glial fibrillary acidic protein expression. J Neurosci Res 78:472-484.

Ye ZC, Wyeth MS, Baltan-Tekkok S, Ransom BR (2003) Functional hemichannels in astrocytes: a novel mechanism of glutamate release. J Neurosci 23:3588-3596.

Zelenin S, Gunnarson E, Alikina T, Bondar A, Aperia A (2000) Identification of a new form of AQP4 mRNA that is developmentally expressed in mouse brain. Pediatr Res 48:335-339.

Zervas M, Millet S, Ahn S, Joyner AL (2004) Cell behaviors and genetic lineages of the mesencephalon and rhombomere 1. Neuron 43:345-357.

Zhang JM, Wang HK, Ye CQ, Ge W, Chen Y, Jiang ZL, Wu CP, Poo MM, Duan S (2003) ATP released by astrocytes mediates glutamatergic activity-dependent heterosynaptic suppression. Neuron 40:971-982.

Zhang Q, Fukuda M, Van Bockstaele E, Pascual O, Haydon PG (2004) Synaptotagmin IV regulates glial glutamate release. Proc Natl Acad Sci U S A 101:9441-9446.

Zhou M, Kimelberg HK (2000) Freshly isolated astrocytes from rat hippocampus show two distinct current patterns and different [K(+)](o) uptake capabilities. J Neurophysiol 84:2746-2757.

Zhou M, Schools GP, Kimelberg HK (2006) Development of GLAST(+) astrocytes and NG2(+) glia in rat hippocampus CA1: mature astrocytes are electrophysiologically passive. J Neurophysiol 95:134-143.

Zhuo L, Sun B, Zhang CL, Fine A, Chiu SY, Messing A (1997) Live astrocytes visualized by green fluorescent protein in transgenic mice. Dev Biol 187:36-42.

Zhuo L, Theis M, Alvarez-Maya I, Brenner M, Willecke K, Messing A (2001) hGFAP-cre transgenic mice for manipulation of glial and neuronal function *in vivo* . Genesis 31:85-94.

Zonta M, Angulo MC, Gobbo S, Rosengarten B, Hossmann KA, Pozzan T, Carmignoto G (2003) Neuron-to-astrocyte signaling is central to the dynamic control of brain microcirculation. Nat Neurosci 6:43-50.